71-4675

MATTSON, James Stewart, 1945-
INFRARED INTERNAL REFLECTANCE SPECTROSCOPIC STUDIES OF THE SURFACE CHEMISTRY OF ACTIVATED CARBON.

The University of Michigan, Ph.D., 1970
Chemistry, analytical

University Microfilms, Inc., Ann Arbor, Michigan

THIS DISSERTATION HAS BEEN MICROFILMED EXACTLY AS RECEIVED

INFRARED INTERNAL REFLECTANCE SPECTROSCOPIC STUDIES OF THE SURFACE CHEMISTRY OF ACTIVATED CARBON

by
James Stewart Mattson

A dissertation submitted in partial fulfillment
of the requirements for the degree of
Doctor of Philosophy in
The University of Michigan
1970

Doctoral Committee:

Associate Professor Harry B. Mark, Jr., Co-Chairman
Professor Walter J. Weber, Jr., Co-Chairman
Assistant Professor Michael E. Bender
Doctor N. James Harrick, Harrick Scientific Corporation
Professor Jack L. Hough

ABSTRACT

INFRARED INTERNAL REFLECTANCE SPECTROSCOPIC STUDIES OF THE SURFACE CHEMISTRY OF ACTIVATED CARBON

by

James Stewart Mattson

Co-Chairman: Harry B. Mark, Jr. & Walter J. Weber, Jr.

The surface chemistry of activated carbons has long been a subject of dispute. A review section which critically discusses past data and conclusions regarding the nature of the surface oxygen functional groups on carbon is the beginning of this thesis.

Extensive study of the adsorption phenomenon involving phenolic compounds in aqueous solution and activated carbon leads to a postulation of a weak donor-acceptor interaction between the relatively electron-poor aromatic ring and an electron-rich site on the carbon surface. It is suggested that the electron-donor surface site is that of a carbonyl oxygen group. Infrared internal reflectance spectroscopic (IRS) studies of several commercial, and several laboratory-prepared, activated carbons tend to support some of the theories regarding surface oxygen functional groups on activated carbons.

The results of the infrared IRS studies of carbon black, powdered graphite, and several activated carbons are presented in the form of spectra, and discussed in terms of their band assignments. Adsorption bands characteristic of dicarboxylic acids, enolic forms of 1, 3-diketones and quinones have been observed on activated carbons.

An Appendix discusses the basic theory behind the application of infrared IRS to the study of high-refractive index, highly absorbing, powdered solids.

ACKNOWLEDGEMENTS

I would like to take this opportunity to express my utmost thanks and appreciation to Professor Harry B. Mark, Jr. for his invaluable advice and generous help in more ways than I could ever enumerate.

I would also like to thank the many individuals who were willing to extend their advice and assistance throughout the period of this research; in particular Professor Walter J. Weber, Jr., Dr. Michael D. Malbin, Dr. Hubert C. MacDonald, Jr., and Dr. N. James Harrick. For his never-ending supply of moral support, I would also like to sincerely thank Clarence E. Schutt.

Finally, I would like to acknowledge the continued and patient understanding of my wife, Carol, for she is the one responsible for keeping all of us, including myself and our two children, on an even keel.

TABLE OF CONTENTS

Chapter

1. INTRODUCTION 1

2. REVIEW OF SURFACE OXIDES 5

I. The Chemisorption of Oxygen on Carbon . . . 5

A. Low Temperature Chemisorption 5
B. Heat of Adsorption 5
C. Desorption of Chemisorbed Surface Oxides 6

II. Physical and Chemical Properties of Activated Carbons Attributable to Surface Oxides 7

A. Acidity, Zeta Potential and Hydrophilicity of Surface 7
B. H- and L-Classification Scheme 9
C. "Aging" of Activated Carbons 9

III. Surface Oxides Which can be Removed as CO, CO_2 and H_2O 12

A. Thermal Evolution of CO and CO_2 12
B. The Relationship of CO- and CO_2-Evolving Surface Oxides to H- and L-Behavior 13
C. Bromination of Surface C=C Bonds after CO_2 Evolution 15
D. Acidity of CO_2-Evolving Surface Oxides 15
E. Adsorption of Water and Methanol by CO_2-Evolving Groups 18
F. Evolution of H_2O on High Temperature Outgassing 18

IV. "Geography" of the Surface Oxides 20

TABLE OF CONTENTS (CONT'D)

Chapter

V. The Determination of Oxygen-Containing Surface Functional Groups by Indirect Methods 22

A. Multi-basic Titrations of Acidic Surface Oxides 24
B. Carboxyl Groups Determined by Acid-Base Behavior 28
C. Identification of Phenolic Surface Oxides Through the Reaction with NaOH 31

VI. Specific Chemical Identification of Surface Functional Groups 32

A. Reaction with Diazomethane 32
B. Reaction with Organic Functional Group Reagents 40
1. Aldehydes and Ketones 40
2. Phenols and Enols 41
3. Carboxylic Acids 41
C. Polarographic Identification of Quinone Surface Groups 42
D. Chemical Reduction of Surface Oxides . . 43

VII. Direct Identification of Surface Functional Groups by Infrared Spectroscopy 45

3. INTERNAL REFLECTION SPECTROSCOPIC (IRS) DETERMINATION OF SURFACE FUNCTIONAL GROUPS 57

I. Experimental 58

II. Samples of a Commercial Carbon Examined by IRS both Before and After the Adsorption from Solution of p-Nitrophenol 74

III. IRS Spectra of Powdered Graphite, Carbon Black, and Microcrystalline Active Carbon 85

TABLE OF CONTENTS (CONT'D)

Chapter

4. IRS SPECTRA OF LABORATORY-ACTIVATED SUGAR CARBONS 98

I. Preparation of Carbons 99

II. IRS Spectra 100

III. Discussion of Results 101

5. ADSORPTION EXPERIMENTS 118

I. Experimental 120

A. Adsorption Isotherm Studies 120
B. Internal Reflection Spectra 125

II. Results and Discussion 126

III. Conclusions 147

APPENDIX — IRS SPECTROSCOPY OF OPTICALLY OPAQUE SOLIDS 153

REFERENCES 167

LIST OF TABLES

Table		Page
1.	Neutralization of Different Bases by the Various Samples of Charcoal and Carbon Black in Relation to CO_2-Complex. From Ref. (12).	14
2.	Bromine Fixed by Charcoal and Carbon Black in Relation to CO_2-Complex Eliminated. From Ref. (12).	16
3.	Water and Methanol Fixed on Carbon Surface Related to CO_2-Evolved. From Ref. (12).	19
4.	Neutralization of Acidic Carbon Surface Oxides with Bases of Differing Strength. From Ref. (4). .	27
5.	Dissociation Constants of Dicarboxylic Acids in Aqueous Solution. From Ref. (36).	29
6.	Effect of Temperature and Oxidation on the Acidic Properties of Carbons and the Reaction with Diazomethane. From Ref. (17).	36
7.	Base Consumption of Sugar Carbons Before and After Methylation followed by Hydrolysis. From Ref. (4).	38
8.	Change in the Quantity of Acidic Groups After Reduction of the Acidic Surface Oxides. From Ref. (4).	44
9.	Band Positions and Relative Intensities for Sugar Carbons Activated in 1% O_2-99% N_2	103
10.	Band Positions and Relative Intensities for Sugar Carbons Activated in 5% O_2-45% CO_2-50% N_2	104

LIST OF ILLUSTRATIONS

Figure		Page
1.	"Adsorption" of Acid and Base by an Activated Sugar Carbon as a Function of Activation Temperature. From Ref. (23)	10
2.	Effect of Heat Treatment of an Ink Black on Acid and Base "Adsorption." From Ref. (25) . . .	11
3.	Infrared Spectra of Carbohydrate Chars. From Ref. (43)	46
4.	A, Infrared Spectrum of Untreated Channel Black of 8-10 mμ Diameter; B, Infrared Spectrum of the Same Black after Treatment with Diazomethane. From Ref. (40)	49
5.	Infrared Spectra of "Carbolac 1" and a Series of Derivatives Prepared by Heat Treatment and Reactions with Diazomethane and Alkali. From Ref. (17)	52
6.	Infrared Spectra of a Series of Sugar Carbons. From Ref. (17)	53
7.	Forward Scattering Spectrum.	60/61
8.	Effect of IRS Crystal on Bulk Absorption	69
9.	Effect of Powder on IRS Spectrum of Thin Film	73
10.	The IRS Spectrum of Nuchar C-115, a Lignin-Based Commercial Active Carbon. 5X Scale Expansion	75/76

LIST OF ILLUSTRATIONS (CONT'D)

Figure		Page
11.	The IRS Spectrum of Nuchar C-115 after the Adsorption of 1.6 meq. p-nitrophenol/gram from pH2 HCl Solution. 5X Scale Expansion. . . .	77
12.	IRS Spectra of Nuchar C-115. Top, before Adsorption; Bottom, after Adsorption of 1.6 meq/g p-nitrophenol. C-O Region.	80
13.	IRS Spectra of Nuchar C-115. Top, before Adsorption; Bottom, after Adsorption of 1.6 meq/g p-nitrophenol. CH Region	82
14.	IRS Spectra of Nuchar C-115. Top, before Adsorption; Bottom, after Adsorption of 1.6 meq/g p-nitrophenol. 1600 cm^{-1} C=O Band	83
15.	IRS Spectrum of Graphite	86
16.	Scale Expansion of 2000-1000 cm^{-1} Region of IRS Spectrum of Graphite	87
17.	Expanded Scale IRS Spectra of C-1000, a Lignin-Based Active Carbon	90
18.	Expanded Scale IRS Spectra of C-1000, with Graphite against the Reference Crystal	92
19.	IRS Spectrum of Carbon Black, 2X Scale Expansion with KRS-5 IRE	94
20.	10X Expanded Scale Spectra of Carbon Black . . .	96
21.	IRS Spectra 10X of Sugar Carbons Activated in 1% O_2-99% N_2 for six hours at 300, 400 and 500°C	105/106
22.	IRS Spectra 10X of Sugar Carbons Activated in 1% O_2-99% N_2 for six hours at 600 and 700°C. .	107

LIST OF ILLUSTRATIONS (CONT'D)

Figure		Page
23.	p-nitrophenol Adsorption Isotherms for Sugar Carbons Activated at 300-700°C in 1% O_2-99% N_2 as a Function of Activation Temperature	110/111
24.	p-nitrophenol Capacities for Sugar Carbons Activated in 1% O_2-99% N_2 as a Function of Activation Temperature	112
25.	IRS Spectra of Sugar Carbons Activated in 5% O_2-45% CO_2-50% N_2 at 300 and 400°C for six hours, and 600 and 700°C for three hours	116
26.	O-H Stretching Region. The Top Spectrum shows the O-H Band of Solid p-nitrophenol (KRS-5, 45°). The Lower Spectrum is that of Active Carbon with p-nitrophenol Adsorbed on the Carbon Surface (KRS-5, 60°, 10X)	122/123
27.	1600-1200 cm^{-1} Region. The Top Spectrum shows the NO_2 Group Bands and C-O Band of p-nitrophenol. The Lower Spectrum shows the same Bands of p-nitrophenol Adsorbed on Active Carbon	127/128
28.	Reduced Concentration Isotherms. The Isotherms obtained at 25°C for Phenol, the Nitrophenols and Nitrobenzene are shown with respect to Reduced Equilibrium Solution Concentration, $C_{eq'm}/C_s$	130/131
29.	Adsorption-Desorption of p-Nitrophenol. A Desorption Isotherm for p-nitrophenol on the Carbon employed in this Study is shown along with the Adsorption Isotherm. Both were obtained at pH 2 and 25°C	133-134

LIST OF ILLUSTRATIONS (CONT'D)

Figure		Page
30.	pH Dependence of p-Nitrophenol Desorption. Equilibrated Samples of p-Nitrophenol and Carbon were subjected to the Desorption Technique Described. Variation of the pH at which Adsorption and Desorption were Carried Out Caused Only the Expected Solubility Effect	136
31.	Reduced Concentration Isotherms for p-Nitrophenol at Different Temperatures	138
32.	Isotherms for p-Nitrophenol at Different Temperatures	140/141
33.	Internal Reflection Spectrum of p-Nitrophenol. Solid p-Nitrophenol, in a Thin Film, ca. 400 A Thick, was Deposited on an IRS KRS-5 Crystal to Obtain this Spectrum	144
34.	Electric Field Intensities for Total Internal Reflection at a Glass/Water Interface. The Energy in the Sample Medium, on the Right, is Exponentially Decaying; while Standing Waves Result in the Internal Reflection Element Itself, on the Left	155/156
35.	For the Case of Attenuated Total Internal Reflection, where Phase Two has a Finite Extinction Coefficient, not only is the Intensity of the Evanescent Field Decreased (on the Right), but the Amount of Energy Reflected in Phase One has Diminished	157/158

LIST OF ILLUSTRATIONS (CONT'D)

Figure		Page
36.	Homogeneous, Highly Absorbing ($K \tilde{=} 0.7$) Graphite will Interact Strongly with the Intense Evanescent Field observed on the Right. The Loss of Energy is Proportional to the Area beneath the Exponentially Decaying Curve	159
37.	Particulate Graphite, with a Thin Film of Air separating the Sample from the IRS Crystal. The observed Interaction, Proportional to the Area beneath the Expoentially Decaying Curve in the Sample Medium (Far Right), is Very Weak	160

CHAPTER 1

INTRODUCTION

"It is by no means to be wondered that, in the science of physics in general, men have often made suppositions instead of forming conclusions. These suppositions, handed down from one age to another, acquire additional weight from the authorities by which they are supported, till at last they are received, even by men of genius, as fundamental truths."

Lavoisier, Elements of Chemistry, 1789

Activated carbon, a product which has been used for at least thousands of years, occupies an interesting position in the field of chemistry. Even though active carbon is employed by nearly all of the chemical industry for the purification (or decolorization) of organic chemicals, and enjoys widespread popularity in the treatment of drinking water to remove taste- and odor-causing organics, the mechanisms by which active carbon specifically adsorbs organic molecules from solution have never been clearly understood. One of the more significant contributions to this singular lack of knowledge has been the lack of direct experimental information on the chemical nature of the surfaces of activated carbons.

This research has been directed towards an examination of the chemistry of active carbon. Our original intent was to employ internal reflection spectroscopy to characterize directly the organic-like functional groups known to be present on active carbon surfaces. This did not turn out to be as simple as it had seemed a priori, and it soon was obvious that there were basic problems extending back several decades which never had been solved. The major hurdle involved in attempting to identify the surface functional groups was in determining the nature of the interaction between the carbon surface and the adsorbate. The theories regarding these interactions were few, based upon minimal information, largely speculative and usually in direct conflict with one another.

While the basic studies reported here of the adsorption process were of necessity somewhat limited (limited primarily to phenols), it did provide some information regarding the types of surface structures to look for spectroscopically. The available literature involving transmission spectroscopic and other experimental procedures was carefully reviewed in order to help interpret the internal reflectance spectroscopic data. Careful spectroscopic studies of commercially prepared materials showed heterogeneities of a broad scope which had not been adequately suspected. Consideration of the temperature and gas concentration gradients

encountered in commercial processes led us to the same step taken by several previous investigators. In order to understand the variety and complexity of surface reactivity involved in the activation process, it was necessary to have considerable control over all of the parameters involved. For this reason, it was deemed necessary to prepare laboratory-activated carbons from a starting material of known high purity, in this case sugar, under conditions of uniform and controlled temperature and atmosphere.

For these reasons, the bulk of the reliable data in the literature on carbon surface chemistry has been obtained with very pure or laboratory-activated carbons, and this is the type of data in which we place the most confidence.

The results of an extensive literature survey, as well as our experimental studies, indicated that, while activated carbons may contain nitrogen, inorganic salts, sulfur and hydrogen as "impurities" as well as oxygen, it is the oxygen functional groups at the surface which are of primary importance. Graphite, carbon black, and activated carbons have long been known to irreversibly chemisorb molecular oxygen (1, 2) at room temperature and below. The chemically bound oxygen is only removable then at elevated temperatures (1). The carbon-oxygen reactions have been under investigation for over a century (2), and the thermodynamic and the kinetic natures of these reactions have been the subject of

studies by several investigators. One of the inadequacies in studies of the mechanisms of adsorption from solution by active carbon has been the lack of definitive information concerning the types of chemical functional groups which are formed at carbon surfaces during the reactions with oxygen.

Previous investigations of the chemistry of these carbon surface oxides has for the most part involved indirect methods of investigation, such as acid-base neutralization of the surface oxides (3-5) and the thermal removal of the surface oxides as CO and CO_2 (6-16). There has been a small amount of direct experimental investigation of surface functional groups utilizing infrared (17-20) and ESR spectroscopy (21-23). Our recent studies employing internal reflection infrared spectroscopy (18-20) provide some new information on carbon surface functional groups. This thesis attempts to examine both the indirect and the direct studies of the carbon surface oxides, in an effort to correlate the various determinations and arrive at a consistent qualitative description of the surfaces of activated carbons.

CHAPTER 2

REVIEW OF SURFACE OXIDES

I. The Chemisorption of Oxygen on Carbon

A. Low temperature chemisorption

Zarif'yanz, et al. (13, 24) examined the adsorption of oxygen on graphite wear dust at low temperatures of -196° C, -73° C, -42° C and -21° C. At -196° C the adsorption was completely reversible, as was the adsorption at -73° C. At -42° C and -21° C, however, the adsorption was irreversible, with an uptake of about 1 μmole O_2/m^2 (13).

B. Heat of adsorption

Zarif'yanz et al. (13) found that the initial heat of adsorption of O_2 on the freshly prepared surface was 40 kcal/mole at -73° C, as compared to 7 kcal/mole on the oxidized (once-exposed) surface (at -73° C). The initial heat of adsorption of oxygen on graphite wear dust at 20° C begins at 100-110 kcal/mole, falling by about a factor of two at higher surface coverages (13). This is indicative of a very strong chemical bonding to the carbon surface.

C. Desorption of chemisorbed surface oxides

On heating graphite wear dust which contains chemisorbed or bound oxygen, the oxygen evolves as CO_2 and CO (6-16, 25). Zarif'yanz et al. (13) examined this evolution of CO_2 and CO as a function of temperature; they found that CO_2 is evolved at temperatures below 600° C, and that CO is evolved between 500 and 800° C. The complete removal of all bound oxygen requires temperatures on the order of 1200° C, under vacuum, and the oxygen is completely removed as CO, CO_2 and H_2O (6, 26).

The fact that activated carbon, regardless of the activation conditions, reacts with oxygen when brought into contact with air at a temperature as low as somewhere between -73° C and -42° C (13) makes it difficult to experimentally study the effects of different activation temperatures and atmospheres on the formation of surface functional groups. Whether it is possible or even necessary to reconcile this problem with respect to the characteristics of activated carbon employed in natural systems is a moot point. Even though the reaction of oxygen with carbon in an isolated vacuum system is important in the study of the formation of chemical structures on the surface, it is important not to lose sight of the fact that all applications of active carbon employ material which has been exposed to the atmosphere for a considerable time prior to use.

II. Physical and Chemical Properties of Activated Carbon Attributable to Surface Oxides

A. Acidity, zeta potential and hydrophilicity of surface

In 1929, Kruyt and de Kadt made the observation that sugar-based carbons which were activated at high temperatures possessed markedly different surface properties with respect to acid-base character, electrophoretic mobility (Zeta potential) and degree of hydrophilicity, than did sugar carbons which were both activated and oxidized[1] at lower temperatures, and even more significantly, that the two types of carbons were reversibly interconvertible (27). The activation of carbon at 1000°C either in pure CO_2 or under vacuum, followed by exposure to oxygen at room temperature, results in a carbon surface which is capable of raising the pH of either a neutral or an acidic solution, is hydrophobic and has a positive Zeta potential (26, 27). By contrast, the oxidation of carbon by exposure to gaseous oxygen at temperatures between 200 and 400°C (27), or by adding it to an aqueous oxidizing solution (3, 4, 27), produces just the opposite surface character, in each of the above respects. This low-temperature oxidized carbon has been shown to be able to lower the pH of a

---

[1] "Activation" refers to the burning out of extensive amounts of original raw material, leaving a porous, microcrystalline product of high surface area and high carbon content. "Oxidation", which is used in its normal context, usually is carried out either (i) in gaseous O_2 at temperatures above 300°C, or (ii) in an aqueous oxidizing medium.

neutral or basic solution, is hydrophilic, and exhibits a negative Zeta potential (26, 27). Frumkin (26) found that it was necessary to heat carbon to at least 1000° C in vacuum or CO_2 in order to produce the ideal high-temperature "activated" carbon, one which could neither raise nor lower the pH of a neutral solution until after exposure to oxygen at room temperature. Kruyt and de Kadt (27), as mentioned above, found that such a high-temperature activated carbon, upon re-exposure to gaseous oxygen at 300° C, could be readily converted to a material which behaved exactly as though it had never been activated at the higher (1000° C) temperature, but instead had all the physical properties of a low-temperature oxidized carbon.

Steenberg (28) and Garten and Weiss (29) demonstrated that one could obtain the same results with high-temperature activated carbons as did Kruyt and de Kadt (27), but without the two-step activation-oxidation step used by the latter (27). They (28, 29) were able to show that exposure to oxygen during high-temperature "activation" resulted in a carbon with the properties observed by Kruyt and de Kadt (27) and Frumkin (26) for carbons activated at high temperature and subsequently exposed to gaseous oxygen at room temperature. They (28, 29) also observed that oxygen must be excluded from the atmosphere in contact with the high-temperature activated and oxidized carbon during the cooling

procedure, or the carbon would take on the properties of a low-temperature oxidized carbon during cooling.

B. H- and L-classification scheme

Steenberg (28) used the uptake of inorganic acid and base as a method of characterizing the carbons activated and oxidized at different temperatures, classifying those low-temperature oxidized carbons which "adsorbed" primarily hydroxide ions as L-carbons, and those which were activated at high temperatures, and thus "adsorbed" acid, were classified as H-carbons. These classifications, which have been found to naturally divide above and below an activation/oxidation temperature of about 500-600° C (28, 29) are adequate today as general classifications. Figures 1 and 2 reproduce the data of Steenberg (28) and Garten and Weiss (29), showing the transition from H to L behavior.

C. "Aging" of activated carbons

Puri found that L-carbon behavior predominated for carbons after long exposure to the atmosphere at room temperature (6). Puri (6) experimented with the aging of active carbon in H_2O-free and humid air, and in pure oxygen. He found that considerable oxygen was bound, primarily as the L-carbon oxide, upon exposure to air for 60 days, or upon exposure to pure oxygen for 12 hours (with little increase observed upon longer aging). This was done (6) with carbons originally oxidized at 350 and 400° C.

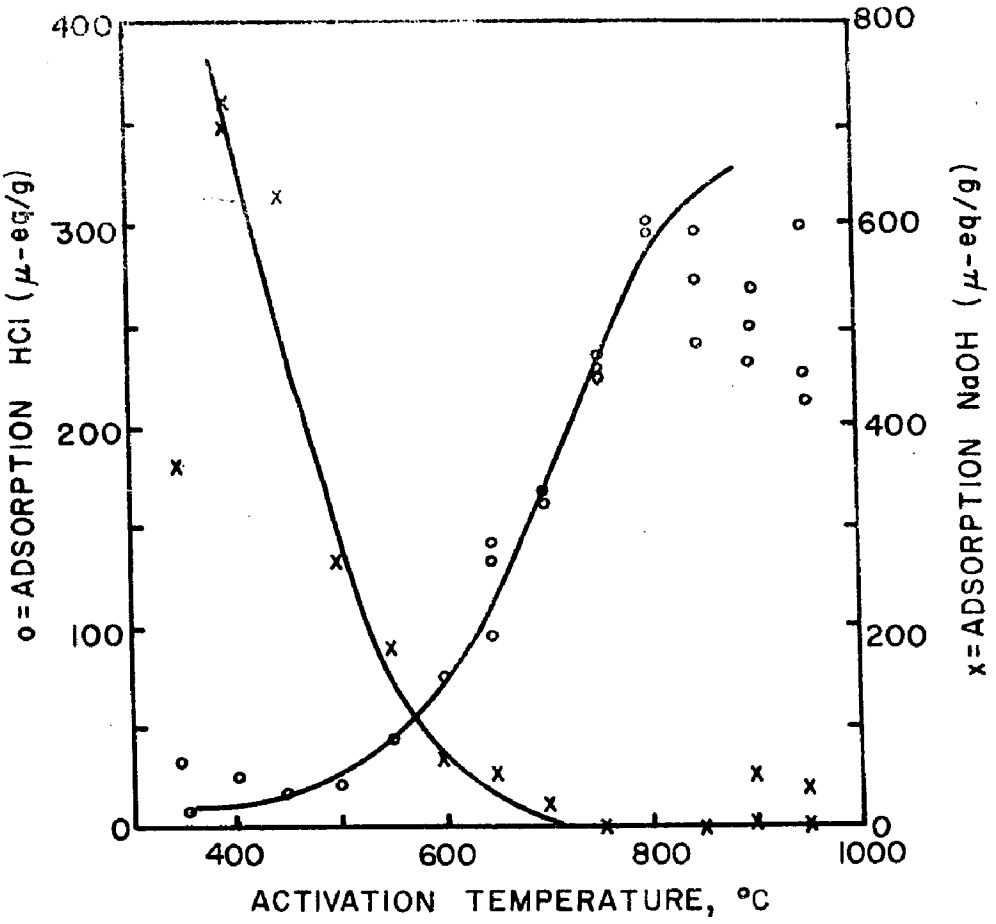

Fig. 1. --"Adsorption" of acid and base by an activated sugar carbon as a function of activation temperature. From Ref. (25)

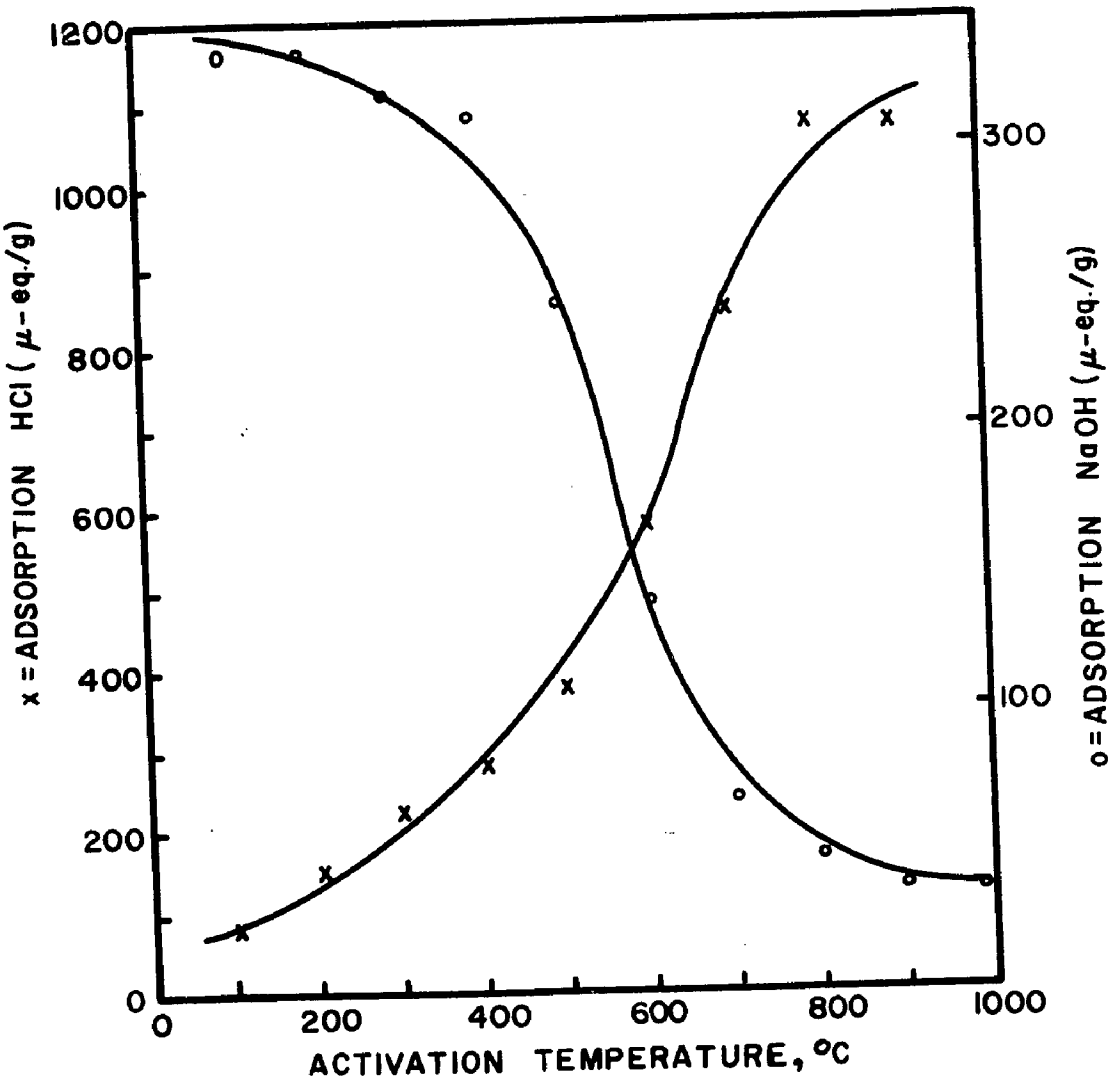

Fig. 2. --Effect of heat treatment of an ink black on acid and base "adsorption." From Ref. (25)

The total amount of oxygen "fixed" to the carbon has been shown to vary considerably with activation temperature, and the amount of this oxygen bound as the H-carbon oxide, has been found to increase considerably as the activation temperature is raised from 400° to 800°C (28, 29). The adsorptive behavior of the carbon is, of course, dependent upon the nature of all of the surface oxides. The atmospheric aging actually only increases the L-carbon characteristics in a relative manner; aging does not decrease the amounts of the other surface oxides.

III. Surface Oxides Which can be Removed as CO, CO_2, and H_2O

A. Thermal evolution of CO and CO_2

Considerable work in this area has been carried out by Puri and his co-workers (6-12), and in studies of "gasification" reactions of carbon with oxygen by other investigators (13, 14). Puri employed an Orsat-Lunge gas analysis apparatus (6) to determine the quantities of CO, CO_2, and H_2O evolved upon the outgassing of samples of carbon under vacuum at 1200°C. These are the only gases that have been found to be removed from carbon under these conditions, and all of the bound oxygen on carbon can be removed in this manner as CO, CO_2, and H_2O.

B. The relationship of CO- and CO_2-evolving surface oxides to H- and L-behavior

Because the respective temperatures at which these gases are evolved coincide with the temperature ranges involved in the production of H- and L-carbons, it has been suggested (6, 12) that the surface oxides evolved as CO_2 are responsible for the physico-chemical properties observed for L-carbons, and that the oxides evolved as CO are responsible for H-carbon characteristics. Garten and Weiss (29) have shown that oxidation of carbon at 800°C produces an H-carbon, while Puri (6-12), Zarif'yanz (13), and Walker (14) have shown that all of the CO_2-producing oxide is removed from the carbon surface at a temperature of 600°C to 750°C.

Recent data of Puri (12) which is consistent with previous results (7-9), is presented in Table 1. This data shows that a close relationship exists between the surface acidity of active carbons (as measured by the uptake of $Ba(OH)_2$, NaOH, n-butylamine and gaseous NH_3) and the amount of CO_2 evolved upon outgassing in vacuum at 1200°C. The carbon used in these experiments (12) was prepared by charring sugar in sulfuric acid. This material was then oxidized in aqueous solution using several strong oxidizing agents (persulfate, chlorine, H_2O_2 and HNO_3), and in each case the capacity of the carbon to neutralize base corresponded to the amount of CO_2 evolved upon outgassing in vacuum at 1200°C. By

Table 1[a]

Neutralization of Different Bases by the Various Samples of Charcoal and Carbon Black in Relation to CO_2-Complex

Description	Amounts of different bases neutralized (m-equiv./100 g)					CO_2 evolved on outgassing (m-equiv./100 g)
	$Ba(OH)_2$	NaOH	n-butyl amine	Aq. ammonia	Gaseous ammonia	
Sugar charcoal, original	655	643	682	354	670	669
Treated with $K_2S_2O_8$	970	985	---	487	898	975
Treated with aq. chlorine	902	888	879	474	825	881
Treated with aq. H_2O_2	810	795	802	402	790	819
Outgassed at 300°	361	366	361	201	347	359
400°	215	209	202	112	198	206
500°	166	163	161	88	159	160
600°	45	43	48	30	38	48
750°	nil	nil	nil	nil	nil	nil
1000°	nil	nil	nil	nil	nil	nil
Outgassed 1000°, treated with HNO_3	1184	1166	---	530	955	1163
Coconut charcoal, original	374	376	381	180	338	384
Treated with $K_2S_2O_8$	749	757	704	362	698	741
Treated with aq. chlorine	678	668	659	342	624	686
Treated with aq. H_2O_2	612	618	614	328	---	---
Outgassed at 300°	308	316	327	172	302	314
400°	56	51	57	22	49	59
500°	3	2	3	nil	nil	8
600°	nil	nil	nil	nil	nil	nil
750°	nil	nil	nil	nil	nil	nil
1000°	nil	nil	nil	nil	nil	nil
Outgassed 1000°, treated with HNO_3	621	612	609	352	584	617
Spheron 6, original	29	28	30	18	---	34
Treated with HNO_3	253	258	250	115	240	257
Mogul, original	139	135	123	68	---	137
Outgassed at 200°	138	133	---	72	---	137
400°	82	79	70	44	69	83
700°	22	22	18	---	---	18
Treated with HNO_3	529	534	524	282	492	524
Mogul A, original	113	115	---	---	---	115
Outgassed at 400°	59	62	61	---	---	59
500°	24	18	19	---	---	24
700°	nil	nil	nil	---	---	nil

[a] Reprinted from Ref. (12), p. 393, by courtesy of Pergamon Press.

first outgassing samples of sugar char at temperatures from 300 to 1000°C, then both (i) neutralizing the surface oxides with base, and (ii) measuring the CO_2 evolved upon outgassing. Puri (12) observed that for pretreatment involving pre-outgassing above 600°C, CO_2 could no longer be removed upon further outgassing at 1200°C, nor could any base be neutralized. These results are consistent with the conclusion that the CO_2-evolving surface oxide functional groups are responsible for the acidic behavior of L-carbons.

C. Bromination of surface C=C bonds after CO_2 evolution

Experiments carried out by Puri (12) on the bromination of these carbons are summarized in Table 2. The correlation between the last two columns of Table 2 indicates that one mole of Br_2 was fixed for each two moles of CO_2 removed previously by outgassing. This suggests that removal of two CO_2-evolving surface oxides results in the formation of a new carbon-carbon double bond at the carbon surface, and that this C=C bond is then readily brominated. The resulting C-Br bonds formed were found to be stable even at the 1200°C outgassing temperature (12).

D. Acidity of CO_2-evolving surface oxides

It is possible, on the basis of Puri's (12) studies, to speculate on the acid strength of part of the surface oxides on activated carbon from the data of Table 1. In the fourth and fifth

Table 2[a]

Bromine Fixed by Charcoal and Carbon Black in Relation to CO_2-Complex Eliminated

Description	CO_2-complex	Bromine fixed	Decrease in the amount of CO_2-complex on outgassing	Increase in amount of bromine fixed on outgassing
Sugar charcoal, original	669	48	---	---
Outgassed at 300°	359	208	310	160
400°	206	292	463	244
600°	48	364	621	316
750°	nil	380	669	332
1000°	nil	391	669	343
1200°	nil	395	669	347
Coconut charcoal, original	384	55	---	---
Outgassed at 300°	314	91	70	36
400°	59	226	325	171
500°	8	232	376	177
600°	nil	242	384	187
750°	nil	248	384	193
1000°	nil	244	384	189
Mogul, original	137	nil	---	---
Outgassed at 400°	83	30	54	30
500°	45	42	92	42
700°	18	62	119	62
1000°	nil	64	137	64
1200°	nil	64	137	64
Mogul A, original	116	nil	---	---
Outgassed at 400°	59	27	57	27
500°	24	48	92	48
700°	nil	61	116	61
1000°	nil	59	116	59

[a]Reprinted from Ref. (12). p. 396, by courtesy of Pergamon Press.

columns of this table, it can be seen that while n-butylamine (pK_b = 3.3) neutralized as much of the surface acidity as did NaOH and $Ba(OH)_2$, NH_4OH (pK_b = 4.8) was capable of neutralizing only from 50 to 60 percent of the total CO_2-evolving groups. As these experiments were carried out in aqueous 0.2 N NH_4OH and 0.5 M n-butylamine (12), it can be estimated that approximately one-half of the total hydroxide-titratable acidic functional groups are made up of surface oxides with a pK_a in the range $6 \lesssim pK_a \lesssim 8$; the other half being somewhat stronger than $pK_a \simeq 6$.

It should be mentioned that, in an isolated set of experiments (6), which are not mentioned in the more recent studies by Puri (12), he found that upon heating a sugar char to 750°C or 1200°C, followed by aqueous oxidation in solutions of chlorine, persulfate, bromate, periodate or nitrate, appeared to result in CO_2-evolving groups (and absolutely no CO-evolving groups) which were not titratable by OH^-. It was suggested (6) that this somehow involved addition of oxygen to double bonds, or in the formation of a non-acidic peroxide structure. The data of Table 1 do not reflect results of this nature. No explanation is available at this time with respect to this once-reported result. Further, as shown in Table 1, an experiment, similar to the immediately preceding experiments, where the sugar char was degassed at 1000°C and subsequently oxidized in nitric acid led to results which were exactly the same

as all the other experiments summarized in Table 1. The so-called non-titratable CO_2-complex reported earlier (6) was not found.

E. Adsorption of water and methanol by CO_2-evolving groups

Puri (12) also found, that for every mole of CO_2-complex present on the carbon surface (determined by CO_2 evolution) it was possible to adsorb one mole of water, and approximately one-half mole of methanol (12). As L-carbons are extremely hydrophilic, it is noteworthy that the L-carbon surface oxide has a one-to-one affinity for water (on a molar basis). The 1/2-to-one affinity for methanol makes a suitable explanation difficult to come by. The data, however, is summarized in Table 3.

F. Evolution of H_2O on high temperature outgassing

We have not discussed the evolution of H_2O on outgassing of activated carbons yet. There are two possible explanations as to why this is observed at elevated temperatures (up to 600°C) (7-11). Because of the recent controversy involving anomalous forms of water near solid surfaces (31-33), it is conceivable that some form of chemisorbed water which has remarkably high temperature stability is responsible for these observations (7-11). It is also possible that adjacent carbonyl groups could split off water to form cyclic acid anhydrides, as in phtahlic acid anhydride, although the temperatures involved are so high as to make this conclusion suspect.

TABLE 3

WATER AND METHANOL FIXED ON CARBON SURFACE RELATED TO CO_2 EVOLVED (12)

Carbon	CO_2 Evolved g/100 g	Water Fixed g/mole CO_2	Methanol Fixed g/mole CO_2
Sugar Charcoal, Original	14.72	19.2	15.3
Outgassed at 300°	7.90	19.3	14.6
Outgassed at 500°	3.52	20.1	16.7
Outgassed at 750°	nil	nil	nil
Cocoanut Charcoal, Original	8.45	16.9	14.6
Outgassed at 300°	6.91	15.3	15.3
Outgassed at 400°	1.23	18.2	15.7
Outgassed at 750°	nil	nil	nil

IV. "Geography" of the Surface Oxides

An important consideration with respect to surface oxides is the question of where on the surface are the oxygen functional groups formed, and in examining the question of "where", one may consider it a "microgeography" problem.

This question was essentially answered by Hennig (16) in one elegant, unambiguous experiment. He had previously examined the oxidation of single crystals of graphite using an electron microscope (15), and noted that molecular oxygen attack on graphite single crystals seemed, due to the extensive nature of such attack, to take place either (i) over the entire graphite surface, or (ii) at the edges of the layer planes alone (either to the extent of 10 monolayers, or at such highly irregular boundaries that they possessed a roughness factor of 10 times the linear dimensions resolvable by the electron microscope).

To resolve this problem, Hennig then employed electron microscope measurements of the alterations in positions of the edges of cleavage planes to show that molecular oxygen preferentially attacks graphite crystals at the edges of the layer planes, estimating the reactivity of the edge atoms to be at least 20 times that of the atoms within the basal planes (16). However, again, it seemed that the amount of surface oxide present after oxidation with O_2 was

excessive when compared to the number of edge atoms calculated to be present from the observable geometry of the crystal edges.

Hennig then (16) performed a measurement of the quantities of surface oxide formed (by measuring the amount of CO_2 + CO evolved at 900°C) both before and after cleaving a graphite single crystal five times. He observed that the same total amount of oxygen was bound by all of the surfaces of the cleaved crystal as was bound by the crystal prior to cleaving. Cleaving the crystal five times, of course, increased the surface area of the basal planes by a factor of six, while keeping the "edge" (prismatic planes) surface area constant. As the oxygen uptake did not increase upon cleavage, the oxygen had to be attacking solely the edge atoms (16).

While single crystals of graphite are not identical to active carbon on a macroscopic scale, on the microscopic scale they are somewhat similar. Active carbon is made up of very small microcrystallites with graphite-like structure. If the layer plane edges on single crystals of graphite are as irregular as was suggested by Hennig's work (16, 17), then one might suspect that the even less graphite-like active carbon microcrystallites would show at least as much, if not more, irregularity. Zarif'yanz et al. (13), using a graphite wear dust for which the particle sizes closely approximate those of finely powdered active carbon, and assuming that the reaction

with oxygen took place only at the edges of the layer planes, calculated (for one case) that the surface area of the prismatic planes was approximately 14 percent of the total BET surface area.

V. The Determination of Oxygen-Containing Surface Functional Groups by Indirect Methods

Nearly every type of functional group known in organic chemistry has been suggested as being present on the surface of activated carbon (3-13, 17, 29). The functional groups most often suggested are carboxyl groups (1), phenolic hydroxyl groups (2), and quinone carbonyl groups (3) (3-13, 17, 29).

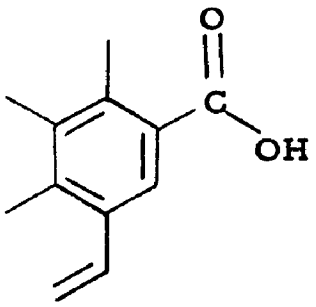

(1)

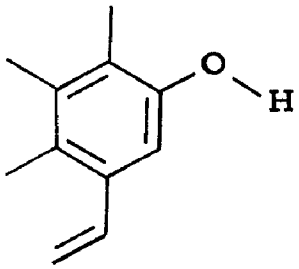

(2)

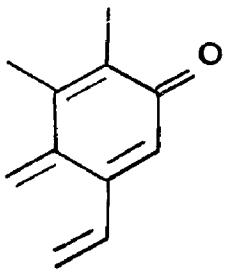

(3)

Slightly less often, there are suggestions of ether, peroxide and ester groups, in the forms of normal-(4) and fluorescein-like

lactones (5) (17), carboxylic acid anhydrides (6) (4, 19), and the cyclic peroxide (7) mentioned above (6).

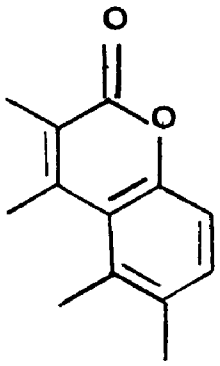

(4)

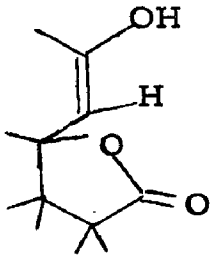

(5)

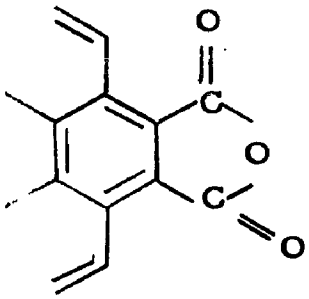

(6)

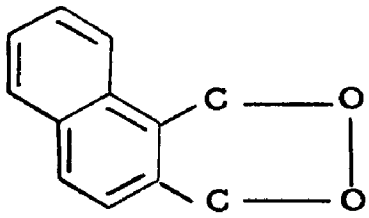

(7)

Because of the experimental difficulties involved in keeping H-carbons from exposure to atmospheric oxygen, there has been a marked lack of interest in the surface oxides of H-carbons. The interest in L-surface oxides is stimulated partially because it is easier to experimentally examine the L-carbon oxides then the H-carbon oxides because of the different relative acidities of the

various surface oxides. H-carbon surfaces are positively charged, and it is considered (26) that the "adsorption" of acid which they exhibit is partially the result of specific adsorption of anions at the positively charged surface, and subsequent secondary adsorption of protons and cations in the diffuse portion of the electrical double layer. It is difficult to indirectly study the actual surface functional groups of H-carbons, at least through acid-base interactions.

L-carbons, however, exhibit a wide range of acid-base interactions, due to a wide range of relative acid strengths of the surface oxides. Boehm et al. (3, 4) have done a considerable amount of work in this area, employing bases of widely differing strengths, in an effort to quantitatively measure and qualitatively identify the types of acidic surface oxides which are present on L-carbons. As the work of Boehm et al. (3, 4) is of major importance in this respect and serves to further subdivide the acidic surface oxides it will be examined closely here.

A. Multi-basic titrations of acidic surface oxides

Boehm et al. (3, 4) employed sugar carbons which were first activated with CO_2 at 950° C. These authors (3, 4) state that cooling under pure CO_2 followed by exposure to the atmosphere resulted in "... only basic surface oxides" (4). Several samples were partially "coked" by first heating them at 1100° C in pure

nitrogen. Oxidation in these cases (3, 4) was done in two ways; either by (i) exposure to oxygen during cooling or at 400 to 450° C for from 5 to 20 hours, or (ii) by oxidation in aqueous NaOCl, $KMnO_4$ or $(NH_4)_2S_2O_8$.

It seems that Boehm et al. (3, 4) chose to venture into a "Pandora's Box" by the selection of an activation temperature at the high end of the CO_2 evolution range and the low end of the CO evolution range which should be expected to result in very complicated surface structures, including both H- and L-surface oxides. The data of Steenberg (28) and Garten and Weiss (29) on sugar carbons (Figures 1 and 2) show that a temperature of about 500°C represents the transition point from L- to H-behavior. Aqueous oxidation of activated or coked sugar chars (4) results in a large amount of L-surface oxides, but as the material was previously activated at 950°C, the H-surface oxides would also be present.

In the work of Boehm et al (3, 4), four bases of widely differing strengths were used; $NaHCO_3$, Na_2CO_3, NaOH and $NaOC_2H_5$. The pK_a's of the conjugate acids of these four bases are 6.37 and 10.25 for H_2CO_3 and HCO_3^- respectively, and 15.74 and 20.58 for water and ethanol. In theory (34, 35) it should be possible to titrate acidic groups with each of these bases with pK_a values at least 2 to 3 units less than the conjugate acid of the

appropriate base. In practice, however, there are difficulties to be overcome with regard to the solvent. Presumably, although Boehm et al. (3, 4) do not mention it, the first three titrations are with aqueous suspensions of the carbon, and the ethoxide titration carried out with ethanol as the solvent. In aqueous solution, it is possible to titrate phenol with 0.05 N OH^- nearly stoichiometrically notwithstanding the acidity of the water (34, 35), but any weaker acid than phenol would not be neutralized completely in aqueous solution.

Thus, it would be possible to, using Boehm's (3, 4) procedure, titrate acidic surface oxides of pK_a's less than ~4.4, ~8.2 and ~10 in aqueous solution using HCO_3^-, $CO_3^=$ and 0.05 N OH^- respectively, while with the ethanolic ethoxide, it would be possible to stoichiometrically titrate a surface acidic group with a pK_a less than ~19.

Some of the neutralization results obtained by Boehm et al. (3, 4) are listed in Table 4. They (3, 4) noted that, in the case of "completely oxidized" carbons, the four bases often were neutralized in the ratio 1:2:3:4, as though to represent equivalent amounts of surface oxides in each of the four ranges of acid strength. This is, however, not a general conclusion and one does not observe that such relative concentrations exist for all activation conditions.

TABLE 4[a]

NEUTRALIZATION OF ACIDIC CARBON SURFACE OXIDES WITH BASES OF DIFFERING STRENGTHS

Sample	Base Consumed, meq/gram			
	HCO_3^-	$CO_3^=$	OH^-	$OC_2H_5^-$
Sugar carbon, coked, oxidized	0.42	0.82	1.24	1.65
Sugar carbon, activated, oxidized	0.21	0.43	0.71	0.89
Sugar carbon, heated to 450° only	0.27	0.50	0.81	—
Sugar carbon, activated coked, and oxidized with $KMnO_4$	0.30	0.45	0.63	0.81
Commercial carbon CK3, coked, then oxidized with persulfate	1.45	2.03	2.69	3.39
Commercial carbon CK3, coked, oxidized	0.14	0.27	0.39	0.70

[a]From Refs. (3, 4)

B. Carboxyl groups determined by acid-base behavior

The individual members, or pK_a groups, of Boehm's series will be examined in turn from the strongest to the weakest acids. The first two surface oxides, the HCO_3^- and $CO_3^=$ titratable groups, include a strongly acidic group ($pK_a \lesssim 4.4$) which can be neutralized by HCO_3^- and a somewhat weaker acidic group ($4.4 \lesssim pK_a \lesssim 8.2$), which cannot be neutralized by HCO_3^- but is neutralized by $CO_3^=$. Boehm (3, 4) suggests that these two may be a pair of adjacent carboxylic acids, a conclusion which appears to be well founded and is discussed later.

Table 5 lists the two pK_a values for several example dicarboxylic acids. Because of the aromatic nature of the graphitic ring structure of the active carbon, and the fact that the surface oxides are found at the edges of these rings, it is important to consider the pK_a values for the phthalic acid isomers. Only the o-phthalic acid, with its two adjacent carboxylic acids, shows a pK_a separation of the magnitude observed in the studies of Boehm et al. (3, 4), and o-phthalic acid has both values of the right absolute magnitudes as well. There is good reason for the separation of the pK_a's of adjacent carboxyl groups. Carboxylic acid groups separated by four or more carbons act like isolated carboxyl groups (30), while the inductive effect of adjacent carboxyl groups strongly affects the dissociation constant for removal of both of the protons.

TABLE 5

DISSOCIATION CONSTANTS OF DICARBOXYLIC ACIDS IN AQUEOUS SOLUTION. From Ref. (36)

Acid	pK_1	pK_2
o-phthalic	2.89	5.51
m-phthalic	3.54	4.60
p-phthalic	3.51	4.82
cyclohexane-1:1-dicarboxylic	3.45	6.11
malic	3.40	5.11
succinic	4.16	5.61
oxalic	1.23	4.19
malonic	2.83	5.69

While the first three samples of active carbon in Table 4 show nearly a 1:1 ratio of the first two acidic groups, those carbons oxidized in solution show a 2:1 ratio of these groups, perhaps indicating a significant increase in isolated carboxyl groups (3, 4). Heating of these solution-oxidized carbons was shown to remove the excess carboxyl groups, leaving behind the 1:1 ratio observed for 400° C oxidized carbons (3, 4). The notable ease with which carboxylic acids undergo decarboxylation on heating (30) also serves to help substantiate the carboxyl group assignment.

From the neutralization data of Puri (12) presented in Table 1, it was stated that approximately one-half of the total CO_2- evolving, OH^- neutralizable surface functional groups must have a pK_a in the range of 6 to 8, the other half being somewhat stronger. From the bicarbonate and carbonate neutralization scheme of Boehm et al. (3, 4) it can be seen that there appear to be carboxyl groups present which fit into two pK_a groups, one group with a $pK_a \lesssim 4.4$, the other with a pK_a between 4.4 and 8.2. Boehm et al. (3, 4), however, noted that additional NaOH was required over the $CO_3^=$ to titrate a group with a pK_a between 8 and 10. Thus there appears to be some discrepancy between the two workers' data, Puri finding the n-butylamine and NaOH-neutralizable groups equal; while finding a difference between NH_4OH and NaOH neutralizable groups; Boehm finding a difference between NaOH and $CO_3^=$ neutralizable groups.

However, as the base strengths of $CO_3^=$ and NH_4OH are not equal, little can be determined from these differences in neutralization data.

C. Identification of phenolic surface oxides through the reaction with NaOH

Boehm et al. (3, 4) have suggested that a phenolic-type hydroxyl group would fit well with the observed pK_a range for the group which was neutralized by NaOH but not $CO_3^=$. Phenol has a pK_a of 9.8; hydroquinone has a pK_a of 10.2, and the range of $8 \lesssim pK_a \lesssim 10$ was previously determined for the acid strength of this group. Garten, Weiss and Willis (17) suggested that phenolic hydroxyl groups were also responsible for the behavior of the titration curve, observed for carbon blacks. Villars (37) has also made the same observation and suggestion, although Garten et al. (17) and others (34, 35) have made the observation that it is not possible to titrate potentiometrically a mixture of phenol and carboxylic acid in aqueous solution, as no observable end-points (inflections) are ever found. Studebaker (38, 39) performed a non-aqueous titration on carbon blacks, as outlined by Moss et al. (34) for phenols, to solve this problem, but even under these conditions he only observed ill-defined end-points.

It is in the assignment of this OH^- titratable, non-$CO_3^=$-titratable group to phenol where the greatest controversy exists.

The presence of phenol-like OH groups has never been shown by infrared spectroscopy (18-20), and perhaps for this reason, most of the investigators who have made phenol assignments via pK_a data tend to suggest that the phenol is only present as part of a larger configuration. The phenolic hydroxyl group could be present as part of a lactone (3, 4, 17, 29) (Structures 4, 5) or an enol (17) (structure 8), and it is not likely to be an isolated hydroxyl group. The data of Hennig (15, 16) regarding the extent to which the edge

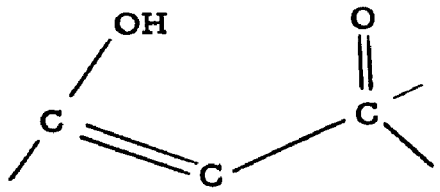

(8)

carbons become saturated with oxygen suggest that none of the functional groups present can be considered as unaffected by neighboring groups.

VI. Specific Chemical Identification of Surface Oxygen Functional Groups

A. Reaction with diazomethane

Studebaker et al. (38) studied the reaction of carbon blacks with diazomethane in an effort to determine and differentiate carboxyl and phenol groups. The reaction of a carboxyl group with diazomethane

(1)

produces a readily hydrolyzable ester, while that with alcohols or phenols (in the presence of an acid catalyst)

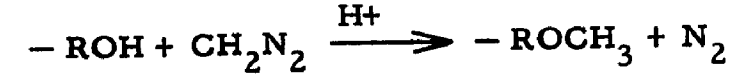

(2)

produces a non-hydrolyzable ether (30). With enols, the hydroxyl group is quantitatively converted, with no catalyst,

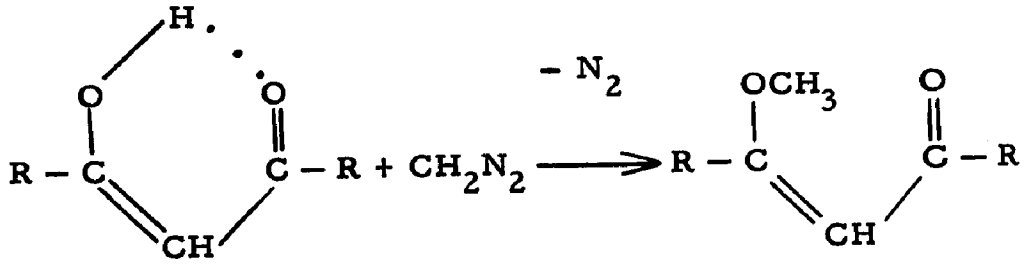

(3)

to the non-hydrolyzable ether (30, p. 693).

With unsaturated carbonyl compounds (i. e., quinones) (30, 38), diazomethane can react to form pyrazoline rings;

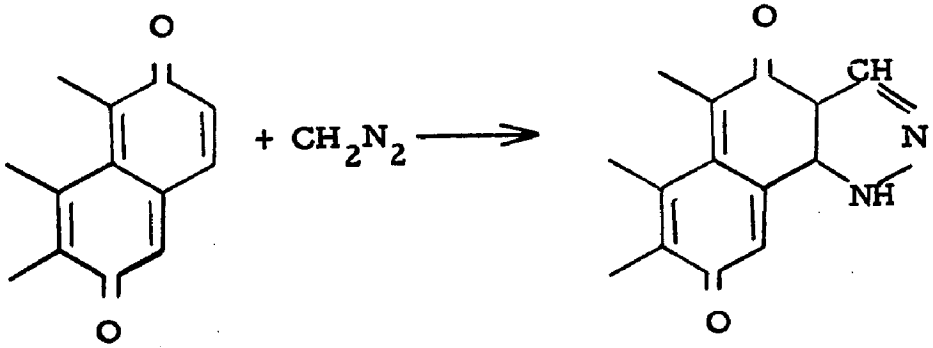

(4)

Studebaker (38) found that, upon reacting carbon black with diazomethane a portion of the methoxy groups could be readily hydrolyzed with HCl, while the remainder was unaffected. Elemental analysis also indicated uptake of nitrogen after treatment with diazomethane. He attributed the hydrolyzable methoxy content to esters formed with carboxyl groups, the non-hydrolyzable methoxy content to ethers formed with phenolic hydroxyl groups, and the increase in nitrogen content to the formation of pyrozoline rings with 1,4-quinone groups. The "phenol" content of twelve carbon blacks (38) accounted for from 5 to 15 percent of the surface oxides which reacted with diazomethane, "carboxyl" groups accounted for from zero to 65 percent of the reacting groups, and "quinones" from 37 to 90 percent of the reacting groups. A considerable amount of the chemisorbed oxygen, however, as determined (by difference) from elemental analysis was found to be completely unreactive to diazomethane (38). This unreactive oxygen amounted to from 45 to 75 percent of the total oxygen content of the carbon black. In one calculation, Studebaker (38) showed that approximately 18 percent of the total bound oxygen was present in quinone form.

Garten, Weiss and Willis (17) also employed methylation of carbon blacks to study surface functionality, and they extended their analyses to include several samples of sugar carbons. In nearly all

cases, the total methoxy content never equalled the amount of NaOH required to neutralize the acidic surface oxides. Their data is reproduced in Table 6.

Garten et al. (17), basically following the procedure of Studebaker (38), did note that the non-hydrolyzable methoxy ethers could be either phenolic or enolic hydroxyl groups (17). Contrary to Studebaker's (38) conclusion that hydrolyzable methoxy esters were the result of carboxylic acids reacting with diazomethane, Garten et al. (17) suggested that the surface group is a lactone ring of the phenolphthalein type (Structure 5). Their suggestion is based on several observations: (i) that a fluorescein or phenolphthalein-like lactone (5) would react with CH_2N_2 to give an ester, while a normal lactone (4) would not, (ii) that the titration curve of a carbon black (17, 37) does not show an end-point in aqueous solution, thus suggesting a pK_a comparable to phenol (phenolphthalein has a pK_a of 9.9), and (iii) transmission infrared data of Garten et al. (17) showed a band at 1760 cm^{-1} which is found for this type of lactone. They (17) also suggested that the difference in NaOH uptake and hydrolyzable methoxy groups was due to the presence of normal lactones (4), a speculation which had very little basis in fact at that time, and is still questionable.

Table 6[a]

Effect of Temperature and Oxidation on the Acidic Properties of Carbons and the Reaction with Diazomethane

Treatment	NaOH required meq/gram	Total $-OCH_3$ meq/g	Non-hydrolyzable $-OCH_3$ meq/g	Hydrolyzable $-OCH_3$ meq/g	NaOH req'd minus total OCH_3 meq/g
Sugar char, heated in air to					
400°C	0.59	0.11	0.05	0.05	0.48
500°C	0.22	0.09	0.05	0.05	0.13
600°C	0.14	0.02	0.01	0.01	0.12
700°C	0.14	0.09	0.05	0.05	0.05
800°C	0.13	0.08	0.06	0.06	0.05
Sugar char, heated in air to 800°C then reoxidized at					
400°C	0.32	0.15	0.05	0.10	0.17
500°C	0.27	0.15	0.04	0.11	0.12
600°C	0.22	0.15	0.04	0.11	0.17
700°C	0.18	0.15	0.03	0.12	0.03
"Carbolac 1" original	1.99	1.46	0.56	0.90	0.42
"Carbolac 1", heated in N_2 at					
400°C	1.74	1.38	0.45	0.93	0.36
500°C	1.54	1.22	0.52	0.70	0.32
600°C	1.06	0.81	0.32	0.49	0.25
700°C	0.61	0.58	0.12	0.46	0.30
800°C	0.43	0.42	0.08	0.34	0.10

[a]Reproduced from Ref. (17), by Permission of Australian J. Chem.

In Table 6, for the sugar carbons, the NaOH neutralization shows just the temperature behavior expected (28, 29). What is very difficult to justify (17) is the lack of variation in the hydrolyzable methoxy content as a function of treatment temperature. If the hydrolyzable methoxy groups were due to carboxyl groups, decarboxylation at temperatures above 600° C should reduce these carboxyl contents to zero. Such is not the case as shown in Table 6. The only set of data, other than the NaOH neutralization, which shows the expected decrease in reactivity with increasing temperature is the last one, the so-called "unreactive" acidic surface oxides! The data of Table 6 does not seem to coincide with the data of any other investigator, and perhaps should be treated with caution in that respect.

Boehm (4) tried a slightly different approach to the methylation experiment. He reacted sugar carbons with CH_2N_2 and followed this by hydrolyzing the ester methoxyl groups with HCl, and measuring the change in NaOH uptake before and after the experiment. Two representative samples of this experiment are shown in Table 7.

It is evident from the data of Table 7 that the formation of non-hydrolyzable methoxy groups blocks the reaction of the group normally titratable with NaOH and unreactive to $CO_3^=$, while leaving unaffected the more acidic groups which react

TABLE 7[a]

BASE CONSUMPTION OF SUGAR CARBONS BEFORE AND AFTER METHYLATION FOLLOWED BY HYDROLYSIS

Sample	Base Consumed		
	$NaHCO_3$	Na_2CO_3	NaOH
Sugar carbon, coked, oxidized, before	0.42	0.82	1.24
Sugar carbon, coked, oxidized, after	0.40	0.84	0.81
Sugar carbon, activated, oxidized, before	0.21	0.43	0.71
Sugar carbon, activated, oxidized, after	0.21	0.41	0.42

[a]From Refs. (3, 4)

with $CO_3^=$. All of the evidence presented thus far suggests that the non-hydrolyzable reaction of diazomethane with carbon is a result of the reaction with a phenolic or enolic hydroxyl group.

This presents one major question. How does one explain the fact that Puri (7-12) observed an equivalence between the evolution of CO_2 and the neutralization of a carbon with NaOH, while Boehm (3, 4) has shown that part of the surface oxide neutralized by NaOH is either a phenolic or an enolic hydroxyl group, which certainly would not be expected to desorb as CO_2. The strength of bases employed by Puri (12) indicate that the pK_a of the weaker portions of the NaOH neutralizable groups lies between 6 and 8. Boehm's titrations suggest a pK_a between 8 and 10. Apparently, the pK_a of the acidic hydroxyl group of interest is somewhere around 8, most likely on the high side, as Puri's (12) neutralization may include some weakly acidic carboxyl groups along with the acidic hydroxyl group. An enol would not be expected to readily decarboxylate, but it is a slightly stronger acid ($pK_a \sim 9$) than a phenol. Acetyl acetone (2, 4-pentanedione) at equilibrium is normally 85 percent in the enol (30) form and it readily forms strong metal chelates with polyvalent metal cations. The chelation is so strong that the whole complex can be volatilized without decomposition in a gas chromatograph. This chelating behavior may be related to the process used in gold refining, in which

activated carbon is employed as an adsorbent for the gold. Chelation behavior in activated carbons has not been carefully investigated; perhaps the suggestion of the presence of 1,3-diketones will provide some ground for such study.

B. Reaction with organic functional group reagents

1. Aldehydes and ketones. — Studebaker (38) attempted to test for the presence of carbonyl groups (as aldehydes or ketones) using the reagent 2,4-dinitrophenylhydrazine. He observed very little reaction (38), amounting to perhaps 2 percent of the total combined oxygen on a sample of Spheron 9, a carbon black. No sugar carbons were tested.

Boehm et al. (4) had suggested that the reaction which they had observed with ethanolic ethoxide, but not with NaOH, was the formation of a hemiacetal with an aldehyde carbonyl. Certainly the reaction does not fit in with the normal acid-base neutralization reactions if this is assumed to be the case, although the reaction might be possible. Reaction with acetyl chloride, which should acetylate alcohols, phenols and carboxyl groups, showed that the ethoxide reaction was not a neutralization of an alcohol, as the acetylation only occurred to the same extent as the NaOH neutralization. Boehm's group tried several specific carbonyl reagents but had no success in relating the amounts of carbonyl groups reacting with identification reagents to the ethoxide reaction.

2. Phenols and enols. — Boehm et al. (3, 4) also carried out qualitative tests for phenols. They (4) employed 2, 4-dinitrofluorobenzene and p-nitrobenzoyl chloride as reagents for phenolic hydroxyl groups. While these reagents will also react with enols, they do not react with carboxyl or carbonyl groups, or with alcohols or even with very weakly acidic phenols. They obtained complete agreement between the amounts of either 2, 4-dinitrofluorobenzene or p-nitrobenzoyl chloride and the difference between NaOH and Na_2CO_3 neutralization quantities.

3. Carboxylic acids. — Additional data was presented by Boehm et al. (4) for the specific identification of carboxylic acids. The weaker carboxyl group, titratable with $CO_3^=$ but not HCO_3^-, was shown (4) to be equivalent to the amount of chloride taken up from reaction with thionyl chloride and subsequently hydrolyzed. Reaction of the stronger of the two types of carboxyl groups with thionyl chloride apparently formed the anhydride, rather than the acyl chloride, suggesting that the stronger of the two carboxyl groups, at least, consists of adjacent carboxyl groups (3, 4). This was also demonstrated by a decrease in the amount of NaOEt required to neutralize the surface, corresponding to one-half the $NaHCO_3$ titer.

Reaction with ammonium hydroxide (3, 4) gave the same result as obtained by Puri (12), and it only appeared to react with the $NaHCO_3$ neutralizable carboxylic acid.

Conversion of carboxylic acids to acyl chlorides, followed by reaction with dimethylaniline and $AlCl_3$ in nitrobenzene, on a carbon which had been wet-oxidized to give a 2:3:4:5 ratio of the four titrants, caused the neutralization values to drop to 1:2:3:4, as though the excess carboxyl groups had participated in a Friedel-Crafts reaction (30).

C. Polarographic identification of quinone surface groups

Hallum and Drushel (40) analyzed a carbon black polarographically. They had carefully extracted their sample to make sure that they were not reducing extractables normally found in the carbon black. The polarogram showed only one reduction wave, rather than the two expected for a 1, 4-quinone, but it did appear that the wave was at the appropriate reduction potential (-0. 68V) for a quinone. On electrooxidation of the same samples, a wave appeared at about +1. 00 V, and Hallum and Drushel assumed this to be the oxidation wave of the hydroquinone. The cathodic wave was seen to disappear completely (40) after reduction with $LiAlH_4$ or MeMgI, and the anodic wave to disappear upon treatment with hydrogen peroxide or diazomethane. Both waves disappeared after heating the carbon blacks to 1950°C. This polarographic data of Hallum and Drushel

appears to have been bolstered recently by a paper describing essentially identical results by Jones and Kaye (41) on samples of activated carbon.

D. Chemical reduction of surface oxides

Reduction of a carbon surface by Clemmenson reduction, Zn(Hg) + HCl, should reduce all of the above mentioned groups to saturated aromatic rings. Boehm et al. (4) found that the quantities of all of the groups were reduced by this procedure, but not completely to zero in each case. Two examples are given in Table 8. Reduction with $LiAlH_4$ or $NaBH_4$ will not normally reduce carboxylic acids, but should reduce phenols, quinones and carbonyls (30). Both of these reductions have been employed in several literature references (i. e., 3, 4, 29, 40) but the results do not agree with any of the previous assignments. For example, in Table 8, $LiAlH_4$ and $NaBH_4$ are seen to reduce group II of Boehm et al. (4), which has been identified above with carboxyl groups, while not reducing group III, supposedly of phenolic character. These results are a cause for concern.

TABLE 8

CHANGE IN THE QUANTITY OF ACIDIC GROUPS AFTER REDUCTION OF THE ACIDIC SURFACE OXIDES. From Ref. (4)

Product	Reduced with	Change in groups (b)			
		I	II	III	IV
SC3, coked, ox. (a)	———	(20)	(21)	(1)	(20)
	Zn/HCl (at 20°C)	+18	-19	-1	-19
SC3, act. ox.	———	(60)	(46)	(61)	(47)
	Zn/HCl (at 20°C)	0	0	-16	-13
	Zn/HCl (at 100°C)	-11	-15	-10	-18
	$LiALH_4$	0	-11	0	-14
	$NaBH_4$	0	-21	-3	-11

(a) This product was obtained by rapid quenching of oxidized sugar charcoal. Practically no groups III were formed during this treatment.

(b) The values in brackets give the content (meq./100 g) in the starting material; the figures without brackets are the changes after reduction.

VII. Direct Identification of Surface Functional Groups by Infrared Spectroscopy

The techniques and experimental considerations involved in obtaining spectra of carbonaceous materials are reserved for discussion in Chapter 3. In this chapter, the essential results of the applications of transmission (17, 38, 40, 42, 43) infrared spectroscopic measurements are examined, the emphasis being on the assignment of the various absorption bands observed.

Brown (42) and Friedel and Queiser (43) examined the transmission spectra of some thin films and mulls of carbonaceous materials. Figure 3 reproduces the spectra of Friedel and Queiser (43) of sucrose and cellulose chars. The sucrose char was prepared (43) under hydrogenation conditions (2500 psi H_2, tin catalyst), while the cellulose chars were obtained from Smith and Howard (44). The carbon contents of these chars are not high, and for this reason they do not adequately represent the type of material obtained after carbon activation, but the band assignments for these chars are instructive. The sucrose char contained 72.1%C, the 190°C cellulose char 45.3% C, the 250°C cellulose char 71.5% C, and the 400°C cellulose char 85.6% C (43, 44).

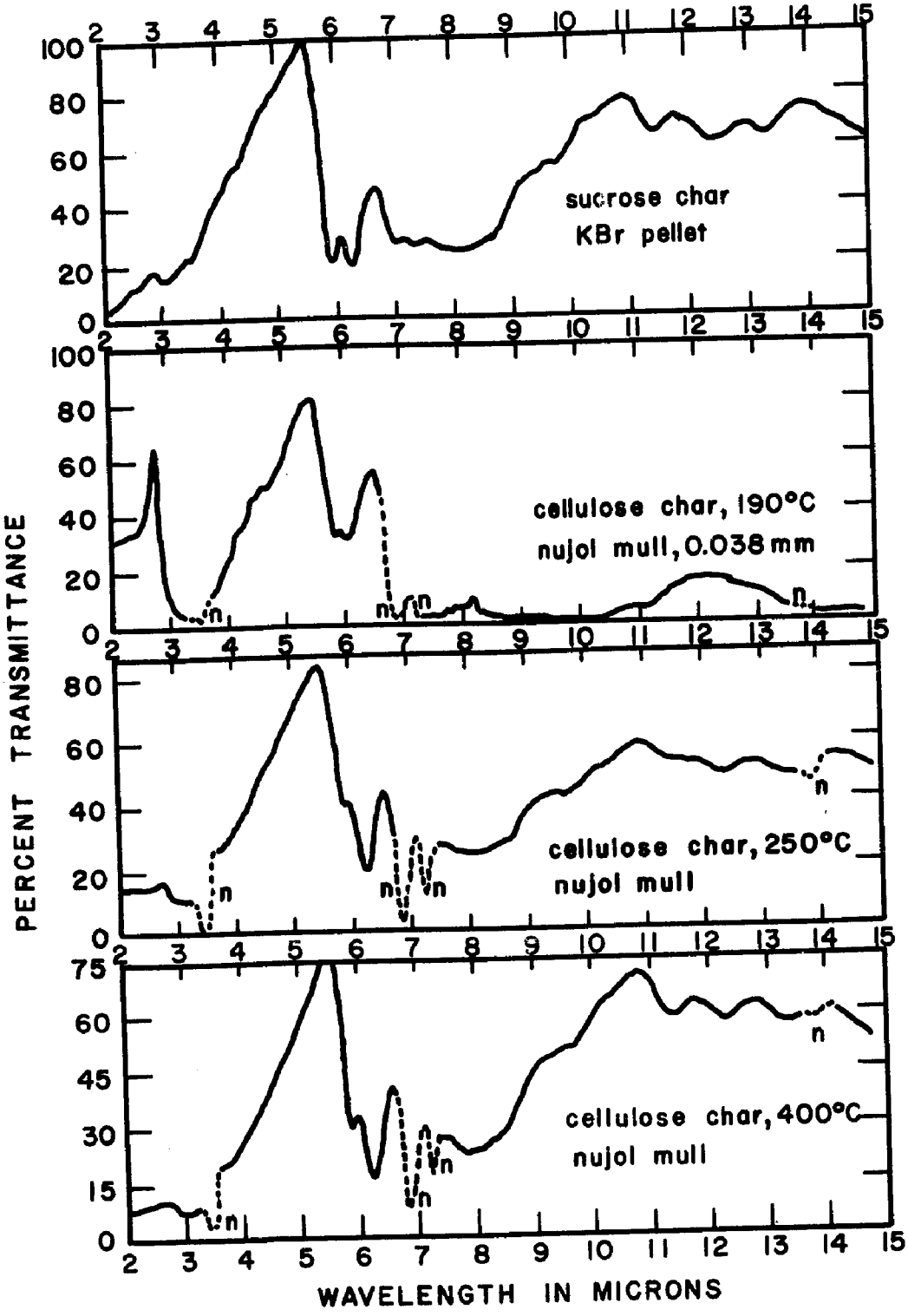

Fig. 3.--Infrared Spectra of Carbohydrate Chars. From Ref. (43).

Certain of the regions of an infrared spectrum are obscured when Nujol (mineral oil) is used as a mulling agent; these are the CH_2 and CH_3 band positions of 2950-2825 cm^{-1}, 1450-1350 cm^{-1}, and ~720 cm^{-1} (3.4-3.55 μ, 6.9-7.4 μ, and ~13.9 μ; as Friedel and Queiser (43) used wavelength rather than wavenumber, the conversions are supplied in the cases where the reproduced figure is in wavelength). With KBr pellets, the 3700-3300 cm^{-1} (2.7-3.0 μ) region is obscured by water adsorbed on the KBr.

In the sucrose char (72.1% C), bands are observed at 3330 cm^{-1} (3.0 μ), 1700 cm^{-1} (5.87 μ), 1605 cm^{-1} (6.19 μ), a broad absorption from about 1415 to 1150 cm^{-1} (7.0 to 8.7 μ), and weak bands at 860 cm^{-1} (11.64 μ), 830 cm^{-1} (12.25 μ) and 750 cm^{-1} (13.29 μ). These bands were assigned by Friedel and Queiser to hydrogen-bonded OH, C=O, a conjugated quinone-like carbonyl group, [aromatic C-O, actually assigned by Friedel and Queiser to absorption at 1250 cm^{-1} (8.0 μ), but freely interpreted here], and three aromatic CH bands respectively. There could be some discussion of the assignment of the 3330 cm^{-1} band to hydrogen bonded OH, but they (43) noted that this band was stable to heating to 370° C in some coal residues, suggesting (43) that it was not water.

In the series of cellulose chars, the 190°C char is apparently nearly identical to the starting material (43), and it shows the same bands as the sucrose char (above it, Figure 3). As the char is heated from 190°C (45.3% carbon) to 250°C (71.5% carbon), the relative intensities of the 1700 and 1605 cm^{-1} bands change, with the lower energy band becoming more intense. The fine structure in the 1400-1000 cm^{-1} (7 to 10 μ) region of the 190°C char becomes identical to the broad band observed for sucrose char when the cellulose is heated to 250°C. Finally, at 400°C, the cellulose char (Figure 3) takes on the aromatic structure of the sucrose char (860, 830, and 750 cm^{-1} bands), while retaining the OH, C=O, conjugated C=O, and aromatic C-O bands.

Hallum and Drushel (40) obtained some transmission spectra of carbon black, before and after methylation with diazomethane (for a discussion of this procedure, see Section VI. A). Their spectra are reproduced in Figure 4. They (40) observed only one distinguishable band in the spectrum of the untreated channel black, that a band at 1600 cm^{-1} (6.3 μ), which they attributed to either (i) aromatic C-C vibrations, or (ii) conjugated, hydrogen-bonded carbonyl groups (40), similar to the assignment by Friedel and Queiser of the (43) 1605 cm^{-1} band of carbonaceous chars. Hallum and Drushel (40) point out that their attempts to obtain transmission

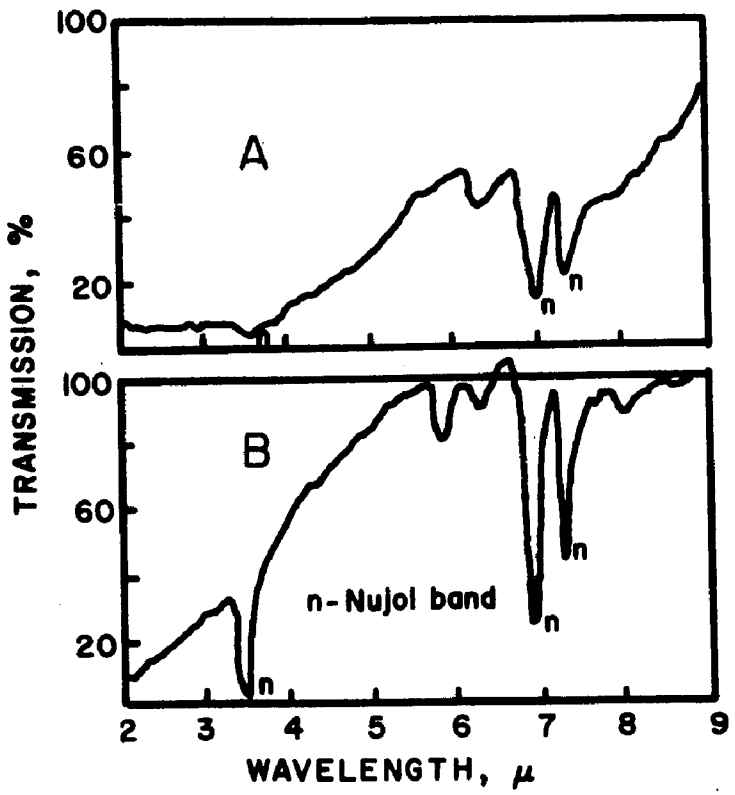

Fig. 4.--A, infrared spectrum of untreated channel black of 8-10 mμ diameter; B, infrared spectrum of the same black after treatment with diazomethane. From Ref. (40).

infrared spectra of carbon blacks were, in general, unsuccessful due to scattering and high light losses. Only this fine (8-10 mμ dia. particle size (40)), highly oxidized carbon black yielded a spectrum, and we would assume that the carbon content of this sample is low, perhaps no greater than 75 to 80 percent (this information was not given in Ref. (40)). After methylation of the carbon black (40), the observed band split into two bands, one at 1700 cm^{-1} (5.85 μ), and the other unchanged at 1600 cm^{-1}. Also observed was the formation (Figure 4B) of a weak band at about 1250 cm^{-1} (8 μ). Methylation of a conjugated carbonyl is shown in reaction (3). This results in the formation of a non-hydrolyzable ether, no longer showing any hydrogen-bonding to the β-carbonyl oxygen (30, 40). The interpretation of Hallum and Drushel's spectrum B in Figure 4 is (40) that [some of] the conjugated, hydrogen bonded carbonyl groups [enols] were methylated to form the β-keto enol ether (reaction 3), thus shifting the position of the 1600 cm^{-1} band to the "normal" 1700 cm^{-1} position expected for a carbonyl oxygen (45). The carbonyl band for this (45) should appear at about 1650 cm^{-1} (~6.06 μ), which is close to the position of the band observed by Hallum and Drushel (40). The band at 1250 cm^{-1} in the methylated carbon black (40) may be due to the methoxy group C-O stretching vibration.

Garten et al. (17), while noting the difficulties inherent in obtaining transmission spectra of carbons, were able to get some results in the 1500-2000 cm^{-1} region of the spectra of some carbon black and activated sugar carbon samples. These are reproduced in Figures 5 and 6. As shown in the left-hand side of Figure 5, Garten et al. (17) obtained the spectra of a carbon black, "Carbolac 1", (a highly acidic carbon black, see Table 6, Section VI. A.) as a function of the temperature of the heat treatment they employed (17). Of the two bands observed, at 1760 cm^{-1} and 1600 cm^{-1}, only the 1600 cm^{-1} band is apparent after heating the sample to 700°C, and after heating to 800°C, neither band is significant (17). The 1600 cm^{-1} band corresponds to that observed by other investigators (40, 43), but the 1760 cm^{-1} band definitely does not. On the right side of Figure 5 the spectra of "Carbolac 1" after methylation, subsequent hydrolysis, and the spectrum of the "sodium salt" of the carbon black (after neutralization by NaOH) are reproduced (17). Methylation (17, Fig. 5) of "Carbolac 1" apparently (17) results in a change in the relative intensities of the 1760 and 1600 cm^{-1} bands, according to Garten et al. (17), which they claim is similar to that which is observed (46) on methylation of humic acids. It does not appear, from what we can see in Figure 5, that any significant change in relative intensities is evident, and upon comparison with

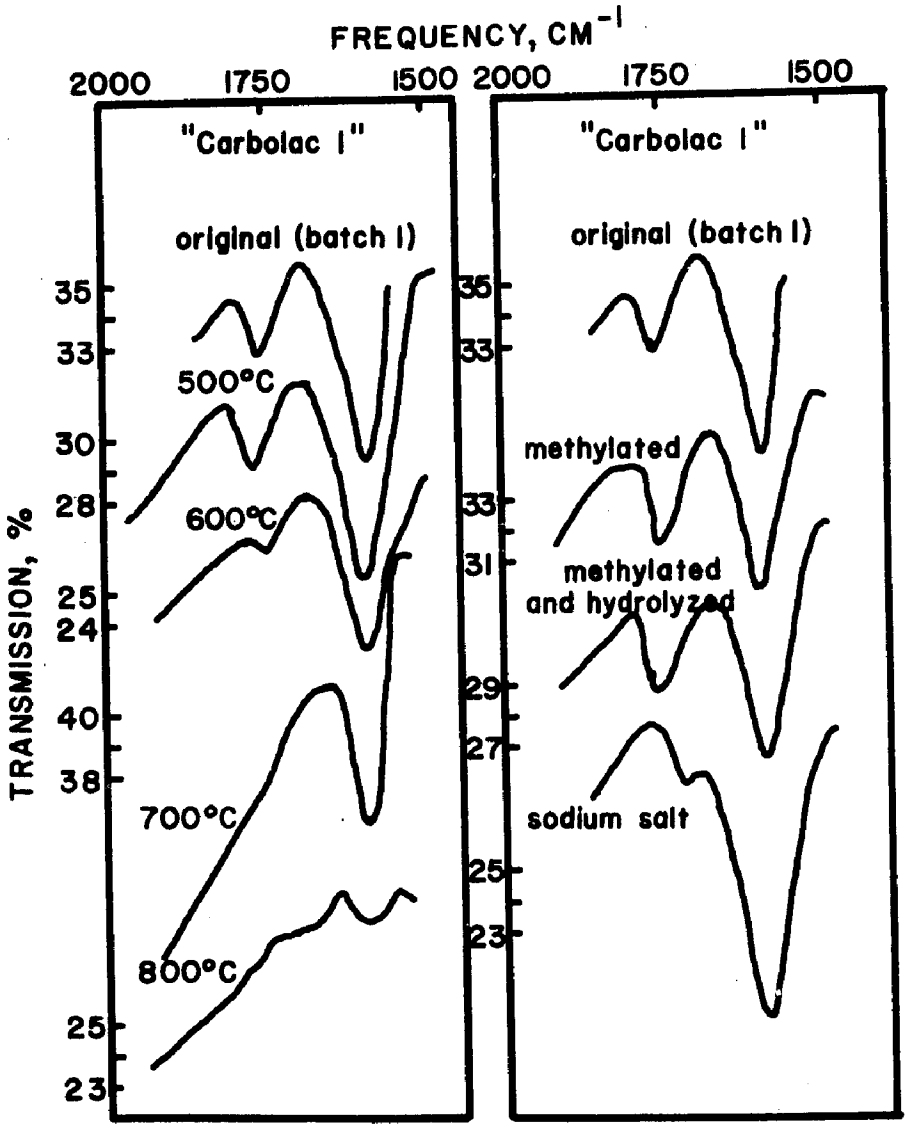

Fig. 5.--Infrared spectra of "Carbolac 1" and a series of derivatives prepared by heat treatment and reactions with diazomethane and alkali. From Ref. (17).

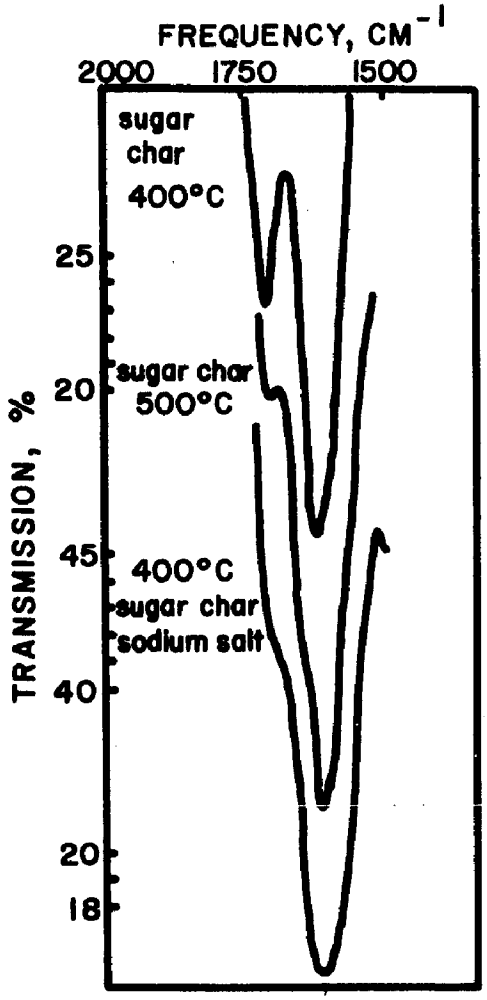

Fig. 6.--Infrared spectra of a series of sugar carbons. From Ref. (17).

Figure 4, it is noted that formation of a 1700 cm^{-1} band after methylation does not seem to take place, in direct contradiction to the observation of Hallum and Drushel (40). Hydrolysis of the methylated product also appears to have no effect on the 1760 and 1600 cm^{-1} bands (17) of Figure 5. The spectrum of the sodium salt of "Carbolac 1", however, does show an interesting characteristic. The 1600 cm^{-1} band shifts [ever so slightly] to 1590 cm^{-1} and broadens (17) [somewhat]. Garten et al attribute this to formation of a carboxylate anion, which should absorb around 1550-1610 cm^{-1} (45), which could account for the observed [?] shift (17). However, the formation of a weak band at 1720 cm^{-1} in the sodium salt of the carbon black, which may be due to a normal carbonyl group, is not explained by Garten et al (17). They (17) contend that the NaOH neutralizes f-lactone groups (5), which should give rise to quinone carbonyl groups (17), with a corresponding absorption at about 1680 cm^{-1} (not observed by Garten et al (17)). In order to account for this, Garten et al. (17) proposed reaction (5) with unsaturated n-lactones which would

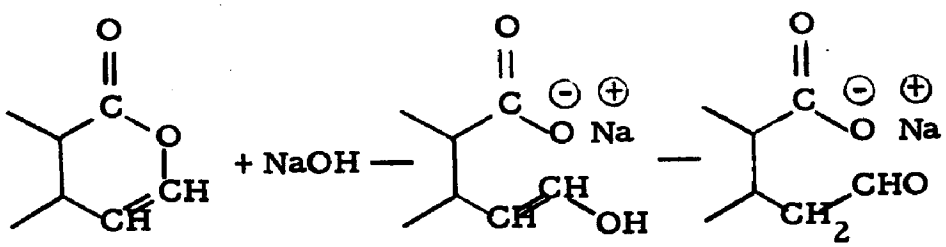

(4) (5)

account for both the formation of a carboxylate anion and a normal carbonyl group in the form of an aldehyde. These "conclusions" [see quotation in introduction] of Garten et al. (17) rapidly diminish in credibility after an examination of Table 6, Section VI. A., where original "Carbolac 1" batch 1 is supposed to have more than twice as much "f-lactone" (5) as "n-lactone" (4) (17). The infrared data and the neutralization and methylation data simply do not agree with the lactone interpretation (17).

In Figure 6, Garten et al. (17) presented the spectra of sugar carbons activated and oxidized at 400°C and 500°C, as well as the sodium salt of the 400°C activated sugar carbon. In agreement with the "observation" made on "Carbolac 1" from Figure 5, the higher activation temperature (500°C) favors the increase in relative intensity of the lower energy band. The bands here (Figure 6), however, are found at 1625 cm^{-1} and 1705 cm^{-1}, in closer agreement with those observed by other workers (40, 43). The 1705 cm^{-1} band may correspond to a normal carbonyl group (17, 40, 43, 45). The disappearance of the 1705 cm^{-1} band after neutralization by NaOH, however, requires an explanation. Garten et al. (17) proposed reaction (6) with n-lactones to explain this phenomenon.

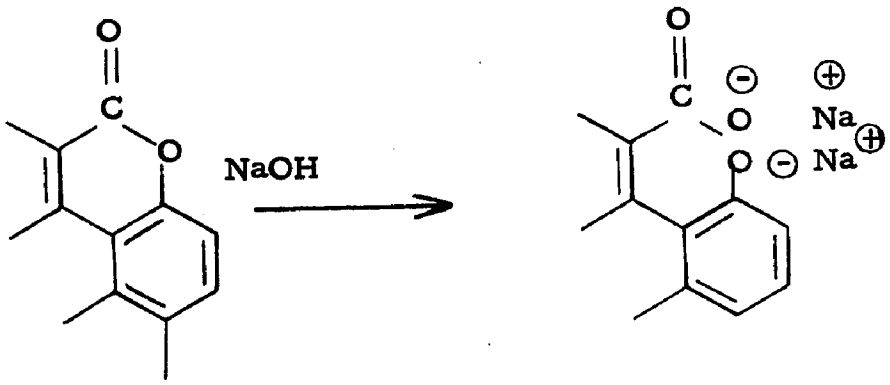

(6)

According to Garten et al. (17), the neutralizable acidity of the 400° C activated sugar carbon was nearly all due to "n-lactones", but this does not explain the discrepancies in Figure 5 mentioned above.

It should be pointed out that no "normal" quinone bands have yet been observed in transmission spectra of carbons, yet the polarographic data of Section VI. C. seemed to positively identify such structures. Also, we would like to suggest that the "lactone-juggling" employed by Garten et al. (17) to explain the various discrepancies in their data does not satisfactorily explain the facts (17, 40, 43).

CHAPTER 3

INTERNAL REFLECTION SPECTROSCOPIC (IRS) DETERMINATION OF SURFACE FUNCTIONAL GROUPS

The basic principles involved in the application of internal reflectance techniques to the study of carbon surfaces are discussed in some detail in this chapter. The reasons that good IRS spectra are easier to obtain than transmission spectra involve the facts that IRS exhibits none of the scattering effects or large light losses common to transmission spectroscopy. Friedel and Queiser, for example, employed a fogged salt plate in the reference beam in an attempt to duplicate the scattering of the carbonaceous particles in the sample beam (43); and it can be seen from Figure 3 that this technique is not notably effective. Garten et al. (17) discussed the difficulties due to scattering in the short wavelength (2-5 μ) region, and in fact were only able to obtain usable spectra on a small percentage of their samples. These problems do not occur with internal reflection spectroscopy (IRS).

I. Experimental

Previous efforts (17, 40, 42, 43) to obtain infrared spectra for carbon black, activated carbon and coal have involved transmission measurements on prepared KBr pellets or Nujol mulls. Although some information regarding structure of the bulk materials has been gained in this manner, transmission techniques have proven rather unsatisfactory for identification of the surfaces of carbon materials because of invariably poor resolution. Ergun (46) and Foster and Howarth (47) have shown that the extinction coefficient of graphite in the infrared spectral range is very high, approaching that of a metal. The average extinction coefficient, k, is about 0.66 in the visible region (46), and varies from about 0.8 to 1.5 through the 1 to 10 μ region of the infrared (47). Common organic compounds or functional groups exhibit extinction coefficients approximately two orders of magnitude smaller than that of graphite, and therefore transmit sufficient radiation to give infrared spectra of reasonable contrast. From the IRS spectral studies of active carbon reported here, it appears that the bulk extinction coefficient of this material is approximately that of graphite. On this basis it is reasonable to conclude that light cannot be transmitted through particles of carbon unless they are extremely thin, in fact, light of 5 micron wavelength will decay to 1% of its initial value after

passing through 3.7 microns of graphite. Thus, infrared light incident upon most microcrystals of active carbon will be totally absorbed, unless it hits at a sufficiently grazing angle to allow the light to be reflected from the particle.

In view of the magnitude of the extinction coefficient for active carbon it appears that the attempts reported in the literature to obtain transmission spectra of this material in KBr or Nujol have actually involved measurement of a complicated type of mixed transmission and reflection spectrum. This type of spectrum results from a combination of forward scattered radiation which misses the particles entirely, as illustrated in Figure 7, as well as radiation which passes through extremely small particles. The resulting spectrum is referred to as a "diffuse reflectance" spectrum (48). This approach to examining the surface of a material such as active carbon is complicated by the fact that light losses due to scattering are inversely proportional to the fourth power of the wavelength, producing huge scattering losses at shorter wavelengths.

It seems obvious that reliable infrared spectra would, in conjunction with indirect observations such as adsorption studies (49, 50), help investigators correlate the nature of surface functionality with heterogeneous adsorptive characteristics and chemical reactivity of activated carbon and carbon black.

Fig. 7. --Forward Scattering Spectrum

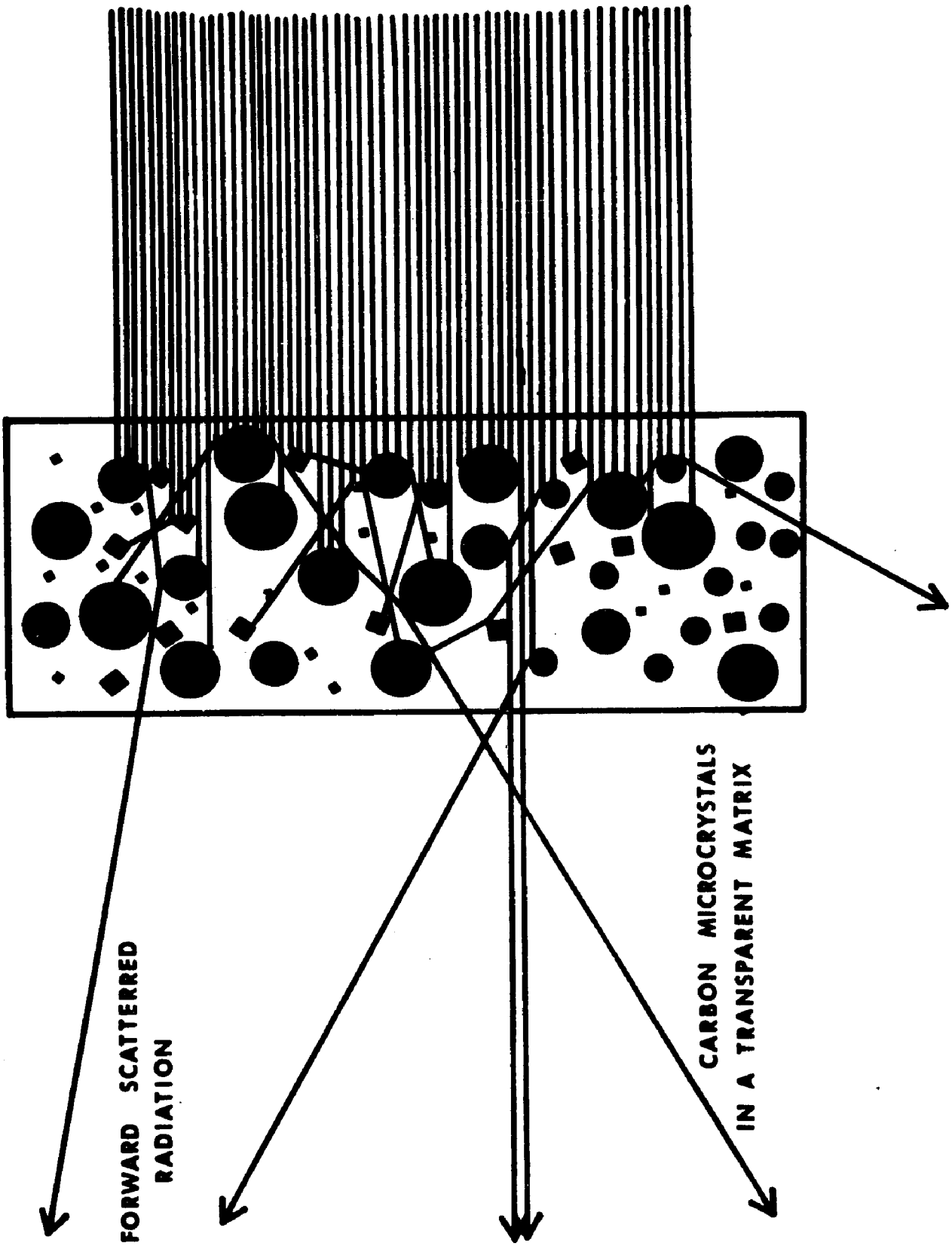
FORWARD SCATTERRED RADIATION
CARBON MICROCRYSTALS IN A TRANSPARENT MATRIX

In the case of bulk carbons, with a typical extinction coefficient (47) of about 0.7, the incident beam in a transmission spectrum arrangement will decay to about 1% of its original intensity after passing through a particle only 3.7 μ thick. As a net result of scattering and large extinction coefficients, attempts to obtain transmission spectra of absorbing powders have resulted in diffuse reflectance spectra. Diffuse reflectance spectra and their complications have been treated by Wendlandt and Hecht (48). It also must be recognized that diffuse reflectance spectra are difficult to interpret accurately, since they will show the influence of bulk characteristics to some degree, and of external reflectance spectra of the surface to some extent, rather than selectively sample one or the other (48). Through the use of internal reflection spectroscopic techniques, these problems are eliminated. However, certain new complications then arise which must be taken into account before using IRS in the study of surfaces of absorbing powders; these are reviewed in the Appendix. While transmission and diffuse reflectance spectra are affected primarily by sample size and extinction coefficient, IRS has several more variables involved which can affect the contrast of a spectrum. These are discussed fully by Harrick (51).

The effect of depth of penetration (51) is extremely important in the IRS spectra of powders. When the rarer phase includes a powdered sample, it becomes a complex mixture of air and irregularly shaped absorbing particles. If one were able to obtain a spectrum of a homogeneous sample in optical contact with the IRS crystal, one would obtain high-contrast spectra with a minimum of reflections, owing to the magnitude of the interaction at the crystal-sample interface. With powders in a supporting medium making up the rarer phase, the interaction at the air-particle interface is generally much smaller than that for homogeneous samples (Appendix), and the resulting reflectance losses are much smaller. This is described by Harrick (51) as the result of the packing characteristics of the powder.

In internal reflection spectroscopy, it is customary to use a non-absorbing ($k = 0$) material as phase 1, the internal reflection element. In the infrared region, KRS-5, AgCl and AgBr fit this description. These materials are used extensively in IRS since they are transparent over the entire infrared region (51). These materials have relatively low refractive indices, however, and for carbon powders with refractive indices anywhere from 1.6 to 4 (47), such low refractive index internal reflection elements (2.0-2.4) prove unsuitable, as they preclude internal reflection for some

samples over large regions of the infrared spectrum. Silicon ($n = 3.5$) and germanium ($n = 4$) would be the best IRE choices for use with carbon powders. Germanium has lattice bands starting at about 12 μ, but by using a carefully matched pair of Ge crystals, reliable spectra can be obtained from 2.5 to 15 μ (4000-667 cm^{-1}). It is quite possible that Ge crystals in this double beam arrangement could be used out to 25 or 30 μ, but the energy losses in both beams due to absorption by the Ge are so high beyond 15 μ that the spectrophotometer response becomes too slow for satifactory use. It is also very difficult to optically balance a pair of Ge crystals in the high absorption region beyond 12 μ. Silicon IRE crystals have not been used because of two reasons: (i) Si probably could not be used much beyond 6 μ because of lattice vibration bands similar to those in Ge, and (ii) Si has a refractive index of 3.5, less than the Ge refractive index of 4, making the Ge the more versatile IRE in that it can assure total reflection even for graphite ($n_{graphite} = 3.5$ at $\lambda = 8$ μ) (47).

For these studies, several different IRS geometries have been employed, varying the IRE's, the angle of incidence, and the number of reflections. Some of the spectra were obtained with germanium, varying the angle of incidence between 45° and 60°, and KRS-5 was used between 50° and 60°. (In each case, the pertinent data is listed in the figure caption.) A pair of Wilks

Scientific Model 9 IRS attachments (Wilks Scientific Corp., South Norwalk, Conn.) were used in a Perkin-Elmer Model 621 infrared spectrophotometer for the spectra reported in this chapter. Using the Wilks Model 9 IRS accessories, the Wilks MIR-29 powder sample holders were found to be the best holders available, because the crystal is held firmly and reproducibly in place in the light beam. With the MIR-29's it is possible to first obtain a baseline spectrum, remove the sample holder from the spectrometer, fill the powder holder, and replace the crystal-sample holder in the instrument without disturbing the optical arrangement. One can then run a spectrum of the powder without losing the optical alignment of the mirror system of the Model 9.

The problems associated specifically with carbon powders are all related to the fact that the samples exhibit a high extinction coefficient as well as high refractive index over the entire infrared region of the spectrum. Below are listed some representative optical parameters for graphite and carbon black (47).

n and k for graphite and carbon black, at 5 μ, from Foster and Howarth (47).

	refractive index, n	extinction coefficient, k
Graphite[a]	3.0	1.3
Carbon black[b]	2.25	0.78

[a]Sample 4 of Foster and Howarth, a polycrystalline graphite.

[b]Sample 5 of Foster and Howarth, a black from natural gas.

From these experimental studies of active carbons, it appears that the n and k of active carbon are in the neighborhood of the values presented above for carbon black. These values generally increase with λ for carbon; $2.0 < n < 2.4$; $0.7 < k < 1.0$ for $2.5\ \mu < \lambda < 10\ \mu$ (47). The optical constants (47) indicate that graphite ($3.0 < nk < 5.0$), and active carbon ($1.4 < nk < 2.4$), will be highly absorbing samples over the entire IR region. For an absorption band of a typical organic compound, the product nk is zero in the neighborhood of the peak, and rises to some small value at the maximum. For p-nitrophenol, for instance, the C-O vibration of the phenolic hydroxyl group shows a maximum nk of about 0.037 (52).

In order to observe such a vibrational band due to a surface functional group, on a highly absorbing substrate, signal amplification must be employed, to see a maximum difference in reflectance of about 1%R (18), as the surface region is thin and the evanescent wave penetrates a considerable distance into the bulk material. The depth of penetration into a homogeneous sample with $n = 2.23$, $k = 0.72$, will be $0.02851\ \lambda$. This value is determined by the equations discussed in the Appendix. This bulk absorption is the main factor in selection of IRS geometry and crystal arrangements, and is discussed in the Appendix. The complex refractive index of

an absorbing medium is given by

$$n = n + ik$$

where k is the extinction coefficient and n the observed refractive index. The energy lost to the absorbing medium in attenuated total internal reflection is given by

$$\int_0^\infty P_x dx = \int_0^\infty \frac{nk\left\langle E_x^2 \right\rangle}{\lambda} dx = \frac{nk\left\langle E_o^2 \right\rangle dp}{\lambda} \qquad (7)$$

where P_x is the power absorbed per unit volume at a distance x into the medium, $\left\langle E_x^2 \right\rangle$ the time average of the square of the amplitude of the electric vector at x, and dp is the depth of penetration (51) into the absorbing medium. Calculation of dp according to Hansen (53), and assuming that the carbon is covered with a 50 Å thick layer of organic molecules gives:

$$\frac{\text{Energy absorbed with organic layer}}{\text{Energy absorbed by pure graphite}}$$

$$= \frac{n_{org} k_{org} (50\ \text{Å}) + n_{Gr} k_{Gr} dp}{n_{Gr} k_{Gr} dp}$$

$$= 1.004$$

After 25 reflections, the ratio is $(1.0004)^{25} = 1.01$. The change in reflectance is about 1%.

Figure 8 shows the effect of bulk absorption at different angles of incidence for a homogeneous sample, with n = 2.25, k_2 = 0.78, and λ_o = 5 μ, for four different IRS crystal materials; germanium (n = 4), gallium arsenide (n = 3.3), silicon (n = 3.5), and KRS-5 (n = 2.4), for a single reflection by a 50:50 mixture of TM and TE polarizations. It can be seen that the bulk absorption losses can be reduced by raising the refractive index of the IRS crystal, or by increasing the angle of incidence, or both. Unfortunately, the bulk extinction coefficients of carbon samples are so high that the angles of incidence required to minimize bulk absorption (losses of < 1-2%) are high, in fact closely approaching grazing incidence, that they are not feasible for normal internal reflection techniques. It is not desirable to reduce the number of reflections below 5 or 6, and in order to obtain multiple reflection spectra with IRS crystals that are thick enough ($\geq$ 1 mm) to handle, an angle much above 60-70° is just not easily obtained.

As the angle of incidence and the refractive index of the crystal are increased, there is also a corresponding loss in sensitivity in the interaction with the surface functional groups. This is because the intensity of the E-fields at the interface decrease rapidly with increasing angle of incidence (51). It is thus necessary to seek an alternative solution, either in the form of high electronic signal amplification, requiring the most stable of

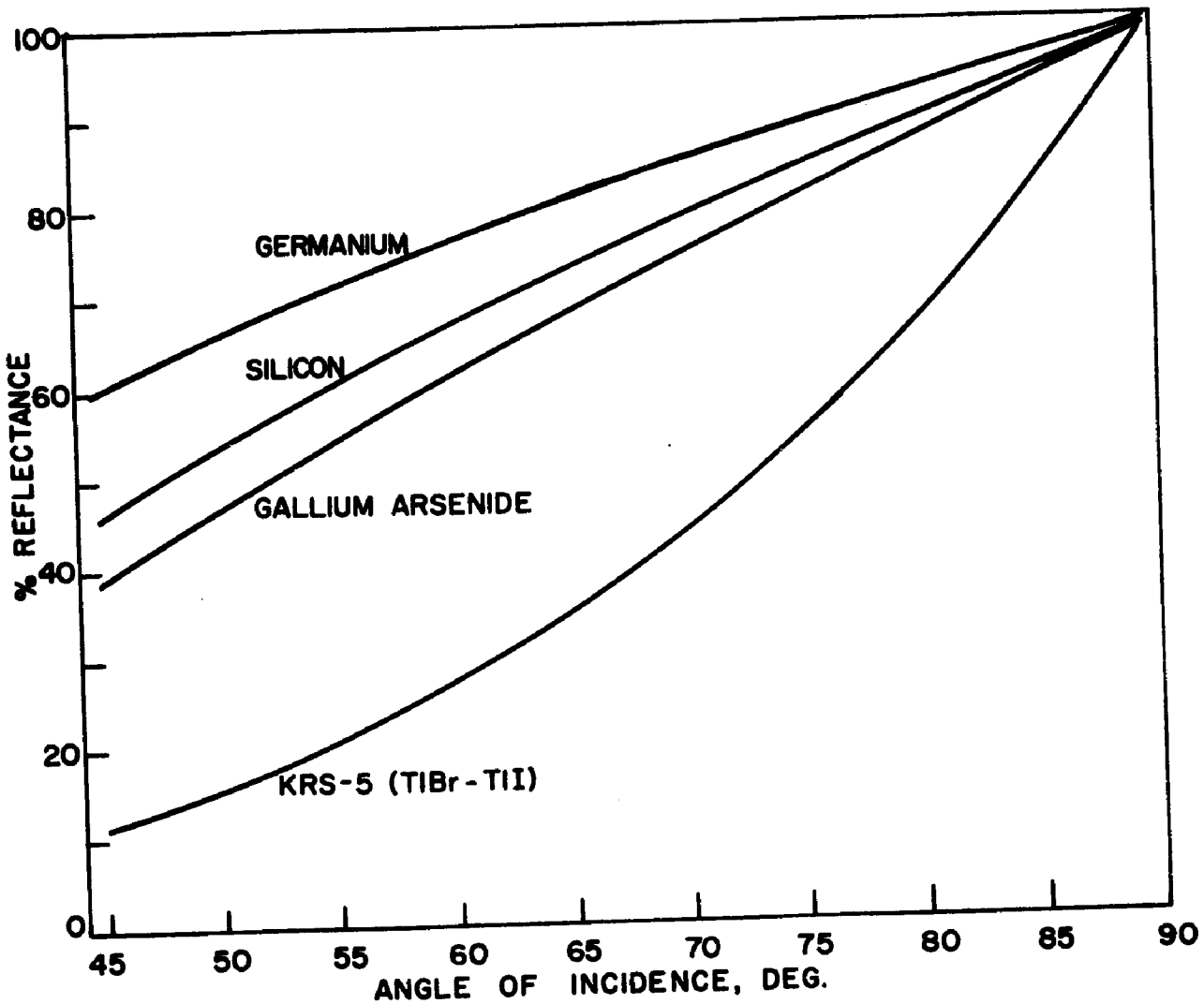

Fig. 8. --Effect of IRS Crystal on Bulk Absorption

commercially available spectrophotometers, or by optically balancing out the reflectance losses caused by the bulk absorption of the substrate. In initial experiments graphite was employed as the optical reference material. The optical constants of graphite and active carbon do not, however, match well enough for graphite to make a very good reference. The ideal reference would be material identical to the sample, but with all of the surface functional groups "stripped off". This, however, is not feasible, and as yet a good reference material has not been found for these studies. Thus, whenever a reference is called for, graphite is used since it is the best available. The graphite has also been shown to contain surface oxygen groups, which serves to further complicate the problem. The graphite employed is a sub-1 μ particle size, spectroscopically pure material (UCP-1, Ultra Carbon Corp., Bay City, Michigan; prepared specially without exposure to N_2 in the heating cycle).

For uncompensated IRS measurements, either germanium or KRS-5 can be used as the IRE, depending on the region of the spectrum to be investigated, amplification desired, sample used, etc. Germanium presents a special problem in these high amplification applications. It is difficult to keep germanium surfaces free from adsorbed organics or surface oxides. It is necessary to check the optical baseline of each crystal often, looking

for evidence of contamination in the 3000-2800 cm^{-1} and 1800-1000 cm^{-1} regions. It is necessary to clean the crystals if contamination shows up at 5X scale expansion in the latter region. This cleaning is accomplished by repolishing the crystal using a slurry of #600 SiC in methanol on a polishing cloth (A. B. Microcloth, available in 10" and 12" circles from Scientific Products, Detroit, Michigan) stretched on a glass plate and held in place with a large hose clamp. The crystal is handled with rubber finger cots and rubbed in a figure-8 motion over the SiC 20-30 times, then moved to a dry portion of the polishing cloth and polished by rubbing 20-30 more times. This procedure is repeated as long as is necessary to obtain a "clean" 5X optical baseline, without attempting to remove all of the C-H contamination in the 3000-2800 cm^{-1} region. The crystals can be washed with almost any solvent, even mild acid or alkali, without damaging the reflecting surface.

The number of reflections to be employed for best results is something which can be determined only on a trial-and-error basis for each sample. It is best to begin with a high angle of incidence and only one side of the crystal covered with powder, and then adding powder to the other side and decreasing the angle of incidence for subsequent runs until the desired contrast is obtained. One of the effects of increasing the amount of powder,

or decreasing the angle of incidence is that the surface coverage of the powder itself increases the quality of the spectrum obtained by decreasing the size of the peaks contributed by contaminants on the crystal. This is shown in Figure 9, where spectrum A is the crystal baseline, showing the C-H peaks of organic material adsorbed on the Ge, B shows the peak decreasing when one side of the crystal is covered with carbon, and C shows that the peak all but disappears when both sides of the crystal are covered with carbon. This is as predicted theoretically by the IRS equations of Hansen (53).

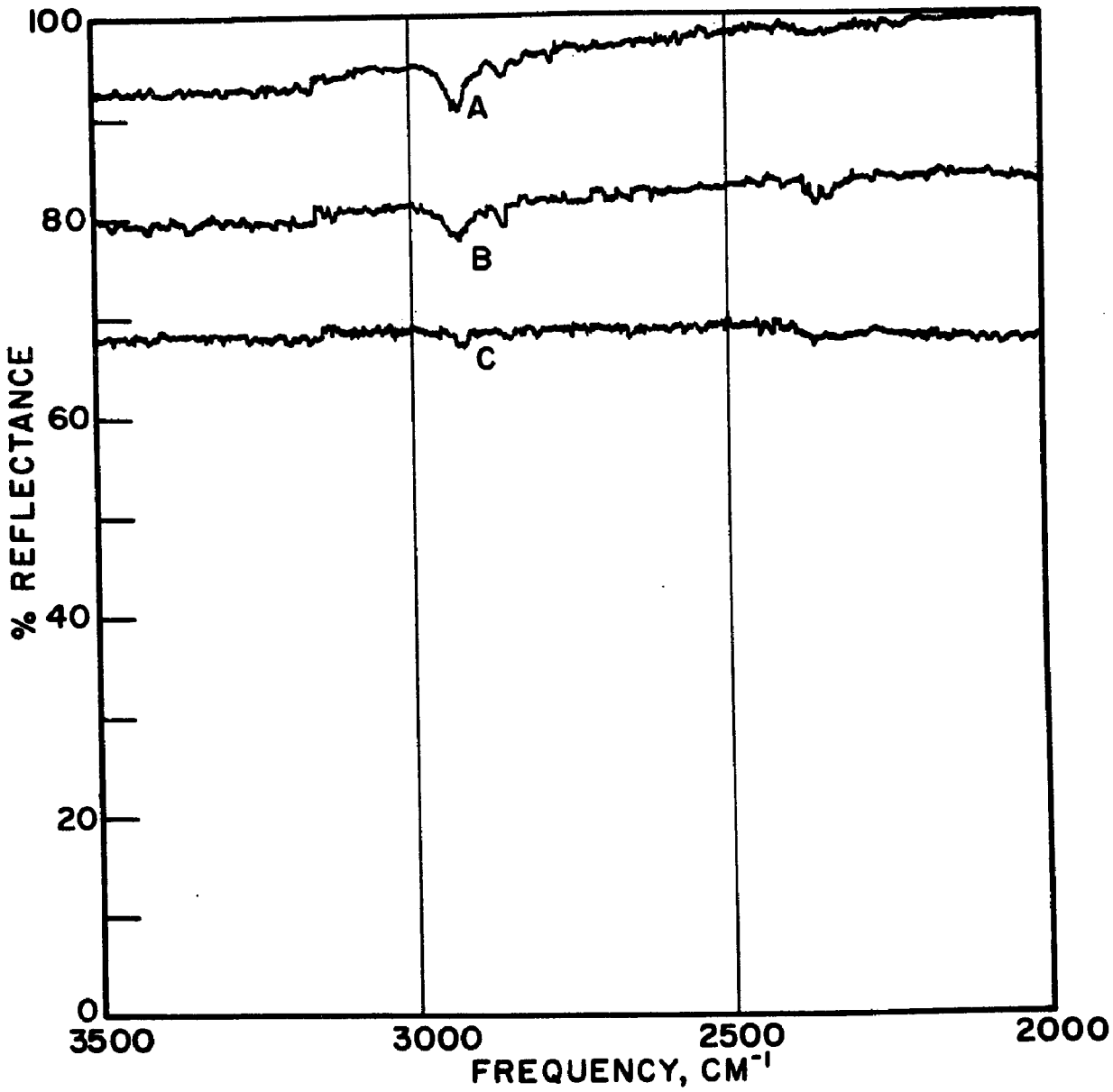

Fig. 9. --Effect of Powder on IRS Spectrum of Thin Film

II. Samples of a Commercial Carbon Examined by IRS both Before and After the Adsorption from Solution of p-nitrophenol

The results of a study on a sample of Nuchar C-115, a lignin based carbon, are discussed first. Spectra were obtained from: (i) the sized, washed, and dried (to constant weight at 200° C) original material, (ii) a portion of (i) which was used for obtaining an adsorption isotherm of p-nitrophenol from a solution of pH2 HCl and subsequently dried at 200° C, and (iii) a portion of (i) which was subjected only to the pH 2 solution of HCl used in (ii) to stabilize the neutral species of p-nitrophenol. The original carbon sample was also subjected to elemental analysis, and was found to contain 92.1%C, 1.3%H, 0%N and 1.1%S, with negligible ash content. The amount of oxygen present, rather than determined by difference, was determined by triton activation (54), giving a value of 5%O.

Figures 10 and 11 show 5X scale expansion spectra of samples (i) and (ii). Some of the absorption peaks observed in these spectra correspond to those observed in the spectra of Garten and Weiss (17), Brown (42), and Friedel and Queiser (43). Since internal reflection spectra, in the case of particulate matter significantly larger than the depth of penetration of the evanescent wave, are solely representative of surface structures, (see Appendix) the results of the analyses of these spectra yield

Fig. 10. --The IRS spectrum of Nuchar C-115, a lignin-based commercial active carbon. 5X scale expansion.

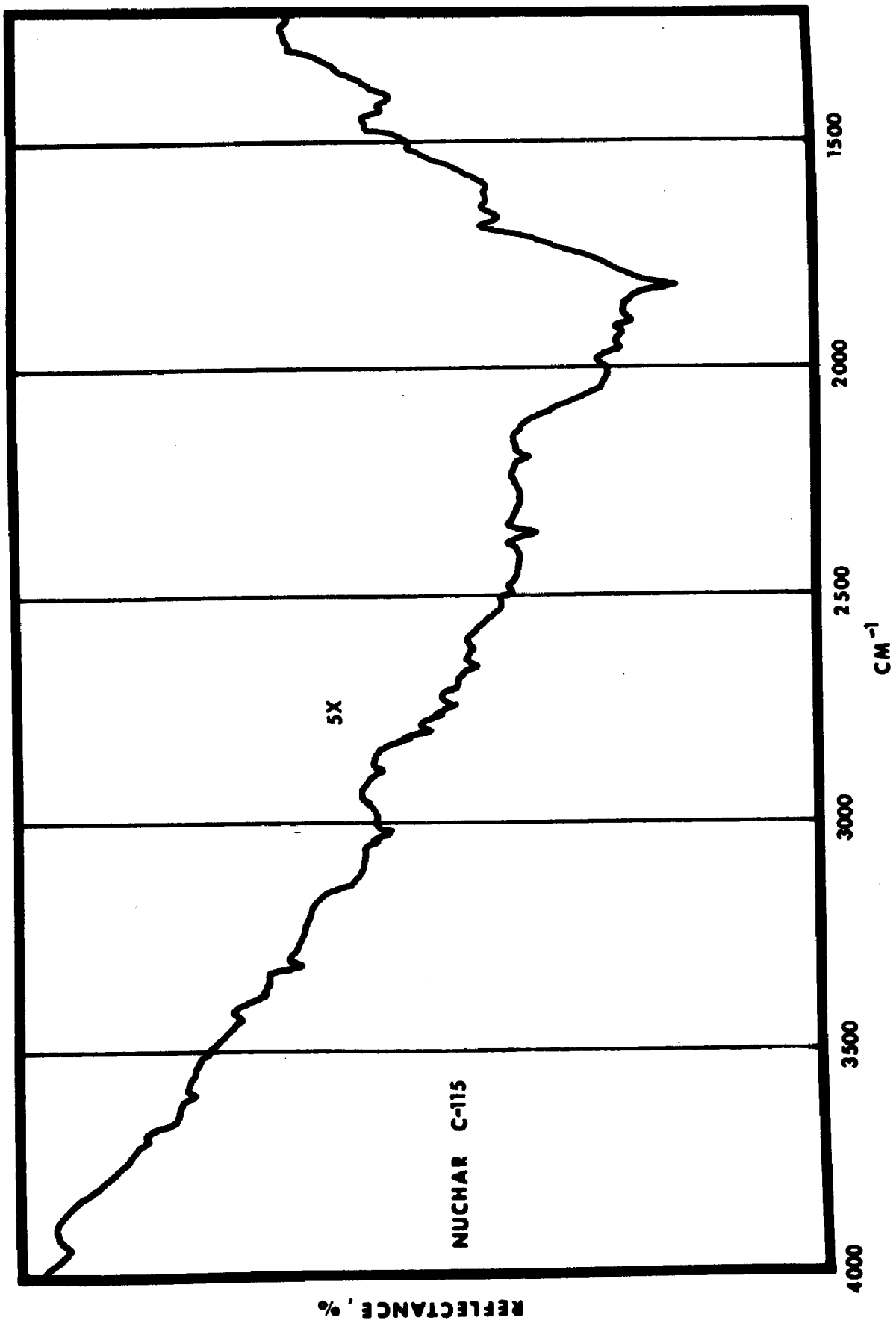
NUCHAR C-115
5X
REFLECTANCE, %
4000
3500
3000
2500
2000
1500
CM⁻¹

Fig. 11.--The IRS spectrum of Nuchar C-115 after the adsorption of 1.6 meq p-nitrophenol/gram from pH2 HCl solution. 5X scale expansion.

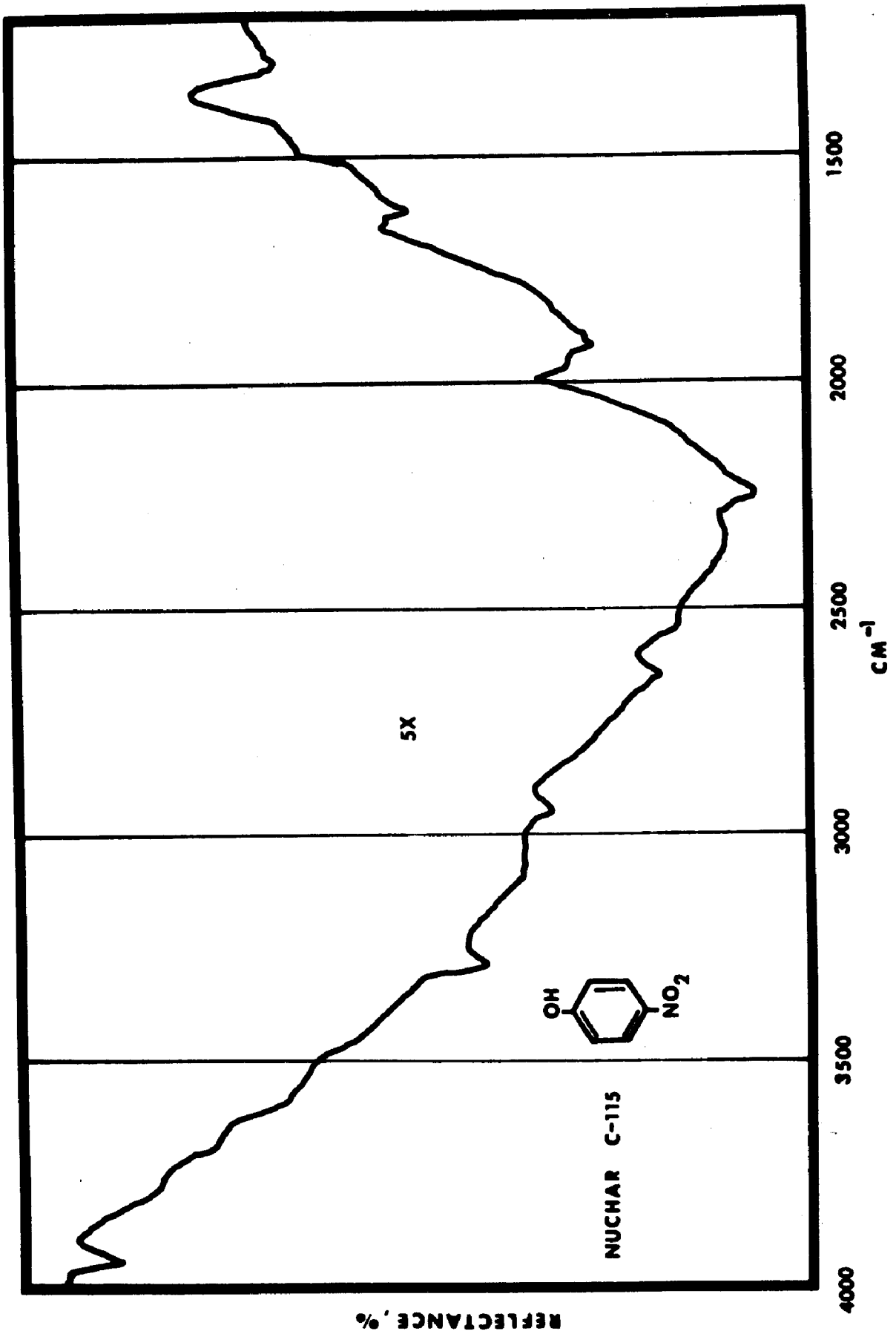
REFLECTANCE, %
4000
3500
3000
2500
2000
1500
CM⁻¹
NUCHAR C-115
OH
NO2
5X

information which is particularly relevant to the external surfaces of the particles (18-20).

The absorption at 3300 cm^{-1} can be seen in both samples (i) (Figure 10) and (ii) (Figure 11), and the size of the band in sample (ii) shows some increase over that in (i). This may tend to lend credence to the assignment (43) of this band to phenolic -OH, but upon thorough drying of sample (ii) at 200° C (the spectrum is not shown), the 3300 cm^{-1} band was no longer observed. Although the latter fact suggests that the absorption is due to tightly bound water, this would require the presence of some specific mechanism which disposes of the -OH vibrational band of the p-nitrophenol upon adsorption. This does take place, and is thoroughly discussed in Chapter 5.

The broad band at 1250-1150 cm^{-1} is not present after adsorption of p-nitrophenol nor does it show up in the spectrum of the sample (iii) which was exposed only to the pH 2 HCl solution. The loss of the band is shown in Figure 12. The appearance of the band before exposure to acid, and disappearance after adsorption suggest either an interaction with the acid or with the p-nitrophenol. The bands in the lower spectrum of Figure 12 have been observed to correspond to p-nitrophenol absorption bands (52), which simply overwhelm the 1250-1150 cm^{-1} band.

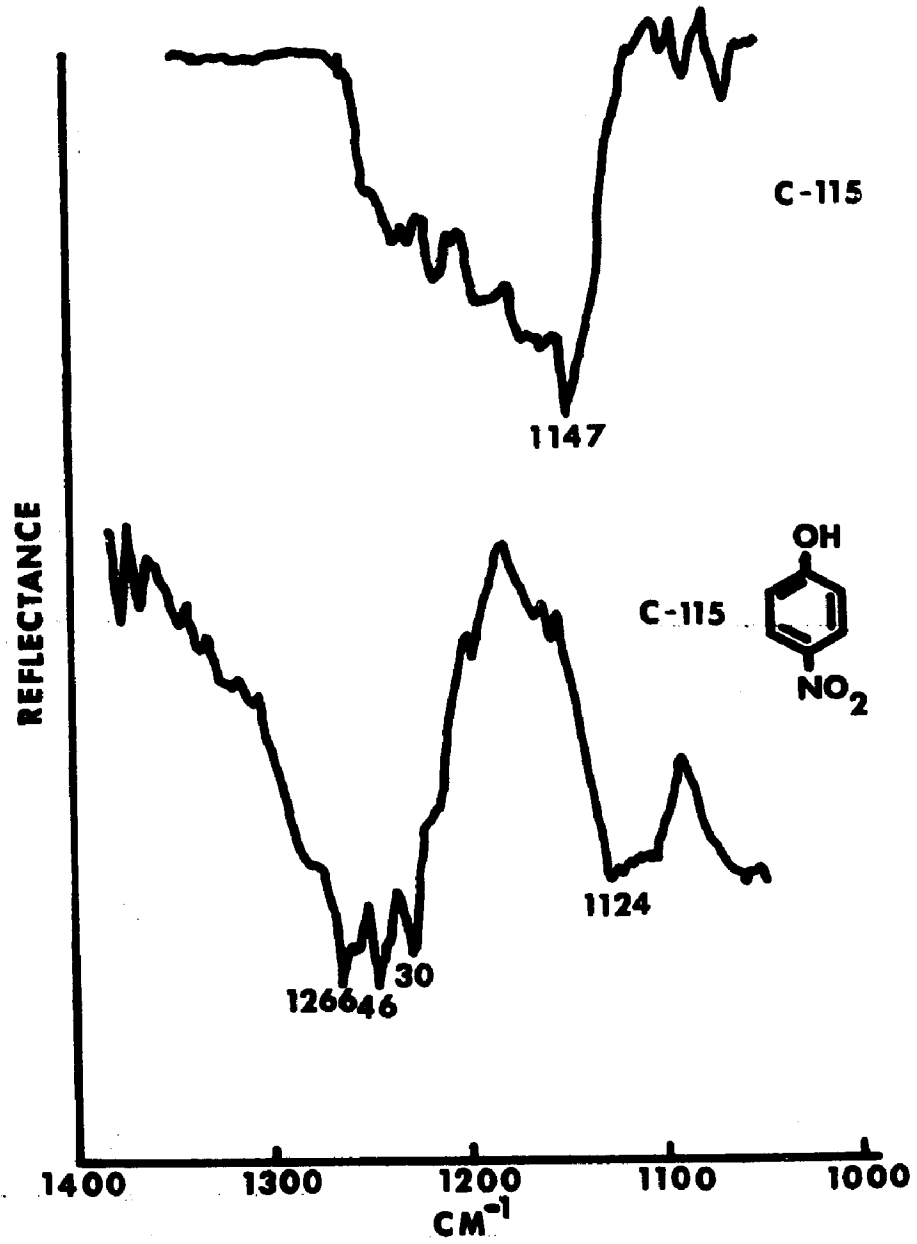

Fig. 12.--IRS spectra of Nuchar C-115. Top, before adsorption; bottom, after adsorption of 1.6 meq/g p-nitrophenol. C-O region.

Figure 13 shows the detail around 2700 cm^{-1}, likely attributable to a C-H bond slightly shifted to lower energy than normal, perhaps as a result of its proximity to carbonyl groups. This peak is unaffected (Figure 13) by the adsorption of either acid or p-nitrophenol. p-nitrophenol does not have an absorption band in this region (52).

Figure 14 shows the strong peak observed at 1600 cm^{-1} (17-20, 40, 43), which has been attributed (17, 40, 43) to the absorption of the enol form of a 1, 3-diketone (shown in reaction 3).

In Figures 10 through 14, the spectra were obtained on the active carbon samples using a germanium IRS crystal, with graphite in contact with the germanium crystal in the reference beam. The carbon samples were of a 1-50 μ particle size, while the spectroscopically "pure" graphite was of a 1 μ particle size.

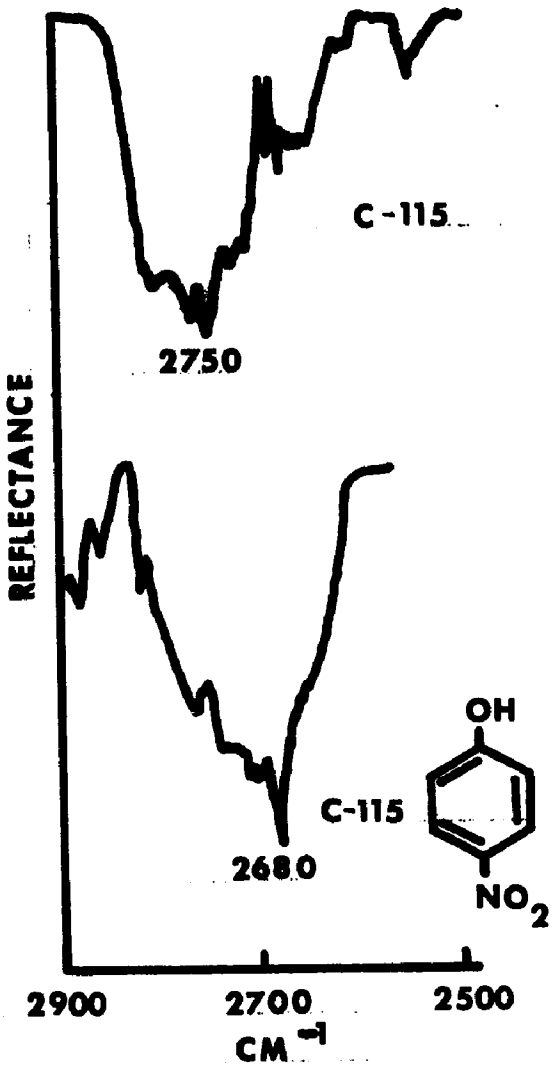

Fig. 13. --IRS spectra of Nuchar C-115. Top, before adsorption; bottom, after adsorption of 1.6 meq/g p-nitrophenol. CH region.

Fig. 14. --IRS spectra of Nuchar C-115. Top, before adsorption; bottom, after adsorption of 1.6 meq/g p-nitrophenol. 1600 cm^{-1} C=O band.

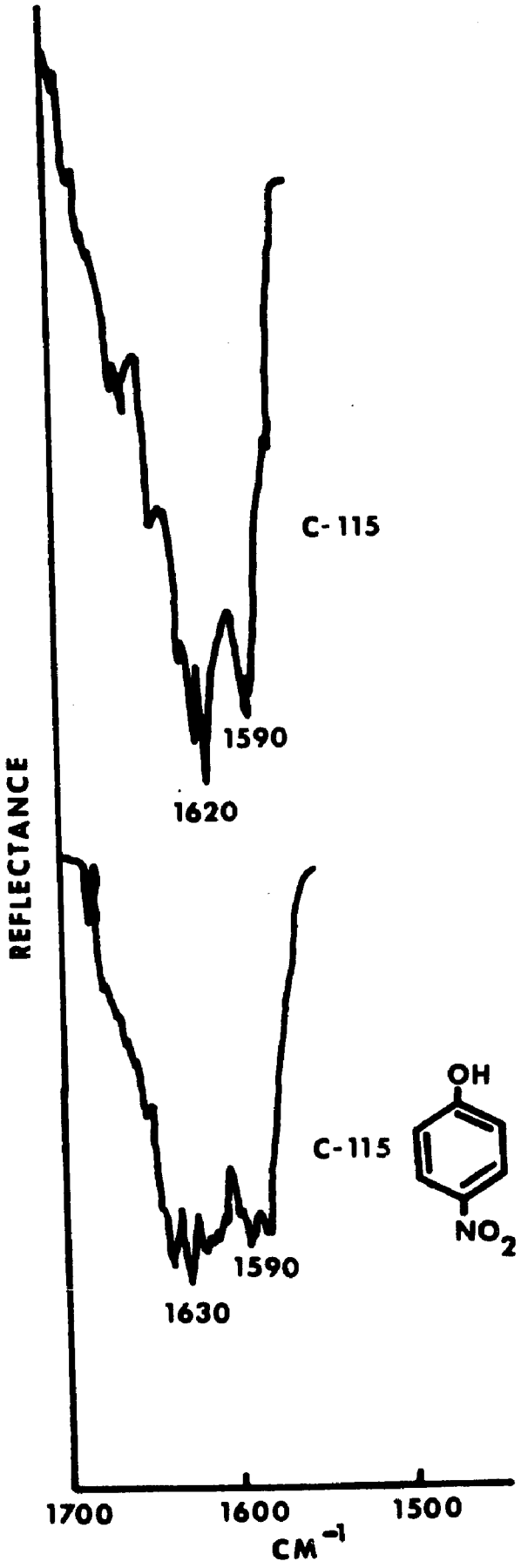
C-115
1590
1620
REFLECTANCE
C-115
OH
NO2
1590
1630
1700
1600
1500
CM-1

III. IRS Spectra of Powdered Graphite, Carbon Black, and Microcrystalline Active Carbon

Figure 15 shows the IRS spectrum of 1 μ particle size graphite, taken with a double beam arrangement on germanium (with just a 60°, 1 mm thick, 52.5 mm long germanium crystal in the reference beam). The number of reflections used was 25. From Figure 15, it can be seen that the graphite shows no distinguishing absorption bands at the normal scale of 1X, although it shows strong absorption throughout the entire 2.5-15 μ (4000-667 cm^{-1}) range. Amplification of this spectrum showed that one broad absorption band was present in the C=O region of the spectrum. This region is shown in Figure 16, which is a 5X and 10X scale expansion of the 2000-1000 cm^{-1} region. In both of the expanded scale spectra of Figure 16, an intense band is observed in the 1800 cm^{-1} region, and a smaller band (doublet) is observed at 1475 cm^{-1}. The band at 1800 cm^{-1} is quite broad, covering between 100 and 200 cm^{-1}.

Because of the low oxygen content, about 1 ppm (55), of the graphite it seems surprising that an absorption band is observed in the C=O region, however, because of the limitation of IRS interactions to the surface regions of the sample (Appendix I) this is explained on the basis of selectivity of IRS spectra for surface structures. More on this is presented below, in relation to the active carbon spectrum, where the 1800 cm^{-1} band is also observed.

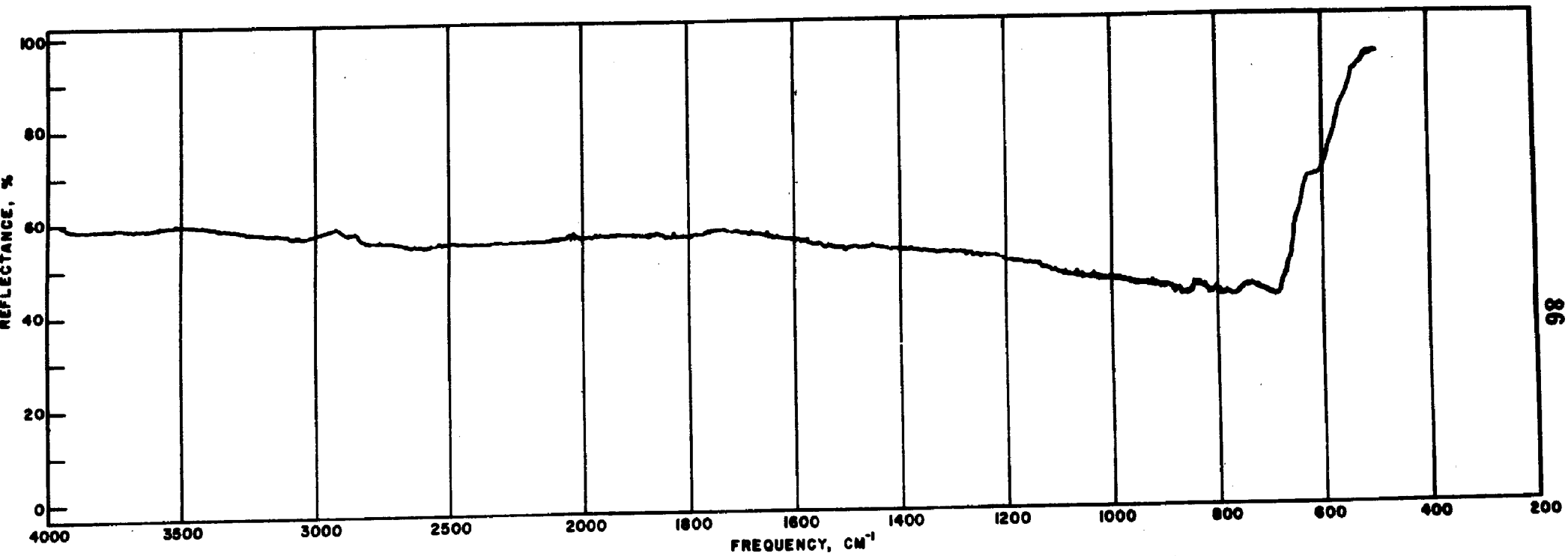

Fig. 15. --IRS Spectrum of Graphite

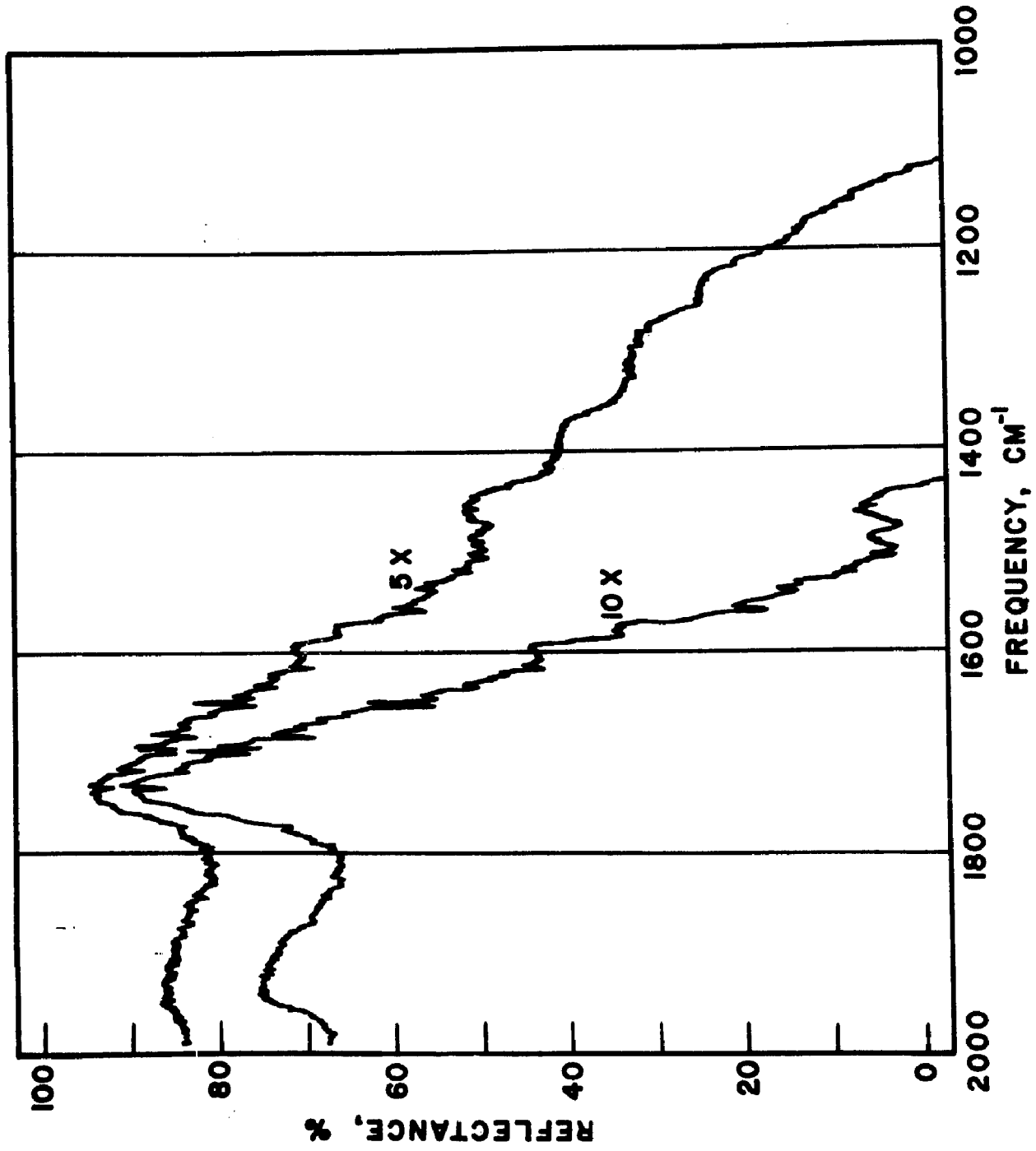

Fig. 16--Scale Expansion of 2000-1000 cm^{-1} Region of IRS Spectrum of Graphite

The fact that the graphite was allowed to cool down in the manufacturing process while in limited contact with air (55) implies that oxygen would have been picked up at the edges of the basal planes during the cooling procedure. The 1800 cm^{-1} band is quite broad, as shown in Figure 16, which might be expected for functional groups placed in a continuous spectrum of energetically dissimilar environments. From the position of the peak, relative to comparable absorption measurements made on solutions (45), the C=O groups would have to be in a strained system, similar to that of a cyclic acid anhydride. It would not be totally unexpected to find that the edges of graphitic planes would contain a large amount of broken rings which, upon oxidation, would give adjacent carboxylic acid groups. In the high temperatures encountered in the manufacturing process, the adjacent carboxylic acid groups would lose water to form the cyclic acid anhydride. However, this interpretation is far from conclusive as germanium oxides also absorb in this region, and it is found that total compensation in the dual beam arrangement is never achieved at such high amplification. Figure 16 shows that the powdered graphite bulk absorption is increasing throughout this region. In combination with uncompensated Ge-oxide absorption, this could give rise to a broad band such as that observed around 1800 cm^{-1}.

The 1475 cm^{-1} band of graphite could be due to an aromatic ring vibration band, usually considerably weaker than C=O bands. Because of the nature of the graphitic structure, however, the fact that the 1475 cm^{-1} band appears to be relatively strong is not contradictory to the conclusion that it is due to the aromatic ring structure. This band is out of the carbon-oxygen region, and is difficult to identify. It should be noted that no phenolic, alcoholic, water or other -OH bands were observed in the graphite spectrum.

The spectrum of a lignin-based active carbon, 10X scale expansion is shown in Figure 17, and the spectrum is strikingly similar to graphite, with broad absorption bands at 1800 (1730-1850) cm^{-1} and about 1475 cm^{-1}. Unfortunately, the details of the manufacturing process for this carbon are not available, and it is more difficult to interpret spectra of this material. However, this particular sample was heated to 200°C for several days and allowed to cool in a desiccator, under vacuum, before the spectra were taken. This procedure is used to drive off the tightly bound water found on this series of active carbons, and this drying procedure may well be sufficient to cyclize adjacent carboxylic acid groups to form the cyclic acid anhydride, as was suggested above for graphite.

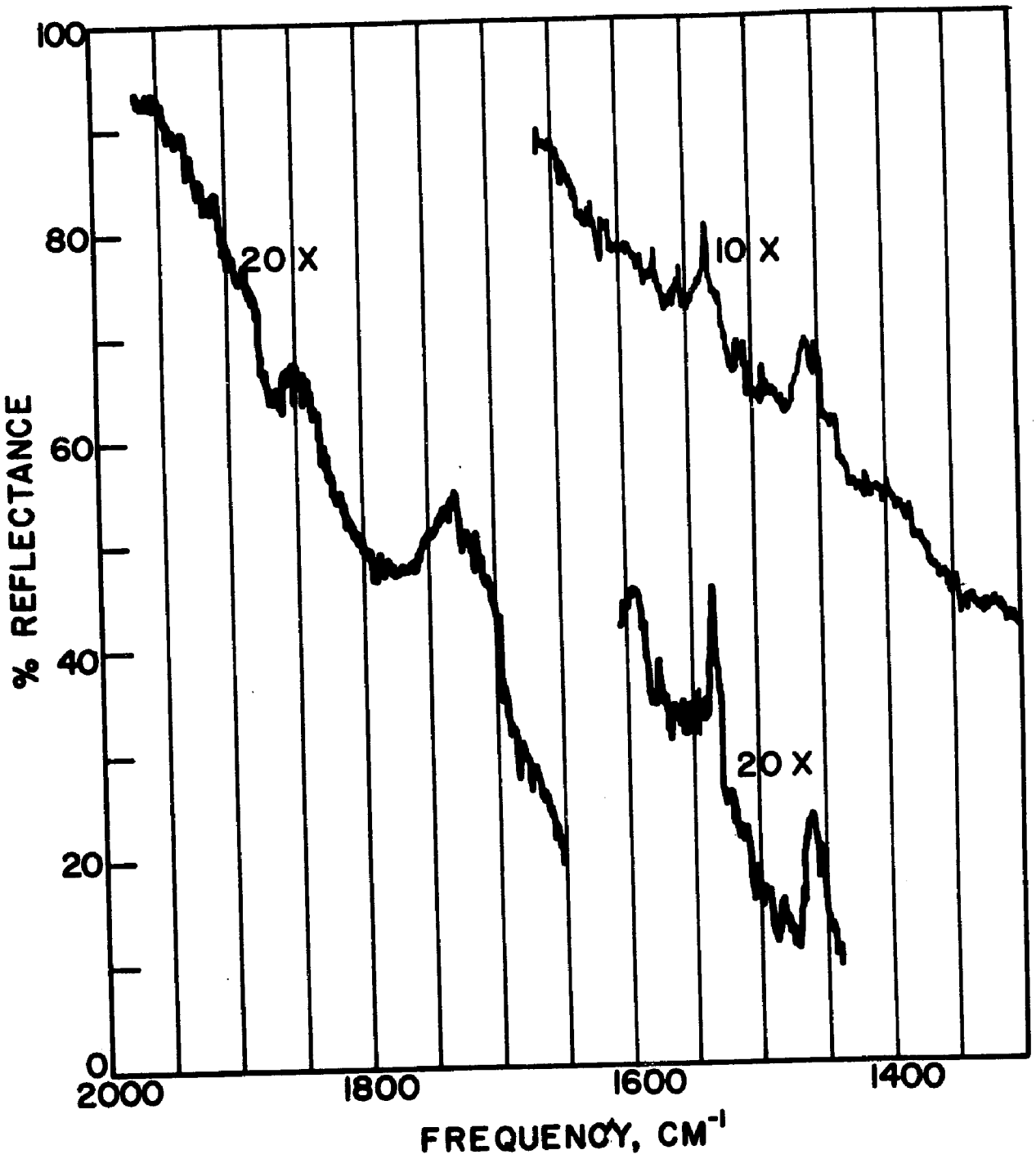

Fig. 17.--Expanded scale IRS spectra of C-1000, a lignin-based active carbon.

The spectrum shown in Figure 18 was obtained by placing the graphite in the reference beam and the active carbon in the sample beam. The disparity in optical constants is responsible for the sloping baseline in Figure 18. This figure clearly shows that the 1800 cm^{-1} band is almost perfectly balanced out by the use of graphite as a reference. There is a sharp rise in the spectrum at 1775 cm^{-1} which is due to uncompensated germanium oxides. The fact that the broad band at 1800 cm^{-1} has been balanced out tends to lend support to the argument that the same oxygen-containing functional group on both the carbon and the graphite is absorbing in this region. The fact that the concentration of oxygen-containing groups on the surface of graphite appears to be about the same as on active carbon is at first surprising. It must be recognized, however, that the external surface areas of the samples, determined by particle size and shape, are about equal, and that the tremendous amount of internal surface area of the active carbon, which accounts for about 99% of its surface area (52), is not accessible to the evanescent wave in IRS because of the very limited depths of penetration encountered. Therefore, the concentration of oxygen on the external surfaces in both samples could be equal even if the total N_2 surface area varied by three orders of magnitude. This is determined by assuming that the total oxygen concentrations are between three and four orders of

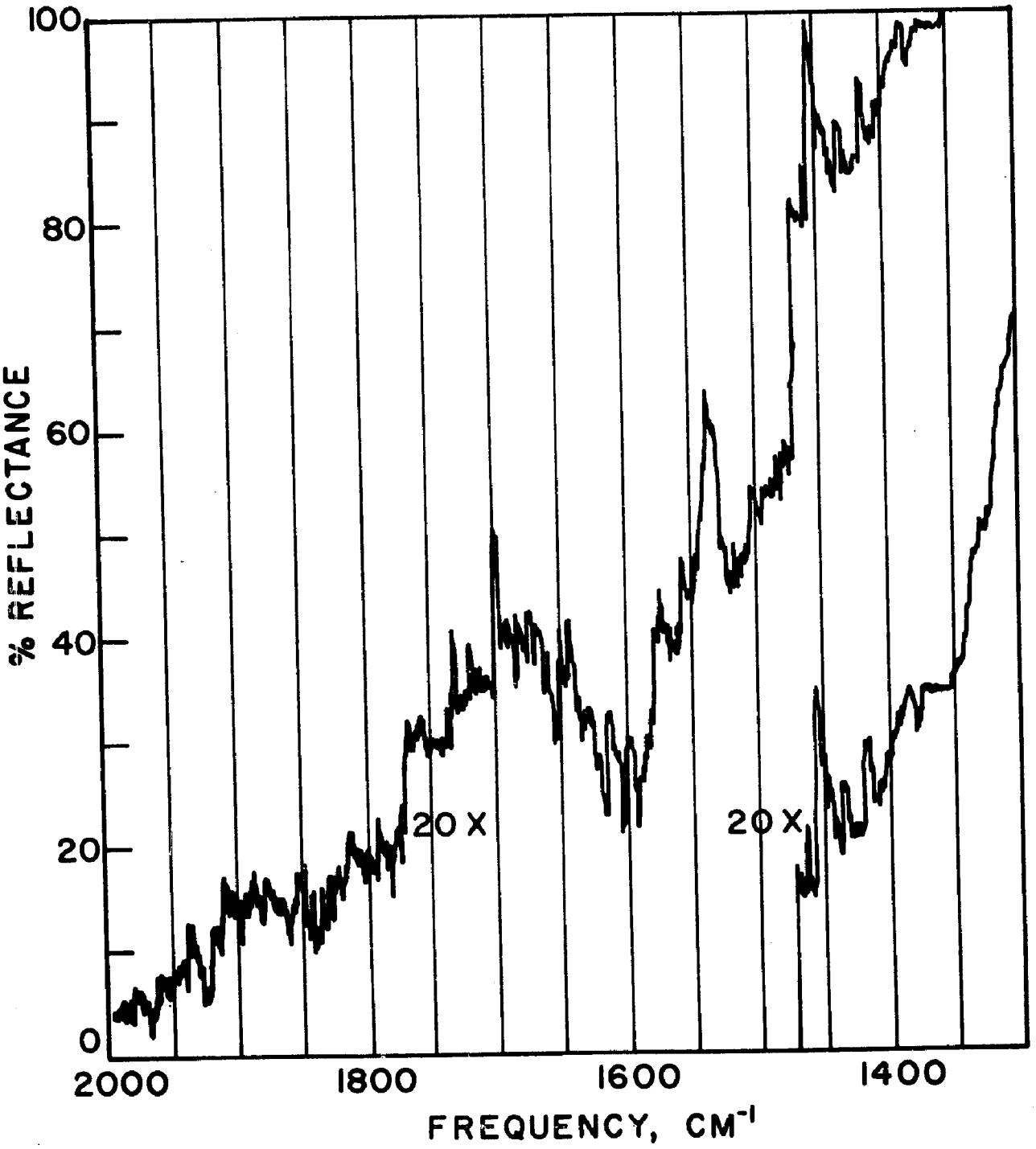

Fig. 18.--Expanded scale IRS spectra of C-1000, with graphite against the reference crystal.

magnitude apart. As it was pointed out (52), the O content of the C-1000 is in the 3-5% range and, that of the graphite is about 1 ppm (55); the surface areas are about 1000 m^2/g for the active carbon (52), and about 1 m^2/g for the graphite (55).

Figure 17 also shows that the 1475 cm^{-1} band of the graphite is not as strong as that in the active carbon, which could indicate a higher proportion of single aromatic rings on the active carbon than on the graphite.

There is a "new" absorption band observed in Figure 18 when the graphite reference is used, which was evidently obscured in the single-IRS-beam spectrum (Figure 17). This is the broad band centered around 1600 cm^{-1} which appears to correspond to the one found earlier and to those observed by other investigators (17, 40, 42, 43) in transmission spectra. This 1600 cm^{-1} band has been discussed (17, 18, 40, 42, 43) as a carbonyl band of an enol and in the light of the observation of a band at 1475 cm^{-1} in both graphite and active carbon, the 1600 cm^{-1} band could not be due to the C-C bonds of the graphitic structure.

Figure 19 shows the entire infrared spectrum of a carbon black (Philblack S315, Phillips Petroleum Co., Bartlesville, Okla.). This carbon black spectrum shows more detail than the graphite spectrum in Figure 15 because (i) the IRE (internal reflection element) was KRS-5, with $\theta_i = 54°$ (see Chapter 5), and (ii) the spectrum in

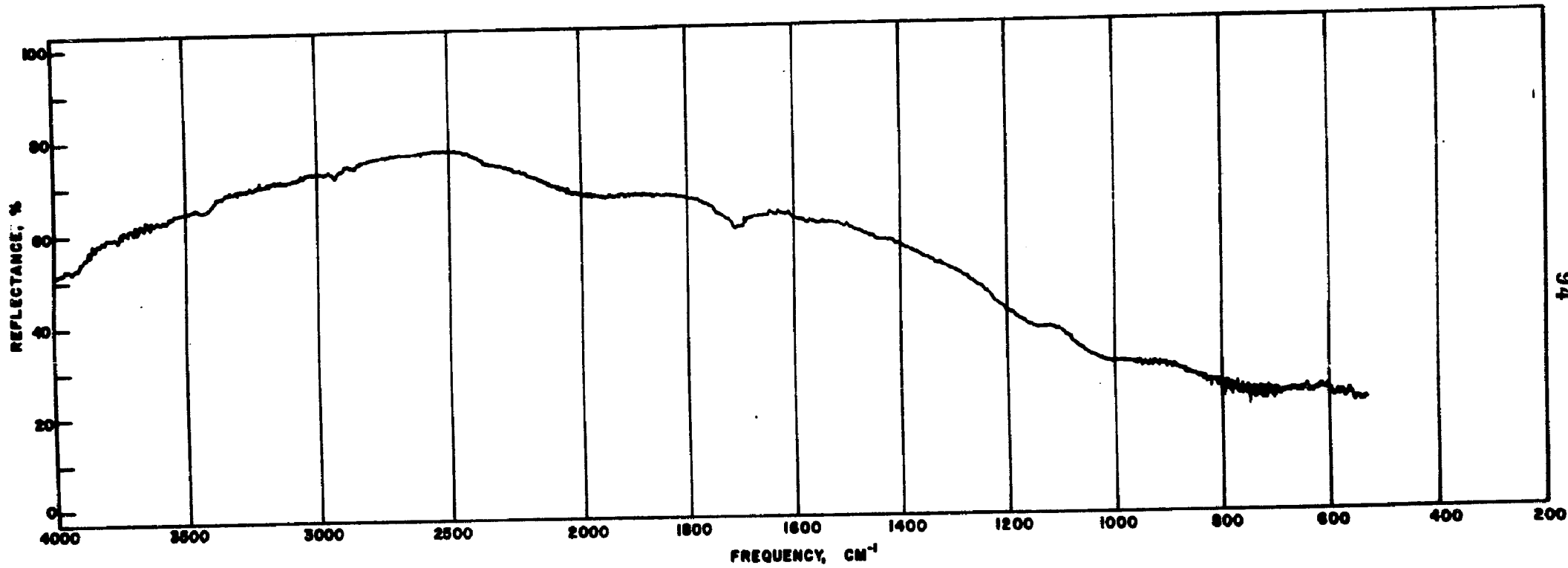

Fig. 19. --IRS Spectrum of Carbon Black, 2X Scale Expansion with KRS-5 IRE

Figure 19 is at 2X scale expansion. This particular IRE selection was made possible by the use of a large particle size sample; the sample was received in pelletized form, and this made it possible to use a lower refractive index IRE because of the thick air layer through which the evanescent wave had to pass prior to interaction with the sample.

The (as received) carbon black had few distinguishing features, observed in Figure 19, and in the expanded scale spectrum in Figure 20. There is a strong band in the carboxylic acid C=O region, at 1700 cm^{-1}, and there is a weaker band at 3400 cm^{-1}, which is in the -OH region, but is also at the right frequency to be the overtone of the band at 1700 cm^{-1}. As this sample had not been dried or otherwise specially treated before the IRS study, assignment of the 3400 cm^{-1} band could be made to either a carboxylic acid -OH (the most likely, considering the obvious carboxylic acid band at 1700 cm^{-1}), or to the overtone of the 1700 cm^{-1} band (the next best possibility), or to a phenolic -OH (the least likely). It should be pointed out that carbon black, by its very nature, would not be expected to show very pronounced graphite-like structural characteristics (47). Since this carbon black sample was not purified or dried as were the graphite and active carbon samples, and considering the fact that this carbon

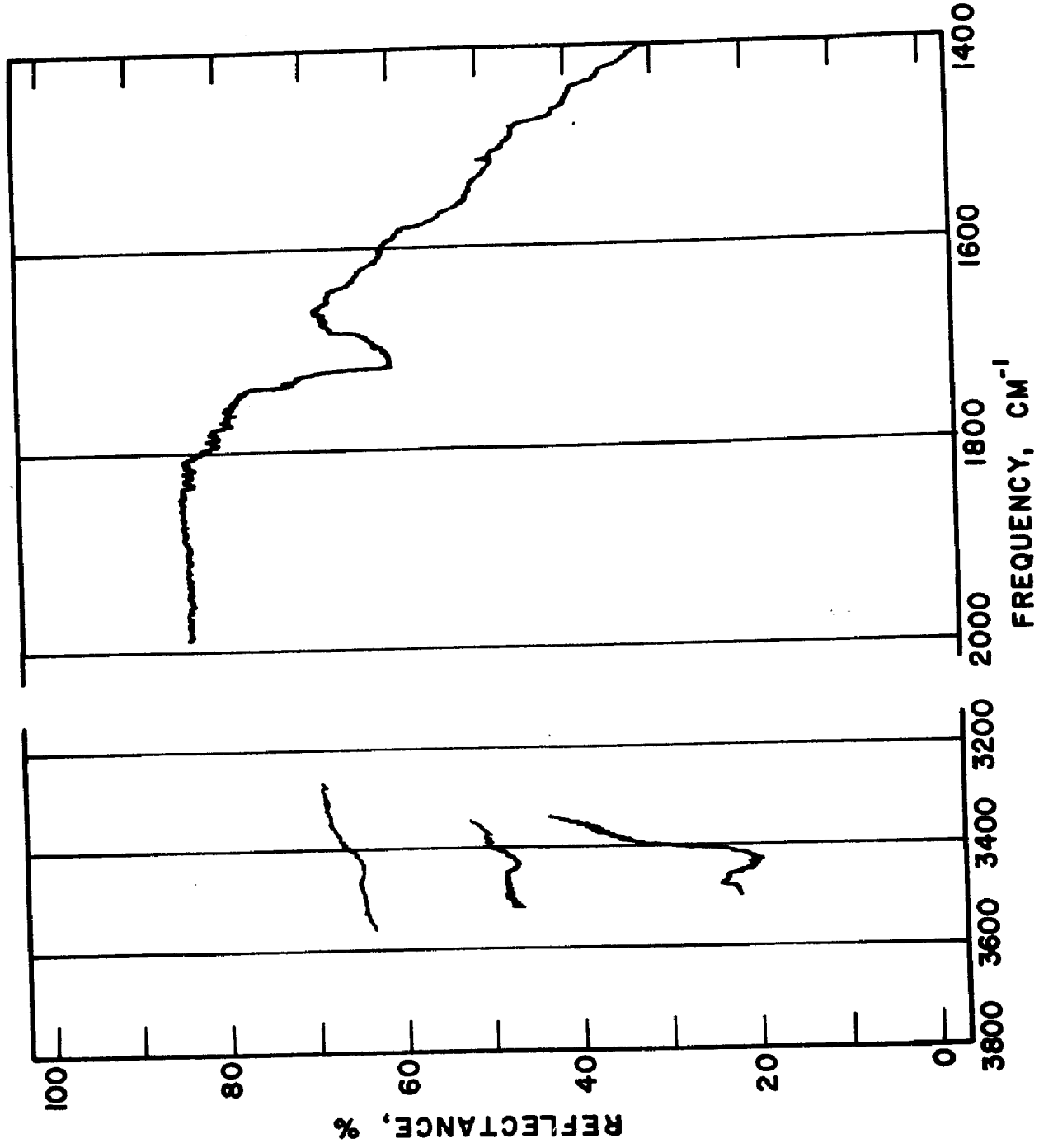

Fig. 20. --10X Expanded Scale Spectra of Carbon Black

black gives a pH of 2.5 in a water slurry, the assignment of the 1700 cm^{-1} band to carboxylic acid seems well supported. It was found that on purification and drying of the carbon black sample[1], the 1700 cm^{-1} and 3400 cm^{-1} bands disappeared and the pH of a water slurry was only 4.2. This indicates that the carboxylic acid group is present as an impurity.

---

[1]The purification was carried out as follows: The sample was washed several times with hot toluene, followed by hexane, then heated at 600°C for 30 minutes, followed by 24 hours at 200°C, then one week at 150°C. It was allowed to equilibrate with the atmosphere during the cooling down to room temperature. The water slurries were made up at a concentration of 1.0 g/100 ml in triply distilled water.

CHAPTER 4

IRS SPECTRA OF LABORATORY-ACTIVATED SUGAR CARBONS

Commercial carbons are generally activated in an atmosphere of CO_2, CO, O_2, H_2O vapor and occasionally other selected gases, at a temperature between 300° and 800° C, often followed by quenching in air or water. Because of the "impure" nature of the raw materials used in the production of commercial carbons, and because of the concentration and temperature gradients that develop within the beds of carbon during activation, very heterogeneous or, at best, difficult to characterize surfaces usually result. These heterogeneous surfaces produce a poor-contrast, difficult to interpret infrared IRS spectrum. Thus, infrared IRS studies were carried out on several series of activated sugar chars, prepared under very uniform and reproducible conditions in the laboratory.

I. Preparation of Carbons

Analytical reagent grade dextrose was charred in porcelain crucibles, with the covers left slightly ajar for exposure to air, in a muffle furnace at 600°C for six hours. The resultant char was ground to pass a 325 mesh (44 μ) screen. The -325 mesh material was then washed several times with triply distilled water, with the fines decanted during washing. The char was then dried at 200°C, and stored in a vacuum desiccator until needed. Ten grams of char was placed in a 25-mm diameter, 20-cm long quartz tube, and retained by quartz wool plugs. The tube was mounted in a tube furnace and held at the desired temperature. Mixed gases of quantitative composition, (concentrations accurate to 1% of stated values, according to supplier), were passed through the tube at a high flow rate (>20 l/hour) for six hours. The tube was then removed from the furnace and allowed to cool with a continuous flow of pure nitrogen flowing through (<0.01% O_2). After the tube had reached room temperature, the carbon was transferred to an evacuable pyrex container with a high-vacuum stopcock affixed. The activated carbons were then kept under vacuum until withdrawn for analysis by IRS spectroscopy.

II. IRS Spectra

A Wilks Model 45DB IRS accessory was employed in the sample compartment of a Perkin-Elmer 621 infrared spectrophotometer. Because of the high refractive index of carbon, it is necessary to use an IRS crystal of either silicon or germanium. It was decided to use germanium crystals in this study, as they can be used, in a double beam arrangement, to 667 cm^{-1} (15 μ). (Silicon could also have been used, as it usefully transmits to about 1000 cm^{-1} (10 μ). The model 45DB utilizes equal and identical sample and reference beam mirror systems (they are actually mirror images in geometry), thus equalizing atmospheric absorption and allowing compensation of the germanium lattice vibrations with an identical crystal in the reference beam.

Both germanium crystals employed were 0.5 mm thick, 5 mm wide, and 12.5 mm long, with 45° face angles. (The Model 45 is designed for only that fixed angle.) This geometry provides 25 reflections (neglecting beam divergence effects) at the crystal interface. The powdered carbon samples were transferred from their evacuated storage containers and placed in physical contact with the IRS crystal. The Model 45 crystal holder was used to hold the powder in place.

A Perkin-Elmer 621 was used because of the inherent electronic stability and large signal-to-noise ratio of the instrument at 5X and 10X scale expansion, which was routinely needed to obtain these spectra.

III. Discussion of Results

It had been previously noted that IRS spectra of commercial carbons showed very broad absorption bands in the 2000-1000 cm^{-1} region. As difficulties were encountered with respect to characterizing the activation conditions of commercial carbons, the logical next step was then to prepare laboratory-activated carbons, utilizing a very pure starting material and uniform activating conditions, in order to attempt to obtain more well-defined IRS absorption bands.

Activated sugar char has been used extensively in the past when such reproducible and well-defined carbons were desired (3, 26, 28, 29). A uniform starting material was prepared by charring dextrose at 600°C, and this material was then activated under controlled atmosphere and temperature conditions. Two different series of activation conditions are reported; a series of sugar carbons activated in 1% O_2-99% N_2 for six hours at 300, 400, 500, 600 and 700°C, and a series of sugar carbons activated in 5% O_2-45% CO_2-50% N_2 for six hours at 300 and 400°C and for three hours at 600 and 700°C.

The IRS spectra for the carbons within each series show the same general features from one sample to the next, but the realtive intensities of the same functional group absorptions show some dependence on the temperature of activation. Tables 9 and 10 summarize the band positions and intensities for the two series of carbons.

Because of the dependence of IRS spectra on the particle size of the material being examined (51, 56), it is possible to make only relative intensity observations among the bands of a given spectrum. However, all of the activated carbons reported on here were prepared from one batch of starting material, so the particle size distributions should be close enough to permit observation of major trends.

In Figures 21 and 22, there are a pair of bands observed at 1710-1750 and 1750-1770 cm^{-1} in each spectrum, from the 300 to the 700°C activated carbon. Figure 22 shows that the 600°C 1% O_2-99% N_2 activated carbon shows a merging of these two bands, and note that the merging is very extensive in the 500 and 700°C carbons. Previously, a broad absorption band in this same region was noted for both commercial activated carbon and "ultra-pure" graphite, but not for carbon black. It was suggested that the absorption band belonged to a carboxylic acid anhydride.

Table 9

Band Positions and Relative Intensities (v-very; w-weak; m-medium; s-strong) for Sugar Carbons Activated in 1%O_2-99%N_2

Band, cm^{-1}	Temperature of Activation, °C				
	300	400	500	600	700
1750-1770	(1765) m	(1750) s	(1770) m	(1770) m	(1750) m
1710-1750	(1740) m	(1710) s	(1750) m	(1720) m	(1710) m
1620-1690	(1640) vw	(1680) vw	(1650) w (1690) w	(1620) vw (1660) w	----
1590-1625	(1590) m	(1625) s	(1595) s	(1590) w	(1590) w
1510-1560	----	(1520) vw	(1550) s	(1560) s	(1520) m
1140-1230	(1150) ?	(1180-1230) s	(1140) ?	(1150) vs	(1140-1180) s

Table 10

Band Positions and Relative Intensities (v-very; w-weak; m-medium; s-strong) for Sugar Carbons Activated in 5% O_2-45% CO_2-50% N_2

Band, cm^{-1}	Temperature of Activation, °C			
	300	400	600	700
1750-1770	(1770) m	(1750) s	(1750) w	(1770) w
1710-1750	(1720) s	(1710) m	(1700) s	(1710) m
1620-1690	(1650) vw	(1670) vw	----	(1660) w
1590-1625	(1600) m	(1605) s	(1600) m	(1590) m
1510-1560	(1555) s	(1520) m	(1565) m	(1450) m
1140-1230	(1210) s	(1180-1240) s	(1200) m	(1140-1220) s

Fig. 21. --IRS spectra (10X) of sugar carbons activated in 1% O_2-99% N_2 for six hours at 300, 400, and 500°C.

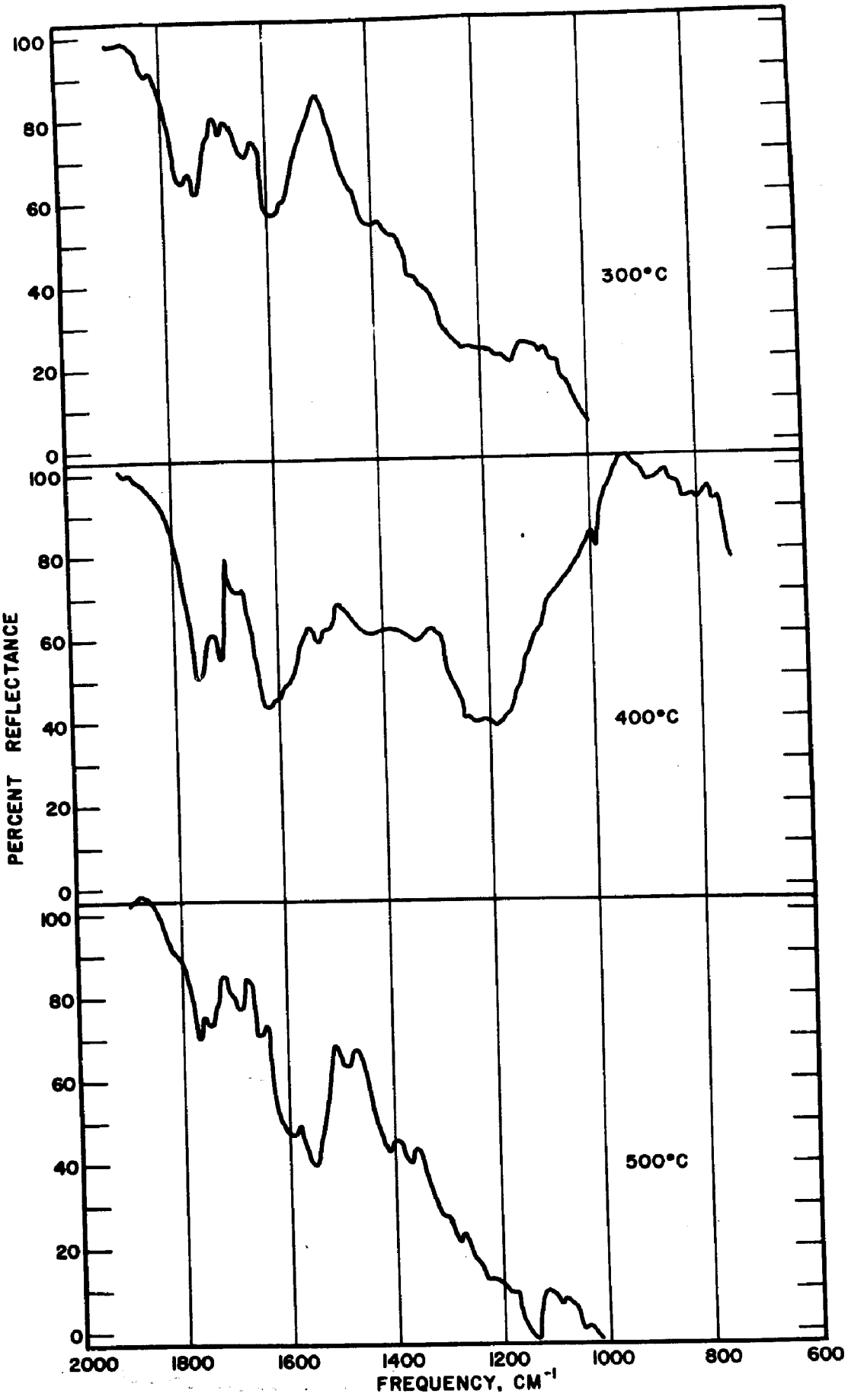
300°C
400°C
500°C
PERCENT REFLECTANCE
FREQUENCY, CM⁻¹
100
80
60
40
20
0
2000
1800
1600
1400
1200
1000
800
600

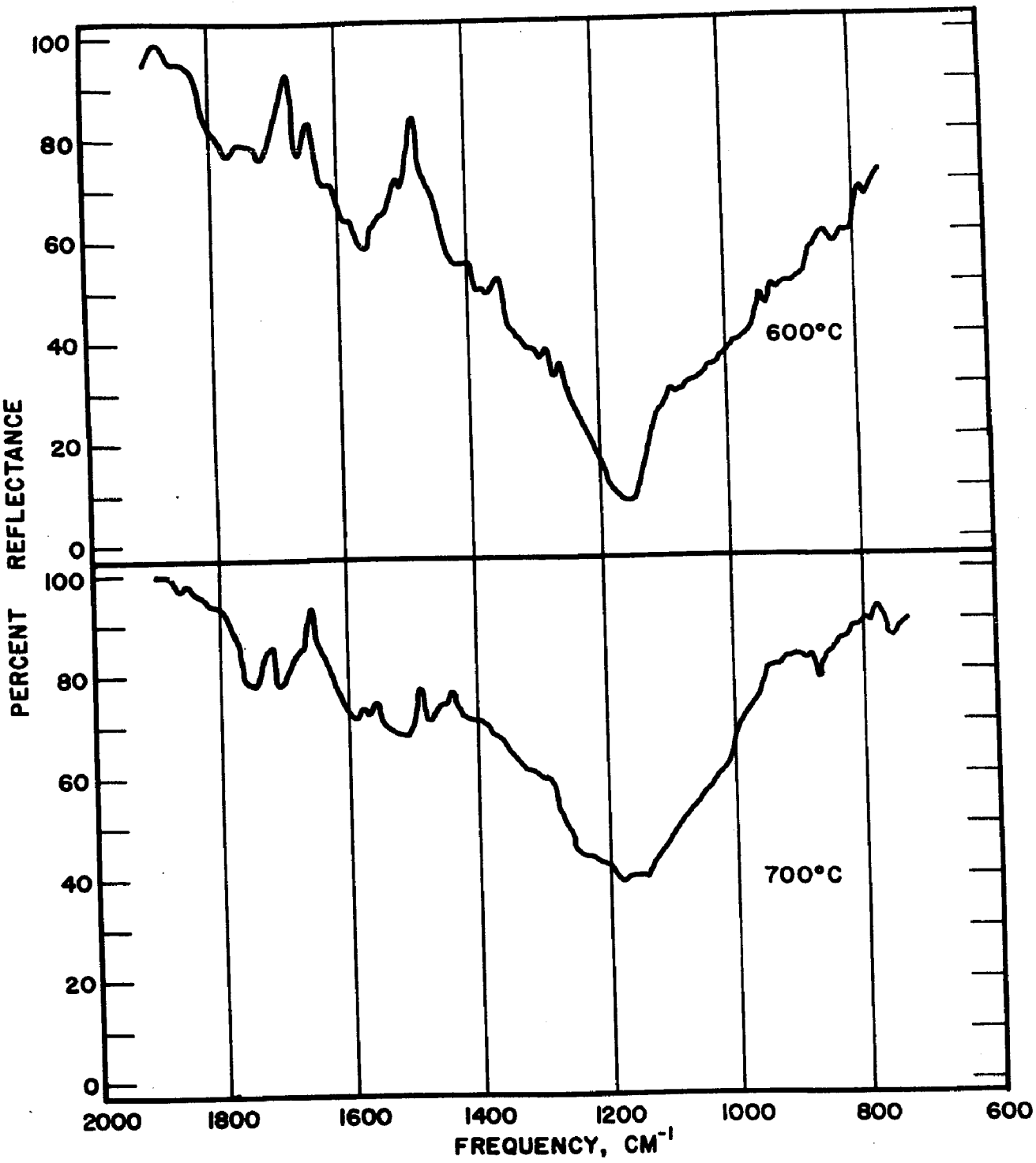

Fig. 22.--IRS spectra (10X) of sugar carbons activated in 1% O_2-99% N_2 for six hours at 600 and 700° C.

In the spectra of Figures 21 and 22, this pair of bands corresponds well with those to be expected for a pair of adjacent carboxylic acids. Because of the ring structure of the carbon basal planes, it is reasonable to expect that aromatic acids, similar to the phthalic acids, would be created upon oxidation of the edges of the ring structure. It is possible that such adjacent carboxyl groups are then responsible for the broad band previously ascribed to an anhydride.

Combined with the data presented in Chapter 2, the infrared IRS data of Figures 21 and 22 appear to confirm the existence of adjacent carboxylic acid groups at the edges of the basal planes, which decarboxylate and evolve CO_2, leaving C=C double bonds between the carbon atoms left at the surface sites.

The other major spectral feature in the carbonyl region of the 1% O_2-99% N_2 activated carbons in Figures 21 and 22 is the pair of absorption bands at 1590-1625 and 1510-1560 cm^{-1} respectively. In the previous discussions of infrared examination of carbon surfaces, intense bands were observed in each case at 1600 cm^{-1} and 1500 cm^{-1} for active carbon, but not always on graphite or carbon black (18, 19) (some absorption was observed around 1500 cm^{-1} on graphite). Garten and Weiss, however, in a transmission IR spectrum noted an intense band at 1600 cm^{-1}

in the spectrum (17) of Carbolac 1, a carbon black. The transmission spectra of the materials in Chapter 2 as well as the IRS spectra of Chapter 3 show a strong band at 1600 cm^{-1}. However, transmission spectra of materials of greater than about 85% carbon do not exhibit any contrast, and it is not likely that exact parallels can be drawn between the spectra of incompletely oxidized carbonaceous materials (40, 43) and activated carbons of high carbon content.

Because of the association of the adsorption of phenols on active carbon to the presence of carbonyl oxygen (see Chapter 5) the carbons activated in 1% O_2-99% N_2 were examined for their p-nitrophenol adsorption behavior. Figure 23 illustrates the experimental data for the adsorption isotherms, obtained as described in Chapter 5, and Figure 24 relates the p-nitrophenol adsorption capacities for an equilibrium solution concentration of 800 μM to the temperature of activation. From Figures 23 and 24, it appears that the surface group responsible for this adsorption mechanism goes through a surface concentration maximum around 500°C activation temperature. From the mechanistic study (see Chapter 5) where donor-acceptor complex formation is proposed involving carbonyl-like oxygen and the aromatic ring of the phenol, it would seem that the spectra of Figures 21 and 22

Fig. 23. --p-nitrophenol adsorption isotherms for sugar carbons activated at 300-700°C in 1% O_2-99% N_2 as a function of activation temperature.

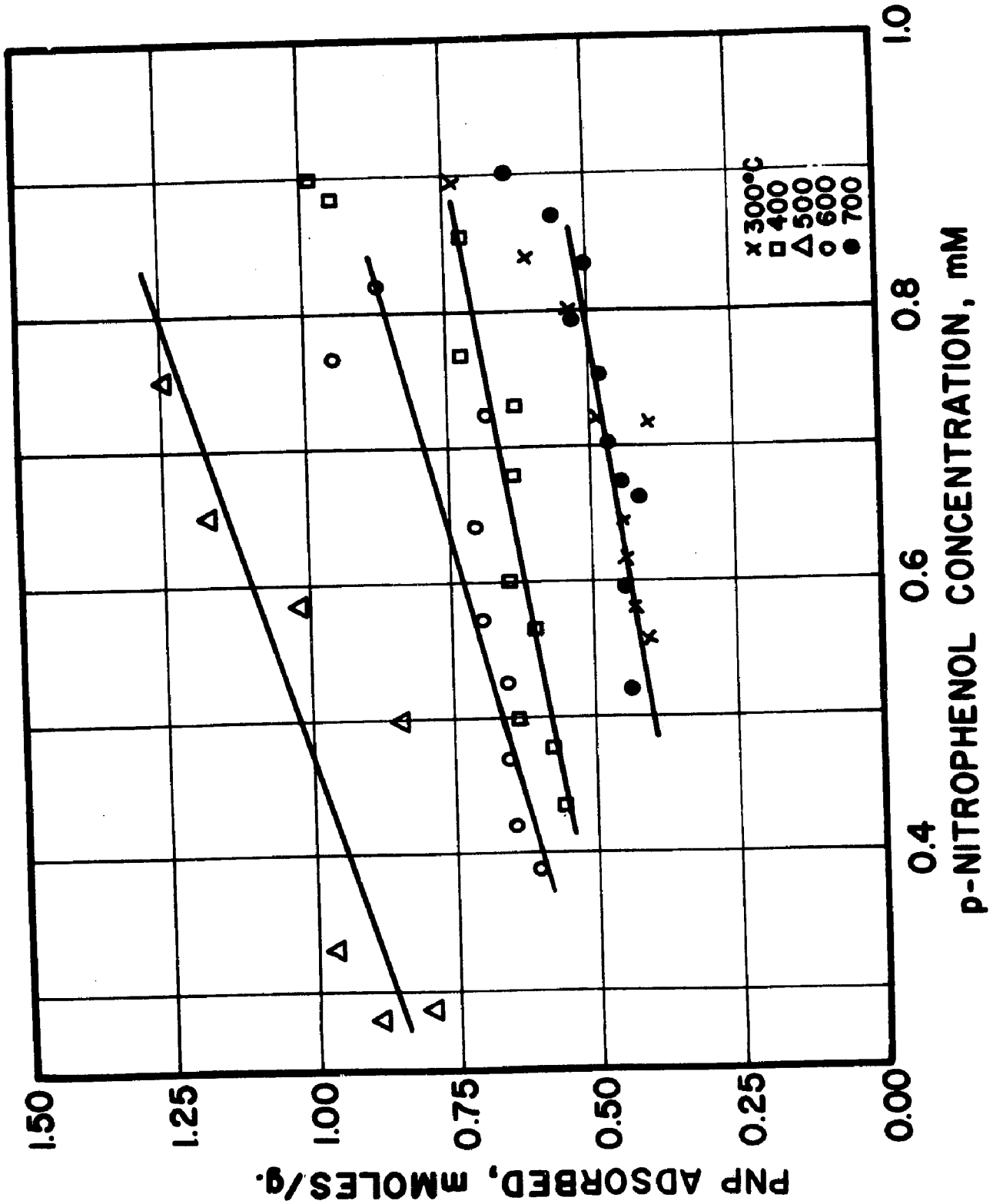
PNP ADSORBED, mMOLES/g.
1.50
1.25
1.00
0.75
0.50
0.25
0.00
0.4
0.6
0.8
1.0
p-NITROPHENOL CONCENTRATION, mM
x 300°C
□ 400
△ 500
○ 600
● 700

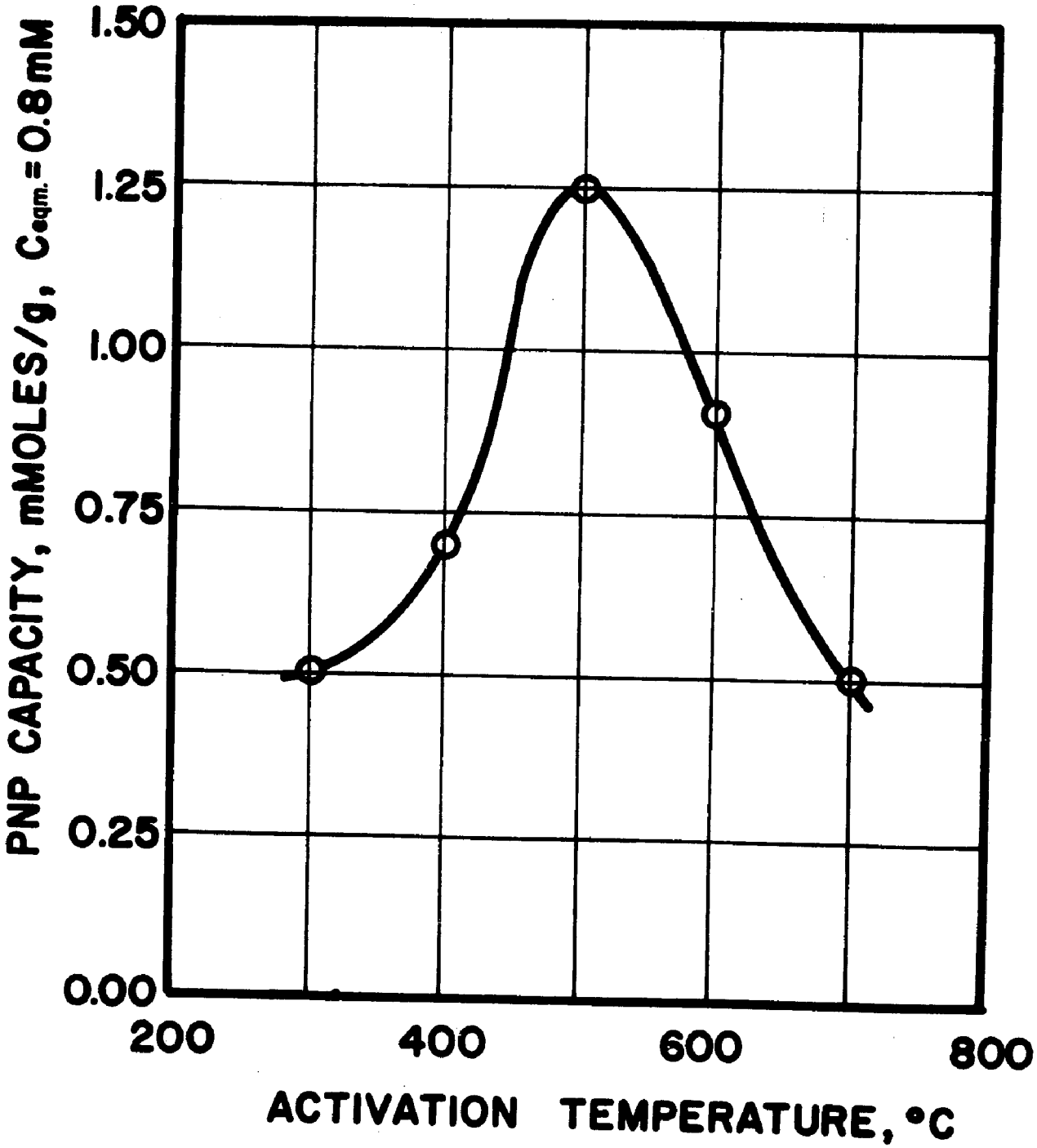

Fig. 24. --p-nitrophenol capacities for sugar carbons activated in 1% O_2-99% N_2 as a function of activation temperature.

should reflect the trend observed in Figure 24 with respect to activation temperature. Careful examination of Figures 21 and 22 along with the intensities and band maxima given in Table 9, reveals only one sequence which matches the adsorption sequence. At 300°C activation temperature, the band on the high-energy side (1590 cm^{-1} in this case) of the ca. 1600 cm^{-1} pair is the only observed band, and it is of medium intensity. In the 400°C carbon, this band (now at 1625 cm^{-1}) is strong, and a very weak band shows up at 1520 cm^{-1}. In the 500°C carbon, the low-energy band (1550 cm^{-1}) is stronger than the high-energy one (1595 cm^{-1}). In the 600°C carbon, the low-energy band (1560 cm^{-1}) predominates, and in the 700°C carbon, both bands are beginning to disappear, although the low-energy band clearly is the more intense.

An aromatic ketone would be expected to appear at 1680-1700 cm^{-1}, and this is clearly not observed. The presence of such a C=O group at the edge of a regular aromatic structure would force the ring system into the cyclohexadiene structure of a quinone, however. An isolated quinone would absorb around 1660-1690 cm^{-1}. Quinones have been identified polarographically on carbon black (40) and on active carbon (41). The presence of an

enol, however, which would involve conjugated 1,3-dicarbonyl structures, would explain the observed spectrum, as the enolic form of such a compound absorbs in the 1640 to 1540 cm^{-1} region (45).

The strange changes in the spectrum in the 1510 to 1625 cm^{-1} region certainly need to be examined carefully with respect to the adsorption phenomena associated with C=O groups. It is quite possible that there is strong interaction all along with edges of the basal planes between carboxyl and carbonyl groups. Certainly the decarboxylation which takes place at these temperatures should result in the type of conjugation required to form enolic groups. These double bonds may also show up in the IRS spectra.

Figure 25 shows the IRS spectra of a series of carbons activated in 5% O_2-45% CO_2-50% N_2. These generally had lower capacities for p-nitrophenol (0.6 to 0.8 mM/g), as the CO_2 had quite an effect of suppression of the formation of surface oxides at these temperatures. The O_2-CO_2-N_2 carbons do not show the same well-defined pair of carboxylic acids seen in Figures 21 and 22, although the absorption band is certainly present throughout (see Table 10). The same general structure is observed in the 1600 cm^{-1} region. A band at 1380 cm^{-1}, observed weakly in the 500 and 600° portions of Figure 22 and not mentioned in Tables 9

and 10, is observed in three of the four spectra of Figure 25. This small band is difficult to assign, however.

The most predominant feature in all of the spectra is the broad band observed in the 1140 to 1230 cm^{-1} region. This band is not temperature dependent, over the range 300 to 700°. It is in the singly-bonded oxygen region, and thus could correspond to a wide variety of functional groups. It may fit with an -OH bending assignment, but there were no bands observed in the -OH stretching region (3750-3000 cm^{-1}). The OH stretching vibration band is normally more intense than the OH bending vibration, and even though IRS will enhance the longer wavelength band (in this case by 8 μ/3 μ = 2.7), this enhancement cannot account for the lack of an OH stretching band.

The infrared spectra of cellulose and its derivatives show a broad, undetermined absorption in the 1150-1250 cm^{-1} region (57), possibly due to mixtures of cyclic and linear ethers and esters, methoxy groups and OH bending vibrations. In the natural lignins, structures such as (8) and (9) are found (58), which may in some way resemble the types of compounds found in carbohydrate derivatives such as chars and active carbons.

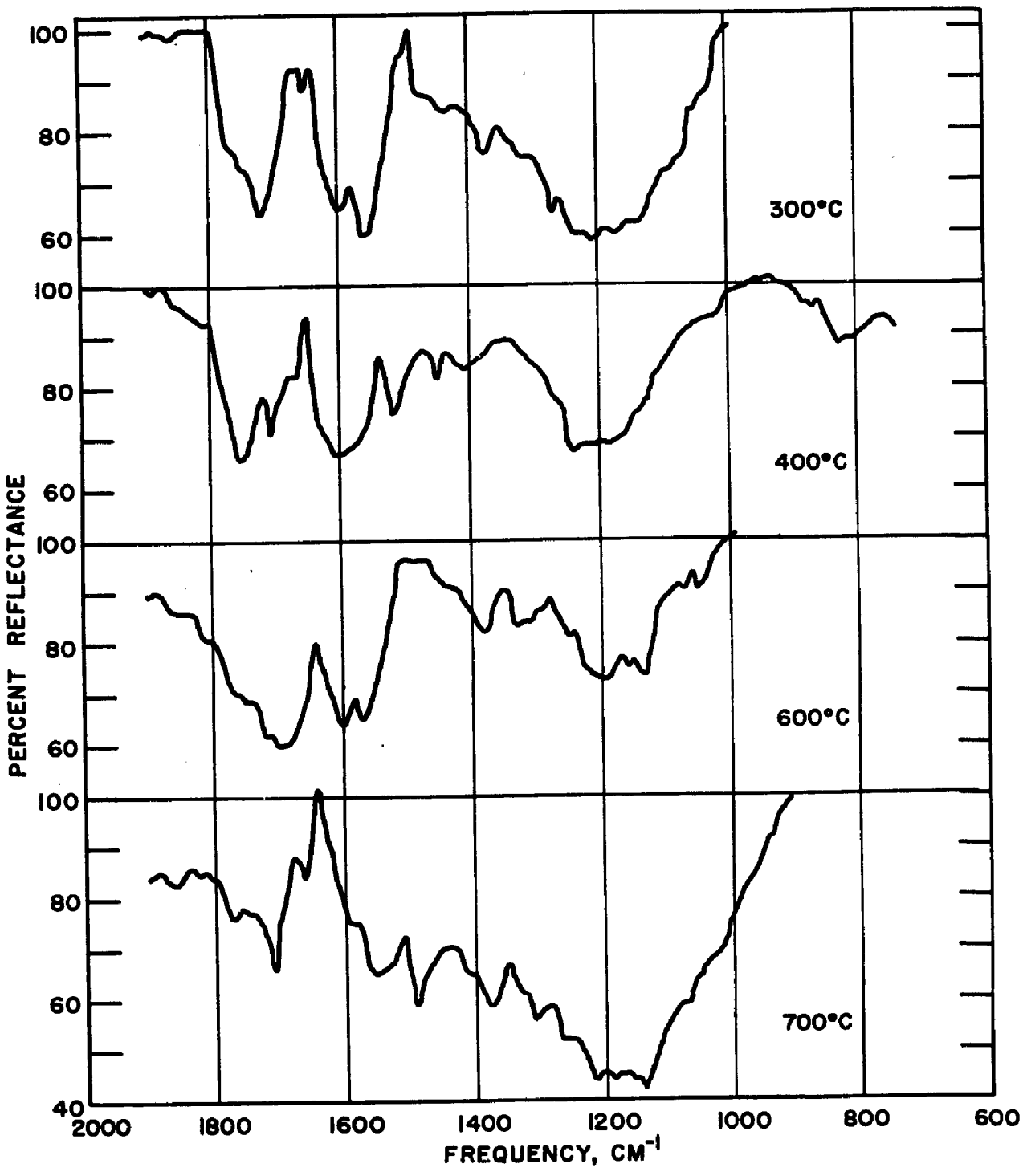

Fig. 25. --IRS spectra of sugar carbons activated in 5% O_2-45% CO_2-50% N_2 at 300 and 400° C for six hours, and 600 and 700° C for three hours.

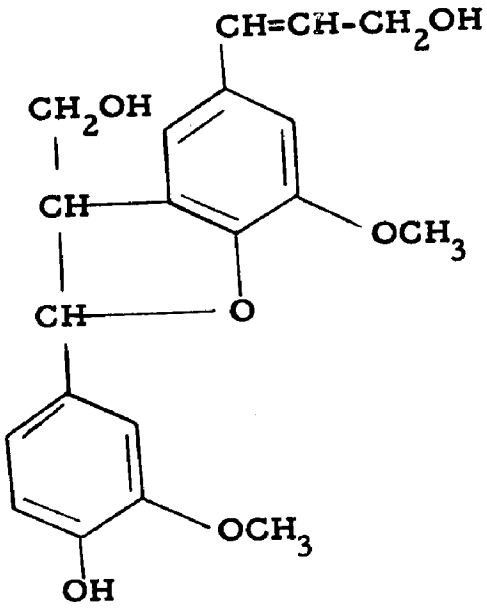

(8)

Dehydrodiconiferal Alcohol

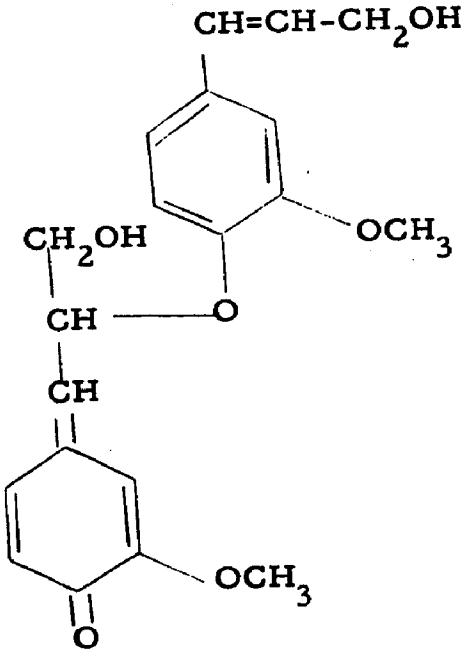

(9)

Quinonemethide

CHAPTER 5

ADSORPTION EXPERIMENTS

Several previous research efforts have recognized the importance of developing information regarding sorptive phenomena associated with active carbon in aqueous solutions of phenols (5, 49, 50, 59, 60). Although different experimental approaches have been employed, all of these studies involved the interpretation of surface properties from measurement of changes in bulk solution parameters.

It has been observed that oxidation and reduction of active carbon markedly influences the nature of the phenol and nitrobenzene isotherms (5). Coughlin and Ezra (5) showed that oxidation of active carbon considerably lowers the capacity of both active carbon and carbon black for adsorption of phenol and nitrobenzene in the low solute concentration regions of the isotherms. They also observed that reduction of the carbon resulted in the opposite effect. It was suggested that adsorption of phenol takes place with the pi-electron system of the graphitic

rings of the carbon basal planes (5, 60), and that the presence of additional acidic surface oxygen groups produced by oxidation of the carbon, at the basal plane edges, serves to withdraw electrons from the pi-system of the basal planes (5). This does not explain (5) how such an electron withdrawal effect makes itself felt over the large distances of the basal ring system, nor does it explain the nature of interaction of the sorbates on the basal planes. It was also stated (5) that the aromatic ring system of the solute could not interact with the carbon surface in the region of an oxygen-containing group because of steric interference.

Giles, et al. (60) pointed out that the adsorption isotherm for phenol on carbon usually shows a two-step process, resulting in two plateaus. The oxidation-reduction studies of Coughlin and Ezra (5) showed that this second plateau was apparently independent of the oxidation state of the carbon surface. Giles (60) suggested that the second step of the isotherm involved an uncovering of part of the surface and readsorption of the phenol molecules in a different orientation. It was suggested (60) that this reorientation involved a change from a flat configuration to an end-on configuration where the hydroxyl group is directed away from the carbon surface.

From consideration of previous speculation, it was evident that considerably more information was necessary with respect to the nature of the adsorption of phenols before the actual mechanism could be resolved. Certain of this necessary information was obtained from the study of adsorption isotherms of phenol, the meta- and para- isomers of nitrophenol, and nitrobenzene on active carbon in the low concentration range of the isotherms presented in this Chapter. This characteristic adsorption data, in conjunction with infrared internal reflectance spectra of p-nitrophenol in the adsorbed state on active carbon are employed as the basis for the postulation of a general theory for this type of interaction.

I. Experimental

A. Adsorption isotherm studies

A lignin-based carbon (Nuchar C-1000) was used in these studies which had a N_2-BET surface area of about 1000 m^2/gram (61). Before use the carbon was first washed in triply distilled water to remove water soluble ash, dried, and then sieved through a 325-mesh screen (44 microns) to obtain a distribution of small particle sizes. The carbon was again washed in triply distilled water to remove fines, then dried. Drying this material was accomplished by heating to 200° C for 12 to 24 hours and allowing it to cool in

a vacuum desiccator. This drying procedure was deemed necessary because both the infrared spectra and the measurement of oxygen content previously had indicated that such carbons contained up to about 8% water after drying at 105°C. (The bottom infrared spectrum in Figure 26 shows that the 3.0 micron O-H peak observed previously disappeared when the carbon was dried as described above.) The samples of carbon were stored under vacuum in a desiccator until used. The p-nitrophenol employed (MCB white label) was recrystallized four times from toluene, and had a 113-4°C melting point. The m-nitrophenol (MCB white label) was decolorized with active carbon in hot toluene and subsequently recrystallized twice from toluene. The purified m-nitrophenol had a melting point range of 97-9°C. Nitrobenzene (MCB white label) and phenol (Mallinckrodt AR) were employed without further purification.

The adsorption isotherms were obtained using 100 ml of solution and from 15 to 150 mg of active carbon per sample. A separate sample was used for each point on the isotherm, and the pH of the solutions was adjusted to maintain a constant value. Samples were continually agitated in bottles with polyethylene-lined caps by rotating them end-for-end in a tumbler. The time required for the equilibration of phenol samples was approximately 20 minutes, while the other solutes equilibrated in less than one

Fig. 26. --O-H Stretching Region. The top spectrum shows the O-H band of solid p-nitrophenol (KRS-5, 45°). The lower spectrum is that of active carbon with p-nitrophenol adsorbed on the carbon surface (KRS-5, 60°, 10X).

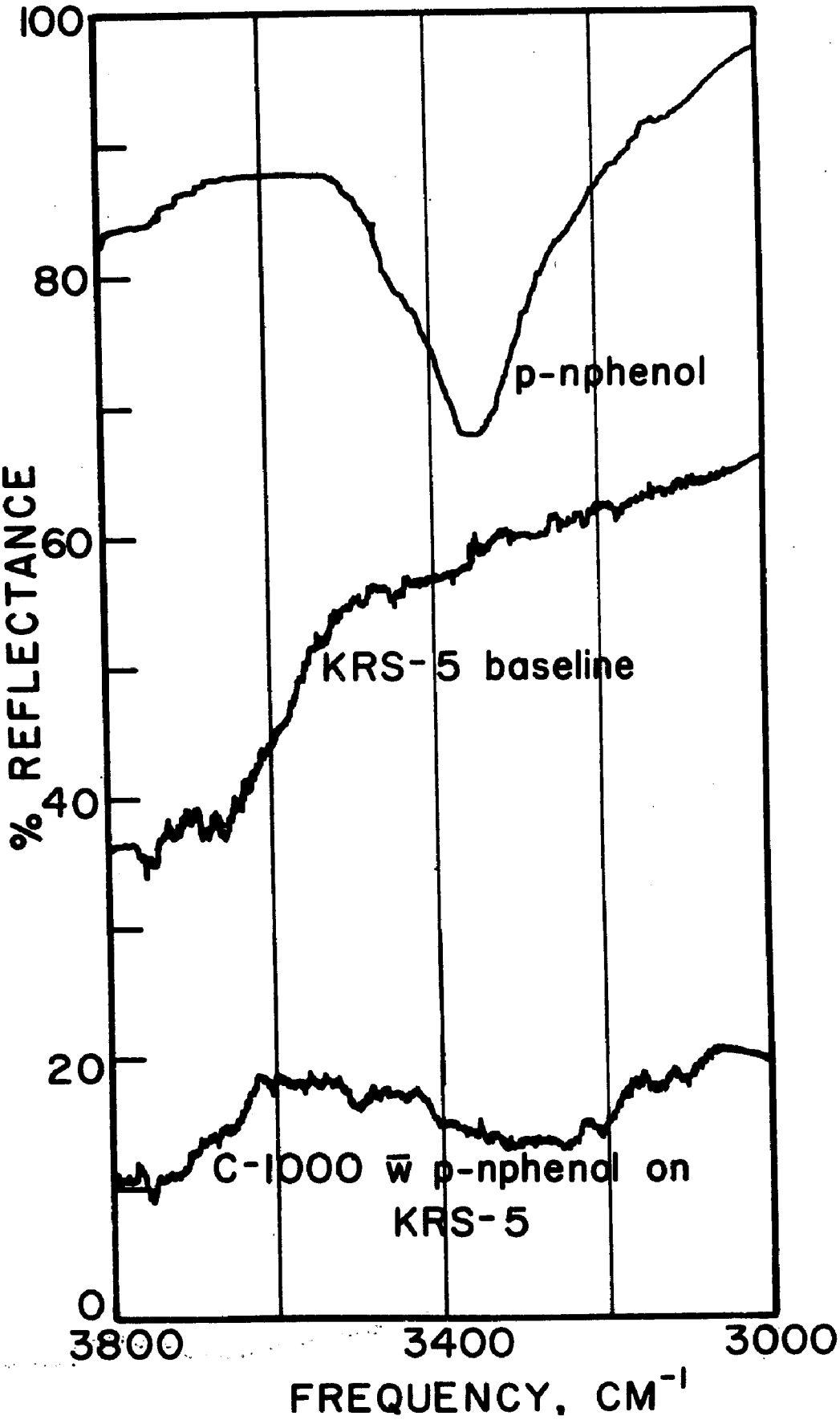
100
80
60
40
20
0
% REFLECTANCE
p-nphenol
KRS-5 baseline
C-1000 w̄ p-nphenol on KRS-5
3800
3400
3000
FREQUENCY, CM⁻¹

minute. However, all phenol samples were allowed 24 hours for equilibration, and the other samples at least 20 minutes. Separation of the carbon from the solutions was done by filtration through microporous filters (Millipore GSWP 0.22 μ). Solute concentrations were then measured with either a Cary Model 14 or a Beckman DU spectrophotometer. Desorption experiments were performed on p-nitrophenol samples by filtering all of the equilibrated solution from an isotherm sample, followed by quantitative transfer of the carbon to a fresh solution of triply distilled water made up to the proper pH with HCl. The cycle was repeated as often as desired (up to 20 times in the studies reported here). The equilibration time was 20 minutes.

Relative rates of adsorption were determined with 5 liters of solution, at room temperature, constantly stirring at a constant rate of 1000 rpm. A total of 50 ml of solution was withdrawn in 5 ml aliquots, at appropriate time intervals, and the carbon separated by filtration through microporous filters supported in a syringe filter holder. (Gelman Instrument Co., Ann Arbor, Michigan, Syringe filter holder no. 4320 and GA-6 0.45 micron filters.)

Phenol was determined colorimetrically at either 2105 A (ϵ = 6,200 l-mole^{-1}-cm^{-1}) or 2700 A (ϵ = 1540); nitrobenzene at

2685 A (ϵ = 11,900); p-nitrophenol at 3170 A (ϵ = 9,800); and m-nitrophenol at 2720 A (ϵ = 5808). The weak acids were colorimetrically determined in pH 2 solution (HCl).

B. Internal reflection spectra

The internal reflectance spectrum of pure p-nitrophenol was obtained with a thin film (ca. 400 Å) of the solid p-nitrophenol by evaporating an acetone solution on a KRS-5, 45°, IRS crystal. By employing this thin film method, there are no significant depth-of-penetration effects, and the spectrum closely approximates a transmission spectrum (51). All IRS spectra were obtained using a pair of Wilks Scientific Corp. MIR-9 IRS accessories in the sample compartment of a Perkin-Elmer Model 621 spectrophotometer. The cell compartment was continually flushed with dry, CO_2-free air to eliminate atmospheric interferences resulting from slightly different path lengths for the sample and reference beams. For the internal reflection spectral studies of the carbon samples, both KRS-5 and Ge IRS crystals were employed. It has been found that it is not feasible to determine the spectra of carbon with adsorbed aromatic compounds using germanium IRS crystals because of the tendency of the adsorbate to migrate to the germanium surface, which results in readsorption on the germanium. Thus, for these studies, KRS-5 was used as the internal reflection element.

It should be noted that the carbon/germanium critical angle is about 27°-31°, while the KRS-5/carbon critical angle is a minimum of 59° at 2.5 microns. At 7.51 microns, the carbon has a refractive index greater than the KRS-5 (n_C = 2.42 (47); n_{KRS-5} = 2.4) and it is not, therefore, possible to obtain total internal reflection under these conditions. Thus, the lower right hand spectrum in Figure 27, where the phenolic O-C band of adsorbed p-nitrophenol is observed using a KRS-5 IRS crystal is not a true internal reflection spectrum, but instead is a metallic reflection spectrum, where the carbon acts as a metallic reflector.

II. Results and Discussion

One might suggest that most adsorption processes involving organic molecules result from a specific interaction between identifiable structural elements on both the sorbate and the sorbent. It would be appropriate therefore, for the purposes of this discussion to designate such interactions as "specific adsorption", as opposed to simple coulombic interactions. It is possible for such specific interactions to exhibit a large range of binding energies, from the very low energies often associated with "physical" adsorption, to the high binding forces usually termed "chemi"-sorption. The mechanism of the adsorptive interactions of aromatic hydroxyl and nitro substituted compounds with active carbon is considered here to be a specific adsorption process.

Fig. 27. --1600-1200 cm^{-1} region. The top spectrum shows the NO_2 group bands and C-O band of p-nitrophenol. The lower spectrum shows the same bands of p-nitrophenol adsorbed on active carbon.

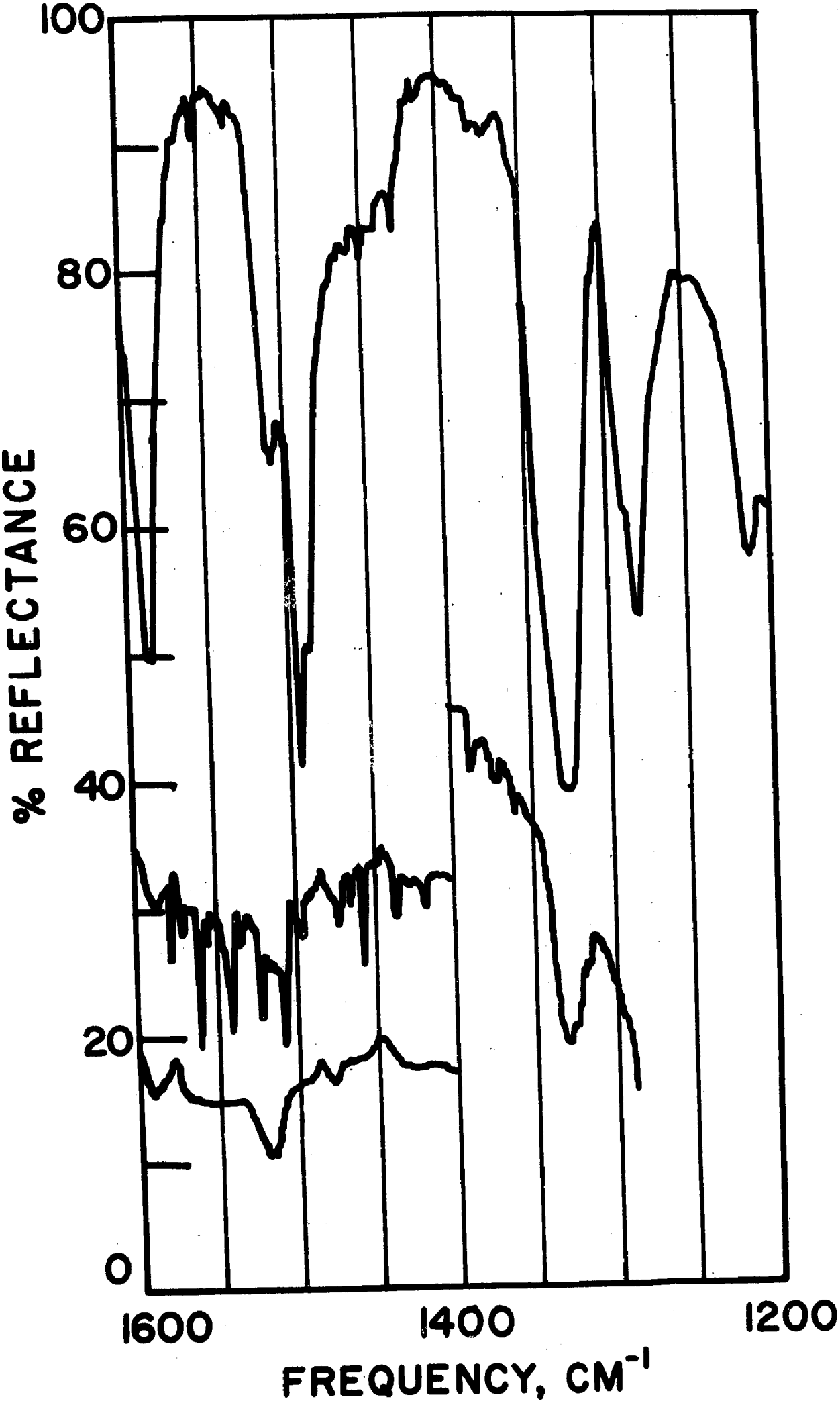
100
80
60
40
20
0
% REFLECTANCE
1600
1400
1200
FREQUENCY, CM⁻¹

The adsorption isotherms for phenol, m-nitrophenol, p-nitrophenol and nitrobenzene on the active carbon are shown in Figure 28. These isotherms are plotted with respect to the reduced concentration of the sorbate in the bulk solution. The solubilities are: phenol (pH 2, 25°C) 0.47M; m-nitrophenol (pH 2, 25°C) 0.045M; p-nitrophenol (pH 2, 25°C) 0.042M; nitrobenzene (pH 2, 25°C) 0.0118M.) From Figure 28 it can be seen that all of these species reach the same limiting surface concentration (ca. 2 mM/gram) in the low concentration range (first plateau) covered by the isotherms, which are measured for solute concentrations of less than 1.5% of the solubility limit. The amount of surface coverage under these conditions does not correspond to the total available N_2-BET surface area (1000 m^2/gram) available in the carbon used. Assuming an average surface area coverage of about 45 $\mathring{A}^2$ per molecule of an aromatic species in planar orientation (5, 60), a surface concentration of 2 mM/gram occupies only about 140 m^2/gram, or about 14% of the total N_2-BET surface. Approximately 40% of the total pore volume of 0.70 cm^3/gram was found to be sub-10 $\mathring{A}$ radius pores, and about 67% to be sub-20 $\mathring{A}$ pores (61-63).

Fig. 28. --Reduced concentration isotherms. The isotherms obtained at 25°C for phenol, the nitrophenols and nitrobenzene are shown with respect to reduced equilibrium solution concentration, $C_{eq/m}/C_s$.

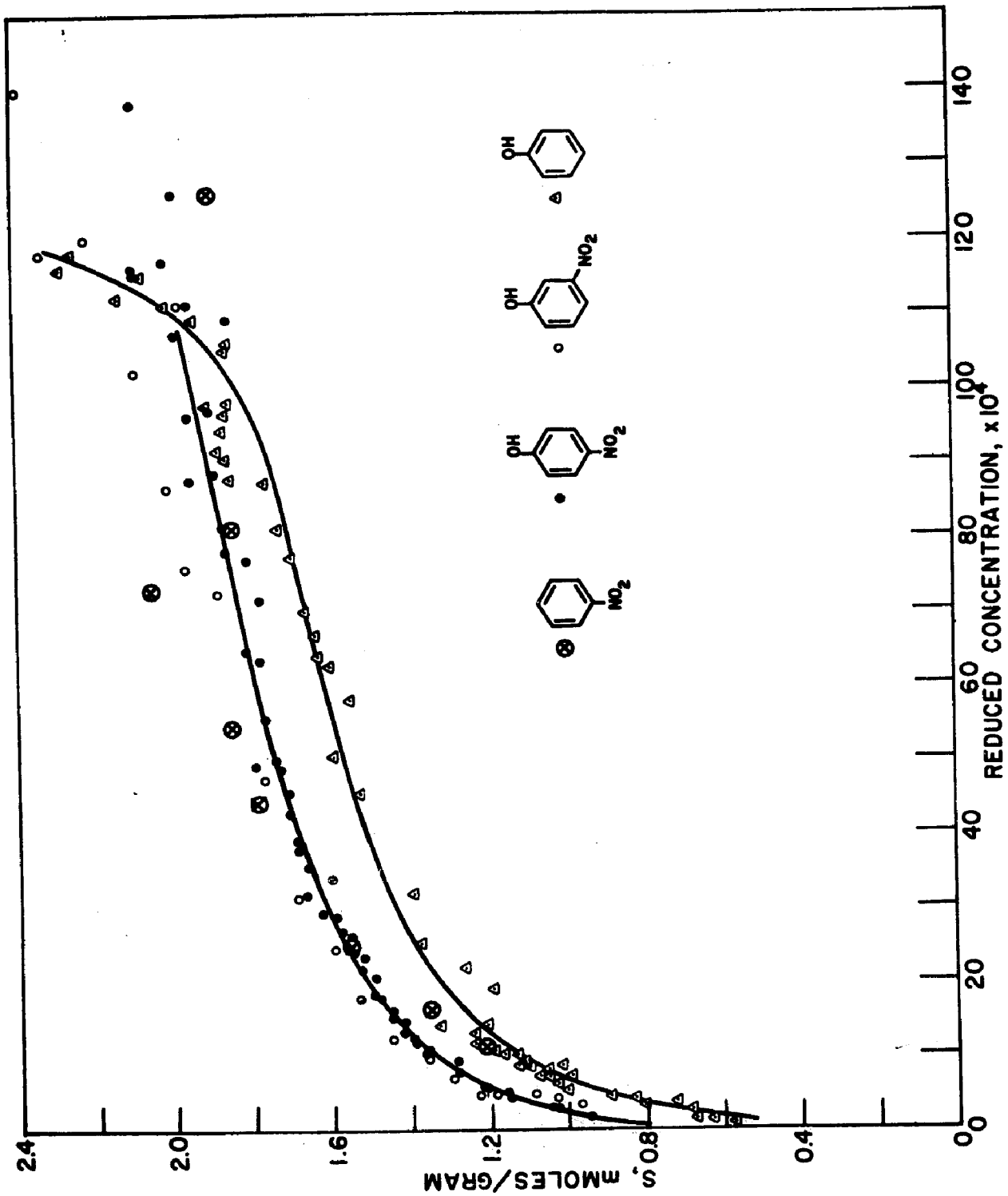
S, mMOLES/GRAM
2.4
2.0
1.6
1.2
0.8
0.4
0
0
20
40
60
80
100
120
140
REDUCED CONCENTRATION, x10⁴
OH
NO2

A particle size analysis on the carbon used in these studies using a dry micro-sieve technique (61), showed that the distribution was as follows: 0-5 micron diameter, 14.5%; 5-20 micron diameter, 22.7%; 20-44 micron diameter, 62.8%. Using weighted arithmetic average diameters from the particle size distribution, the minimum external surface area for smooth spheres would be about 0.2 m^2/gram. Allowing for a surface roughness estimated from visible microscopy, a roughness factor would give an approximate upper limit for the external surface area of 2 m^2/gram. Approximately 140 m^2/gram of surface area is occupied by adsorbed solute at the isotherm plateau in Figure 28, indicating that the majority of adsorbed molecules are on internal surfaces. From the pore size distribution, it would be expected that a large amount of the solute is in very fine pores. In Figure 29, a desorption isotherm for p-nitrophenol as well as the corresponding adsorption isotherm is shown. There is a marked hysteresis effect observed in the desorption curve which indicates that there is an irreversible step in the adsorption-desorption cycle. This behavior is probably due to the oxidation of p-nitrophenol by the surface of the carbon. The amount of

Fig. 29. --Adsorption-Desorption of p-Nitrophenol.

A desorption isotherm for p-nitrophenol on the carbon employed in this study is shown along with the adsorption isotherm. Both were obtained at pH 2 and 25°C.

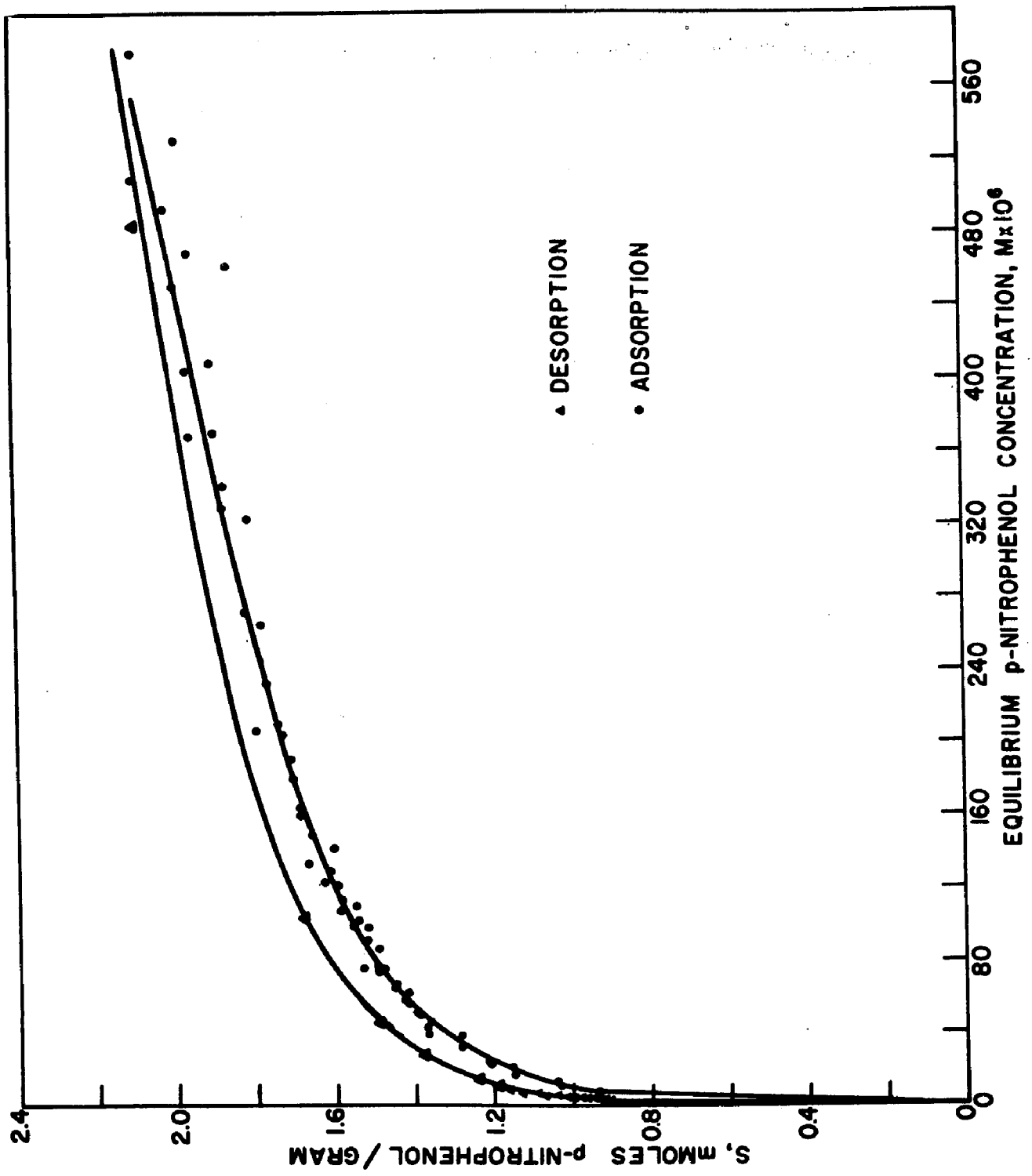
S, mMOLES p-NITROPHENOL / GRAM
2.4
2.0
1.6
1.2
0.8
0.4
0
0
80
160
240
320
400
480
560
EQUILIBRIUM p-NITROPHENOL CONCENTRATION, M x 10⁶
▲ DESORPTION
● ADSORPTION

hysteresis is, however, small and it does not significantly disturb the expected positions of the isotherms under conditions of varying bulk solubility (see Figure 30).

In Figure 28 the adsorption isotherms for all four solute species are given in terms of their reduced concentrations, and it is important that the relevance and limitations of the use of reduced concentration be understood. Traube's rule can be qualitatively expressed by the relation, $\underline{K \cdot C_s}$ = Constant, where $\underline{K}$ is the surface-solution partition coefficient and $\underline{C}_s$ the solubility. This concept can be used to normalize adsorption isotherms. The use of reduced concentrations, or $\underline{C}_{eq'm}/\underline{C}_s$, normalizes the amount of energy required to bring a molecule of solute from the bulk to the surface of the solution. This normalization is valid only for dilute solutions. Traube's rule can be applied to show that the adsorption of iodine on Graphon is a purely coulombic interaction, as the temperature dependence of the solubility can be used to account for shifts in the iodine-Graphon adsorption isotherm with temperature (63, p. 102). The extension of Traube's rule to a monofunctional homologous

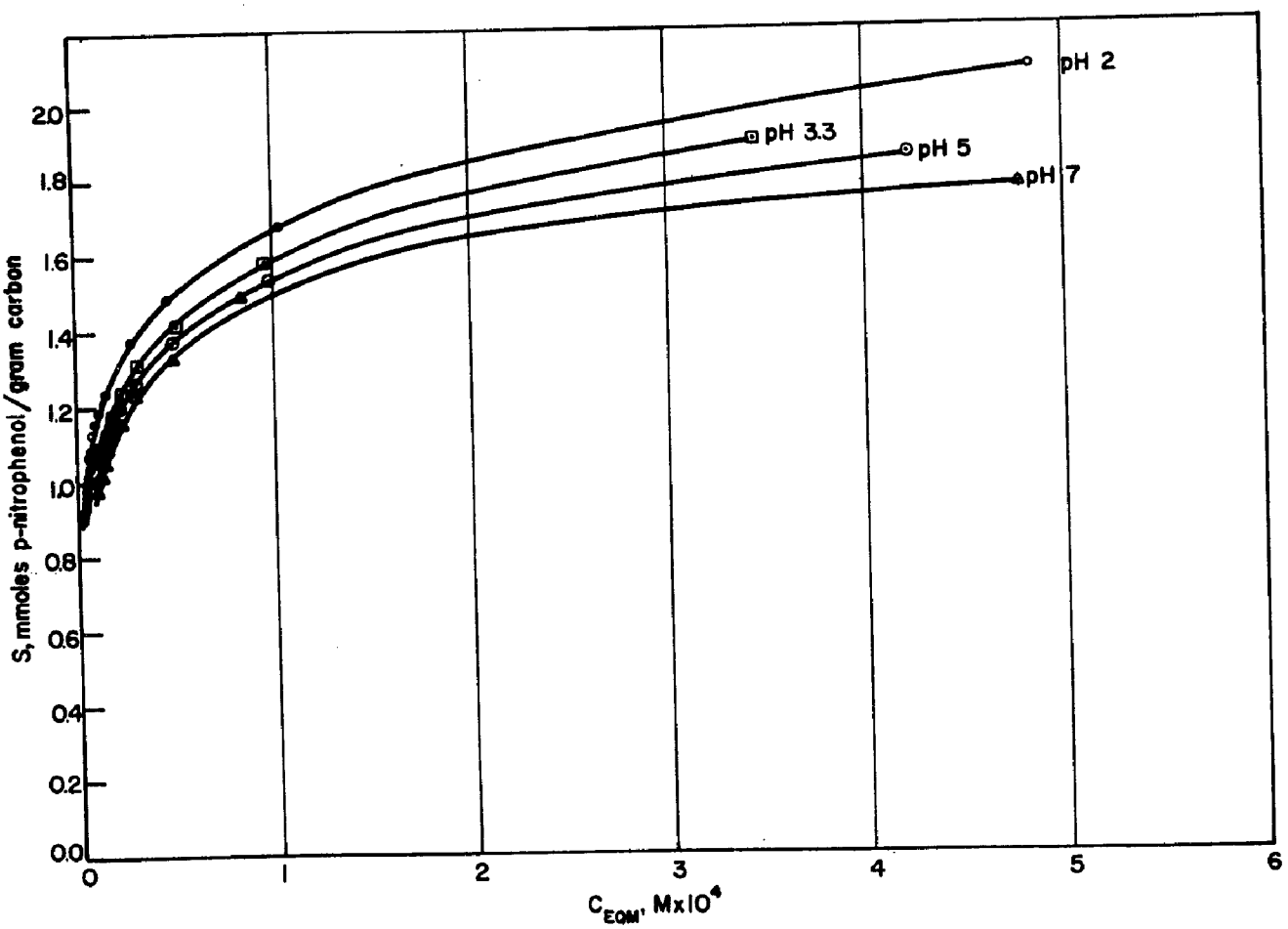

Fig. 30. --pH Dependence of p-Nitrophenol Desorption. Equilibrated samples of p-nitrophenol and carbon were subjected to the desorption technique described. Variation of the pH at which adsorption and desorption were carried out caused only the expected solubility effect.

series of organic compounds requires that the interaction, not now restricted to coulombic effects, be the same in each case, so that only solubility differences will affect the isotherms. This was shown by Hansen and Craig (62, p. 405) for the adsorption of a homologous series of fatty acids on Spheron 6. By using the reduced concentrations, the adsorption isotherms were found to coincide (for dilute solutions).

In Figure 28, it can be seen that the reduced concentration isotherms for the nitrophenols both fit well onto one curve, while that for phenol is shifted to the right until it reaches the plateau, and nitrobenzene appears to fall in between the two. The coincidence of the isotherms for p- and m-nitrophenol indicates that the interaction for each is the same, regardless of the position of the NO_2 group on the ring. The strong adsorption of nitrobenzene indicates a slightly stronger interaction than in the case of phenol, which seems to point to the nitro group as a stronger contributor to the adsorptive interaction than the hydroxyl group.

In Figure 31, reduced concentration isotherms for p-nitrophenol are given at temperatures of 16.3°, 25.0° and 40.3°C. Between 16.3° and 25.0°C, the solubility only changes from 0.037 to 0.042M, but at 40.3°C the solubility is 0.243M (all measurements were made at pH 2). Thus one observes, from

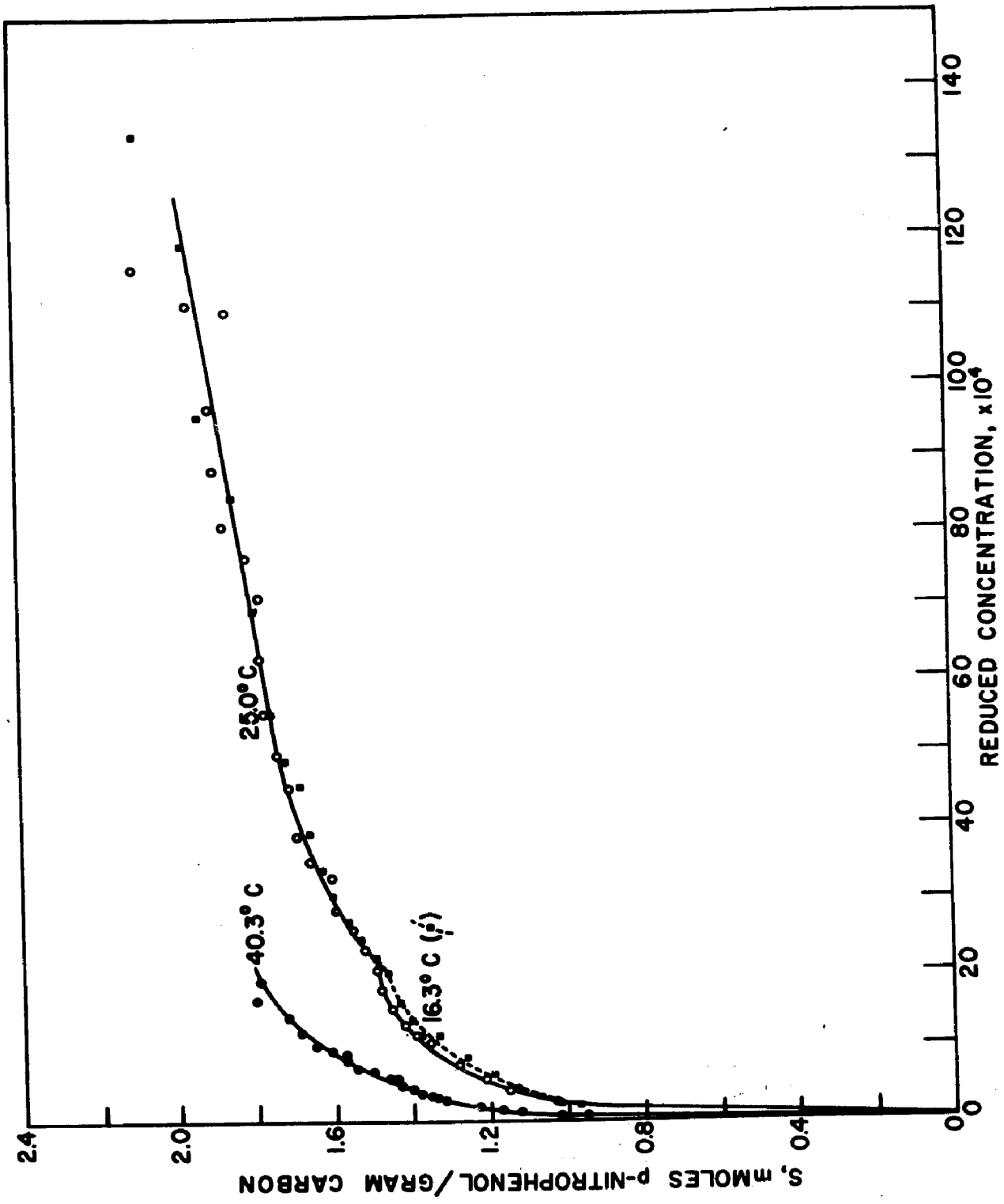

Fig. 31. --Reduced concentration isotherms for p-nitrophenol at different temperatures.

Figure 31, that p-nitrophenol adsorption does not follow Traube's rule with respect to temperature. This implies that the adsorptive mechanism involves more than just coulombic interaction and suggests that some specific interaction is involved.

In many of the p-nitrophenol isotherms (see Figures 31 and 32), there seems to be a break at a surface coverage of about 1.4 mmoles/gram. Snoeyink et al (50) have reported a similar break for phenol and p-nitrophenol using a different active carbon. There have been previous observations of breaks in the isotherm for the adsorption of phenol on carbon (5, 60), but usually these occurred at much higher equilibrium solution concentrations. (This higher concentration break in the phenol isotherm is evident in Figure 28 at the extreme right end of the isotherm.) The break at high concentration in the phenol isotherm has been attributed (60) to an uncovering of part of the surface and readsorption in a different orientation. Although this break observed at low equilibrium further study would be required to establish its precise meaning and significance.

The possible effects of pH on these adsorption experiments are threefold. First, because three of the solutes are weak acids their solubilities are pH dependent, which results in a solubility

Fig. 32. --Isotherms for p-nitrophenol at different temperatures.

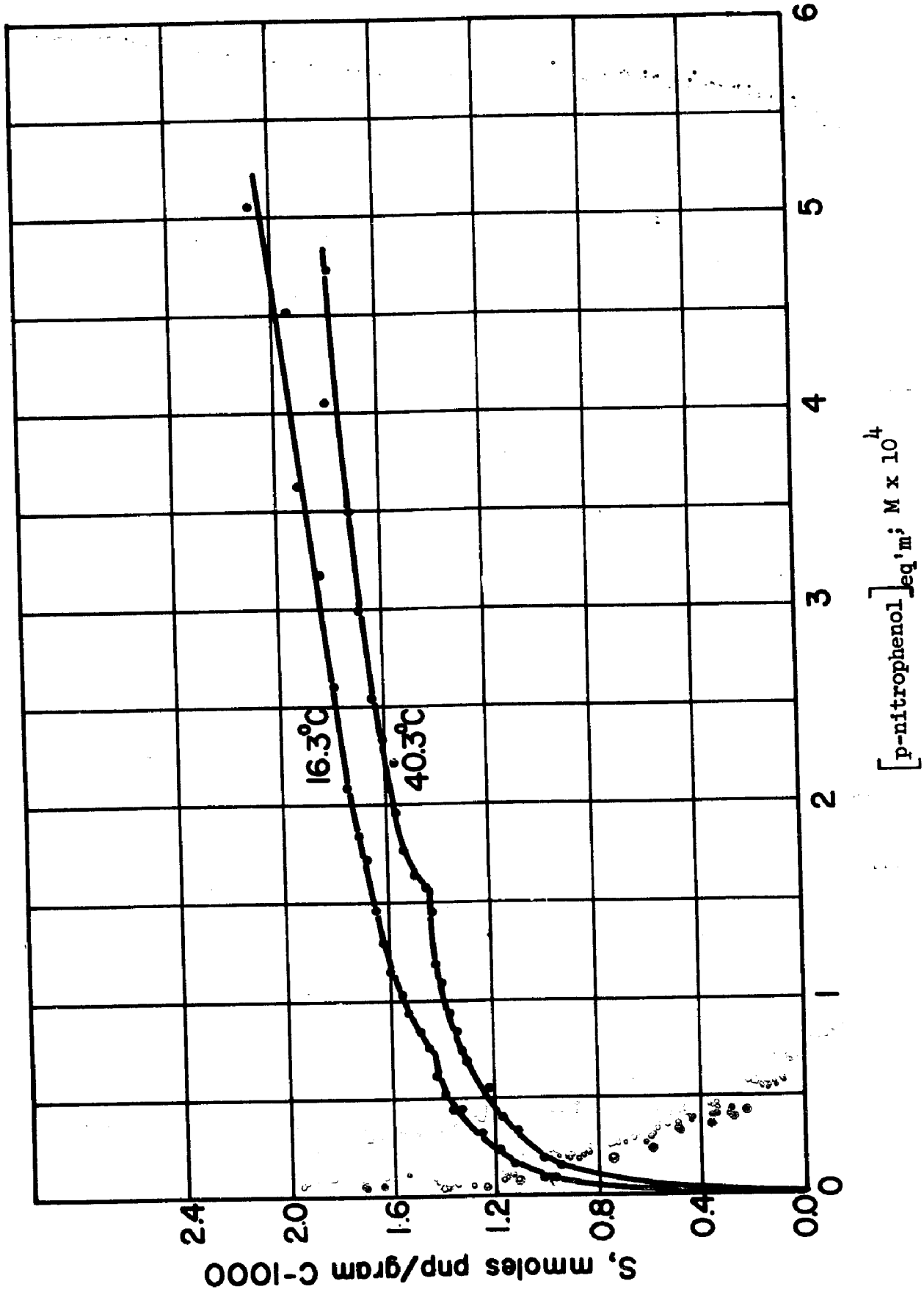
16.3°C
40.3°C
S, moles pnp/gram C-1000
0.0
0.4
0.8
1.2
1.6
2.0
2.4
0
1
2
3
4
5
6
[p-nitrophenol]eq'm; M x 10^4

dependence of the isotherms as a function of pH. This can be seen in Figure 29, where the effect of pH on p-nitrophenol desorption is shown. Second, the charge on the carbon surface will depend upon the relationship of pH, and the isoelectric point of a carbon similar to the one used in this study is at pH = 2.4. The fact that the desorption experiments in Figure 29 do not show any significant differences other than solubility effects indicates that the net charge on the carbon surface is not the determining factor in these adsorptions. The third effect is competitive adsorption of H^+ ions. Monitoring of pH in adsorption and desorption experiments indicated that there was no significant proton concentration change during the course of the experiments (except in the desorption of p-nitrophenol at pH 7). Thus it can be assumed that competitive adsorption effects were held constant throughout the experimental work by using HCl solution at pH 2 for all studies. It is important, of course, that pH be held constant in the adsorption studies of weak acids to avoid solubility effects on the isotherm which would unnecessarily complicate the interpretation of isotherm data.

In order to observe the structural changes undergone by these compounds after adsorption on active carbon, infrared spectra of the surfaces after adsorption were obtained by an

internal reflection technique described in Chapter 3. The IRS spectrum of solid p-nitrophenol is shown in Figure 33. The observed bands are identified as follows: the broad 3100-3500 cm^{-1} band is due to the O-H stretch of strongly intermolecularly hydrogen bonded O-H; the bands at 1611, 1590 and 1506 cm^{-1} are aromatic C-C stretching vibrations; the bands at 1497 and 1284 cm^{-1} are NO_2 bands; the strong band at 1330 cm^{-1} is due to the phenolic C-O stretch; the band at 1214 cm^{-1} is the O-H bending vibration; the bands at 1165 and 1110 cm^{-1} are aromatic ring vibrations; and the triplet around 850 cm^{-1} is due to ring C-H vibrations. The broad absorption around 1300-1100 cm^{-1} and the shoulder at 1200 cm^{-1} are due to a Teflon O-ring holding the crystal in place.

Spectra obtained by the IRS technique developed for carbon surfaces cover the entire group frequency region of the infrared spectrum (2.5 to 15 microns with Ge; 2.5 to 40 microns with KRS-5), and can be used to infer how the organic solute molecules interact with the carbon in the adsorbed state. With the carbon used in this study, the external surface area was approximately 1-2 m^2/gram, and the average surface coverage was only about 14% of all available N_2-BET surface area, so that it was necessary to push the internal reflection technique to the limits of its sensitivity in order to obtain good spectra.

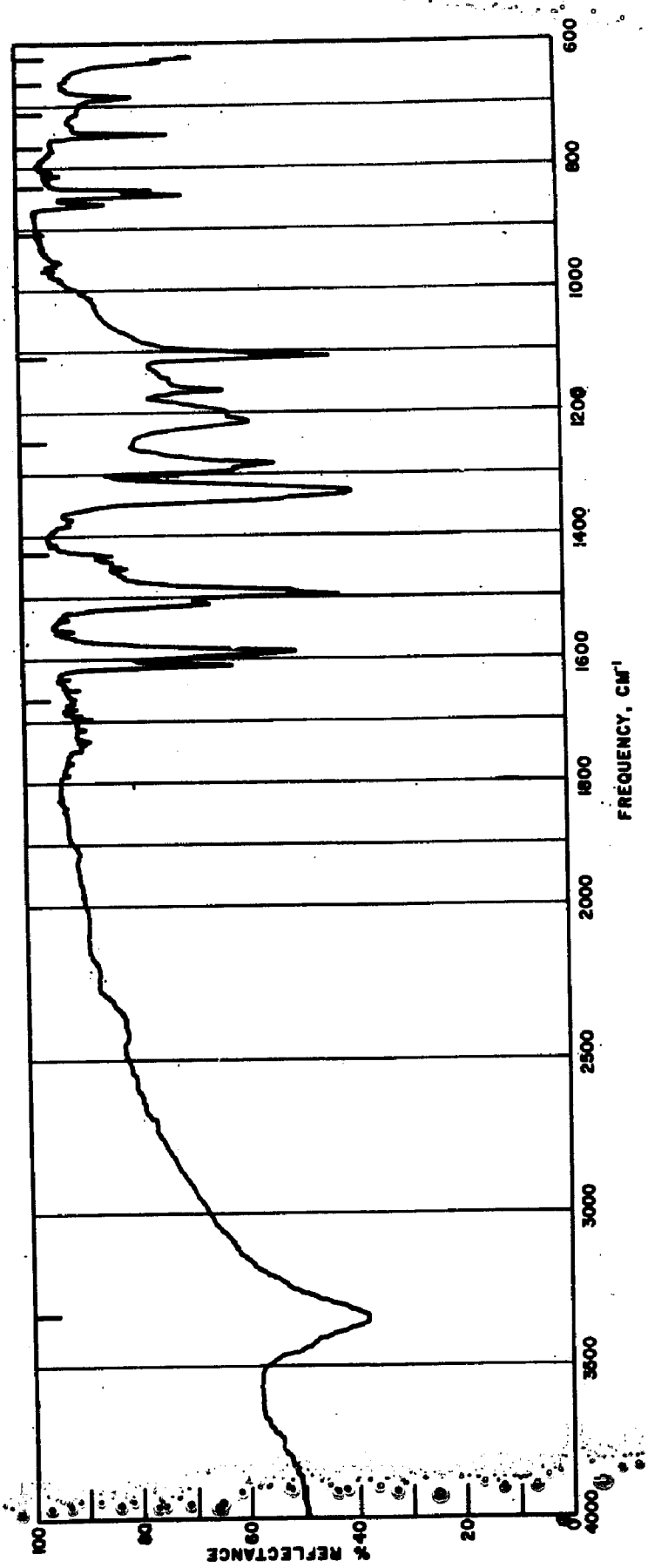

Fig. 33.--Internal reflection spectrum of p-nitrophenol. Solid p-nitrophenol in a thin film, ca. 400 A thick, was deposited on an IRS KRS-5 crystal to obtain this spectrum. (See text for technique and band assignment.)

Figure 27 shows several IRS spectra taken in the 1600-1200 cm^{-1} region. The uppermost of these spectra is reproduced from the pure p-nitrophenol spectrum in Figure 33. The lower right spectrum, from 1400 to 1280 cm^{-1}, was taken on a sample of carbon after the adsorption of p-nitrophenol. The sample was equilibrated at S = 2.0 mmoles p-nitrophenol/gram, and subsequently desorbed to S = 1.6 mM/gram, then washed and dried to assure that no p-nitrophenol was left on the surface from evaporation of interstitial solution. The procedure was checked by re-immersing a portion of the dried sample in the last equilibrium solution and measuring the uptake of solute. The losses were calculated to be less than 6% of the equilibrium S value. This spectrum clearly shows that the phenolic C-O vibration is in the same position, and has the same shape as in the pure p-nitrophenol spectrum. This spectrum was obtained using 20X scale expansion of a 6 reflection spectrum of carbon on KRS-5 (60°). The adjacent spectrum in the lower left part of Figure 27 was taken with the same IRS geometry, but is a 10X scale expansion. This spectrum, which has been corrected for partial interference of water vapor in the beam, shows that the nitro group peaks are essentially unchanged with respect to their positions before adsorption.

Figure 26 reproduces the intermolecularly hydrogen bonded O-H band (O-H···O), and below this spectrum are (i) a 60° KRS-5 10X baseline, and (ii) the spectrum of the carbon with adsorbed p-nitrophenol. Both (i) and (ii) were taken at 10X scale expansion. It is clear from Figure 26 that the strong O-H···O band has disappeared upon adsorption.

From these spectral data, some definite conclusions regarding the surface structure of p-nitrophenol can be drawn. First, since the phenolic C-O band is unchanged after adsorption, the oxygen cannot be directly associated with the surface in any specific interation, since any such interaction would be expected to alter the 1330 cm^{-1} band observed in Figure 27. Second, it is evident that the phenolic hydrogen is either gone, or is in an energetically symmetric environment which significantly reduces its infrared activity by virtue of symmetry. Loss of this hydrogen does not agree with what is observed regarding the C-O bond. Such a loss would cause the p-nitrophenol to revert to its most stable anionic structure, which is a quinoid structure. This would give the C-O bond considerable double bond character, and shift the peak up into the 1600-1660 cm^{-1} region. No such new bands were observed in the spectra taken in this region, nor were any C=C bands of a quinoid structure observed. Thus it is most likely

that the hydrogen is involved in intracomplex hydrogen bonding, within the surface complex itself. It has been shown in Gould (65) that the O-H stretching vibration in such a case will considerably diminish, broaden, and possibly even disappear altogether.

III. Conclusions

The reversibility of the adsorption (Figure 29) and the amount of temperature dependence not corrected for by solubility effects (Figure 31) indicate that a weak chemical interaction probably accounts for the adsorption of these compounds. In this respect, the adsorption characteristics of the various solutes are examined on the basis of their structures and their reactivities in homogeneous solution. This information is correlated with the spectral data in an attempt to determine the most likely mechanism which is consistent with all that is known about the systems. The structure of the solutes can be divided into three reactive functionalities, (i) the O-H group, (ii) the $-NO_2$ group, and (iii) the aromatic ring pi-electron system.

The surface of activated carbon has been described as a collection of organic functional groups containing oxygen, with these groups occurring primarily at the edges of broken graphitic planes, and the basal planes consisting of large fused aromatic ring systems in a graphite-like structure. Hydrogen bonding by the phenolic

protons with these oxygen groups is one possible surface interaction in light of the typical interactions observed in solution. This would not account, however, for the fact that nitrobenzene, which has no such proton, is adsorbed as strongly as the phenolic molecules (Figure 28). If this mechanism were of primary importance, it would be expected that the isotherms of these weak acids would correlate on the basis of their relative pK_a values. Thus major differences would be expected between p-nitrophenol (pK_a = 7.15), m-nitrophenol (pK_a = 8.2) and phenol (pK_a = 9.8). Such differences are not observed (Figure 28). Any interaction based on the electron donating ability of the phenolic oxygen would be discounted by the same pK_a argument, as well as the spectral evidence for the non-involvement of the oxygen. On the basis of the disappearance of the O-H stretch in Figure 26, as well as the position of the nitrobenzene isotherm between phenol and nitrophenol, it is evident that there is some hydrogen bonding with surface groups involved, but this interaction is small and is not the primary cause for adsorption of phenols.

If the nitro group were primarily responsible for the adsorption of the nitrophenols and nitrobenzene, one would not expect the strong adsorption observed for phenol (Figure 28). Also, the spectral evidence in Figure 27 shows that the nitro group does

not undergo significant changes upon adsorption. Thus, one must conclude that the nitro group is not directly involved in the solute-carbon interaction.

The interaction of the aromatic ring with the surface of the active carbon must, therefore, be considered the major influence in these processes, interacting through the pi-electron system of the ring. There is considerable evidence in the literature for the formation of donor-acceptor complexes between phenol and several kinds of electron donors (66). A donor-acceptor complex is a complex resulting from a small amount of orbital mixing between an electron-rich and an electron-deficient species. The binding energies of donor-acceptor complexes can range from 2 to 15 Kcal/mole (66), and is partially covalent (less than 10%) and partially coulombic in nature. Although donor-acceptor complex is the accepted term, frequently the same phenomenon is described as a charge-transfer complex (67). One can say that two factors will influence the stability of such complexes; (i) the availability of electron density in the donor, and (ii) the electron affinity of the acceptor.

It is well known (66, 67) that the electron density of an aromatic ring is strongly influenced by the nature of the substituent groups. A nitro group acts as a strong electron withdrawing group in reducing the overall electron density in the

pi-system of the ring. Thus, nitro-substituted aromatic compounds act as acceptors in such complexes and form stronger donor-acceptor complexes with a given donor than phenol, because the phenol has no low-lying acceptor orbitals (67) and forms complexes with very strong donors. The isotherms for m-nitrophenol and p-nitrophenol are essentially identical, indicating that the net energy of interaction at the surface is comparable for both. (Figure 28.)

Drago (67) has shown that phenol forms strong donor-acceptor complexes with oxygen groups, and it is known that the oxygen group dipole moment is the determining factor in the strength of the donor-acceptor complex formed. Carbonyl oxygen has a larger dipole moment than carboxylic acid oxygen, and thus would be expected to act as the stronger donor (66, 67). Thus, it is suggested that these aromatic compounds adsorb on active carbon by a donor-acceptor complex mechanism involving carbonyl oxygens of the carbon surface acting as the electron donor and the aromatic ring of the solute acting as the acceptor. These complexes would be expected to behave reversibly; and because of the pi-system interaction, it is expected that the solute molecules would adsorb in the planar orientation.

As mentioned in the introduction, Coughlin and Ezra (5) observed that a change in the adsorptive capacity for phenol and nitrobenzene took place upon oxidation and/or reduction of the carbon surface. They (5) observed that upon oxidation of the surface, both capacities decreased, and with reduction, both capacities increased. Boehm (3, 4) and Coughlin and Ezra (5) show that the oxidation of the carbon surface increases the amount of strongly acidic oxygen-containing functional groups through the oxidation of carbonyl groups. They interpret the reduction as being the reverse of the above process. As it cannot be expected that the C-C bonds broken in oxidation will rejoin upon reduction, much of the original carbonyl groups are not reformed, hence the capacity may not fully recover to its original value. Thus, it is reasonable to expect that the capacity of carbon for electron acceptors would go down upon oxidation of surface carbonyl groups to carboxylic acid groups. It is interesting to note that the data of Coughlin and Ezra (5) also seem to indicate that the second phenol plateau is not affected by oxidation of the surface, which would lead one to expect that the second step in the phenol adsorption is the formation of a donor-acceptor complex with the fused ring system of the basal planes of the carbon.

All of the data support the mechanism of a donor-acceptor complex with surface carbonyl oxygen groups, with adsorption continuing after these sites are exhausted by complexation with the rings of the basal planes. It should also be mentioned that the relative rates of adsorption of the various compounds studied were measured in order to determine the time necessary for equilibration of isotherm samples. These relative rates are consistent with the proposed mechanism, since the nitro-substituted compounds would be expected to react faster from a linear free energy argument. If the proposed mechanism is correct, then it should be possible to predict the behavior of di- and tri-nitrophenol as well. DiGiano and Weber (49), in recent adsorption studies, examined the relative amounts of adsorption of 2, 4-dinitrophenol and p-nitrophenol on the same active carbon, and found that the di-nitrophenol isotherm was shifted considerably to the left of the p-nitrophenol isotherm, indicating a much stronger interaction for di-nitrophenol. This is exactly what is predicted by the proposed mechanism. Although no data is available it would be expected that tri-nitrophenol will adsorb even more strongly on active carbon than any of the species mentioned here. Known tri-nitrophenol charge transfer complexes (picrates) are often so stable that they can be isolated and crystallized from solution.

APPENDIX

IRS SPECTROSCOPY OF OPTICALLY OPAQUE SOLIDS

There are two drawbacks to any transmission method. If the refractive index of the powder is different from that of the support, or if the powder has a finite extinction coefficient, each particle will act as a Rayleigh scattering center. The scattering is increasingly more pronounced at shorter wavelengths, and for particles with diameters $<<\lambda$, (λ - the in vacuo wavelength of the incident light) the scattering is proportional to λ^{-4}. For absorbing powders, the light beam is also attenuated in the region of an absorption band. This attenuation is the principle of transmission spectroscopy, but for particles of reasonable size and large extinction coefficient the light losses from both scattering and absorption are severe.

It has been shown that internal reflectance spectroscopy can be effectively applied to the study of absorbing powders. While transmission techniques are dependent primarily upon the physical size and optical constants of the particulate matter, IRS has several more controlling variables with which the contrast of a spectrum

can be determined. These include: the refractive index of the internal reflection element, the geometry used, the number of reflections, etc. In order to explain the selection of experimental parameters for a specific application, it is important that the basic features of IRS be understood. The particular problems encountered in the study of powders or turbid samples are discussed below.

The interaction which results in attenuated total internal reflection (ATR) can best be explained by reference to Figures 34-37, which have been obtained from computer calculations of the electric fields according to equations 1-57 of Hansen (53). The incident plane wave can be polarized either parallel to (TE) or perpendicular to (TM) the plane of incidence. In the coordinate system shown in Figures 34-37, the electric field of TE light has only a y-component, while the electric field of TM light has both x- and z-components. For the case in which light is totally reflected from a glass-water plane interface, with no attenuation, the electric field components are as shown in Figure 34. In Figure 34, the electric field components in phase one (the internal reflection element) are standing waves, formed by the superposition of the incident and reflected waves. In the rarer medium (phase 2), the electric field components exhibit an exponentially decaying intensity in the z direction. This set of exponentially

Fig. 34. --Electric field intensities for total internal reflection at a glass/water interface. The energy in the sample medium, on the right, is exponentially decaying; while standing waves result in the internal reflection element itself, on the left.

GLASS/WATER
NO ABSORPTION, THETA=60 DEG.
NEAR CRITICAL ANGLE

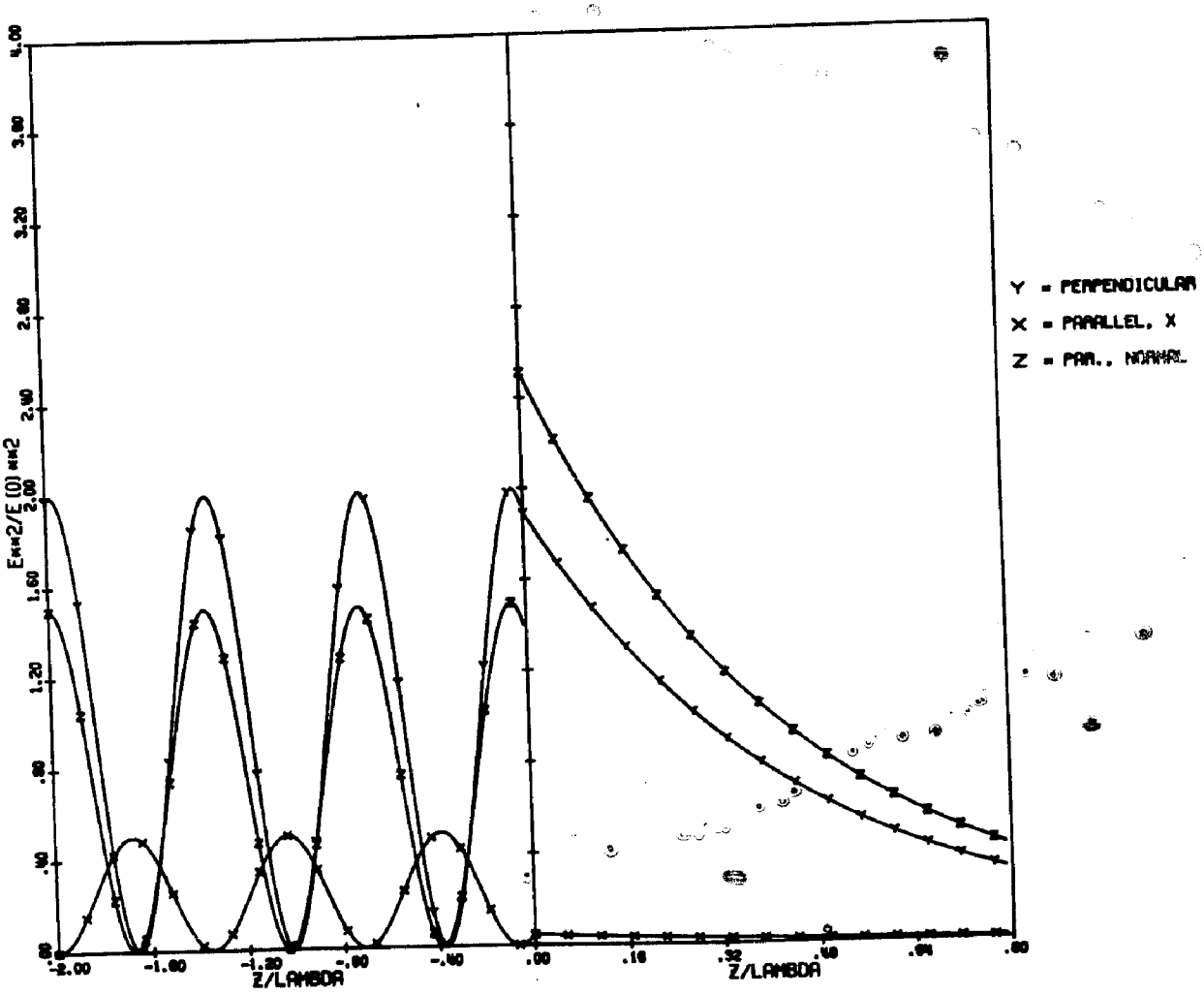

Fig. 35. --For the case of attenuated total internal reflection, where phase two has a finite extinction coefficient, not only is the intensity of the evanescent field decreased (on the right), but the amount of energy reflected in phase one has diminished.

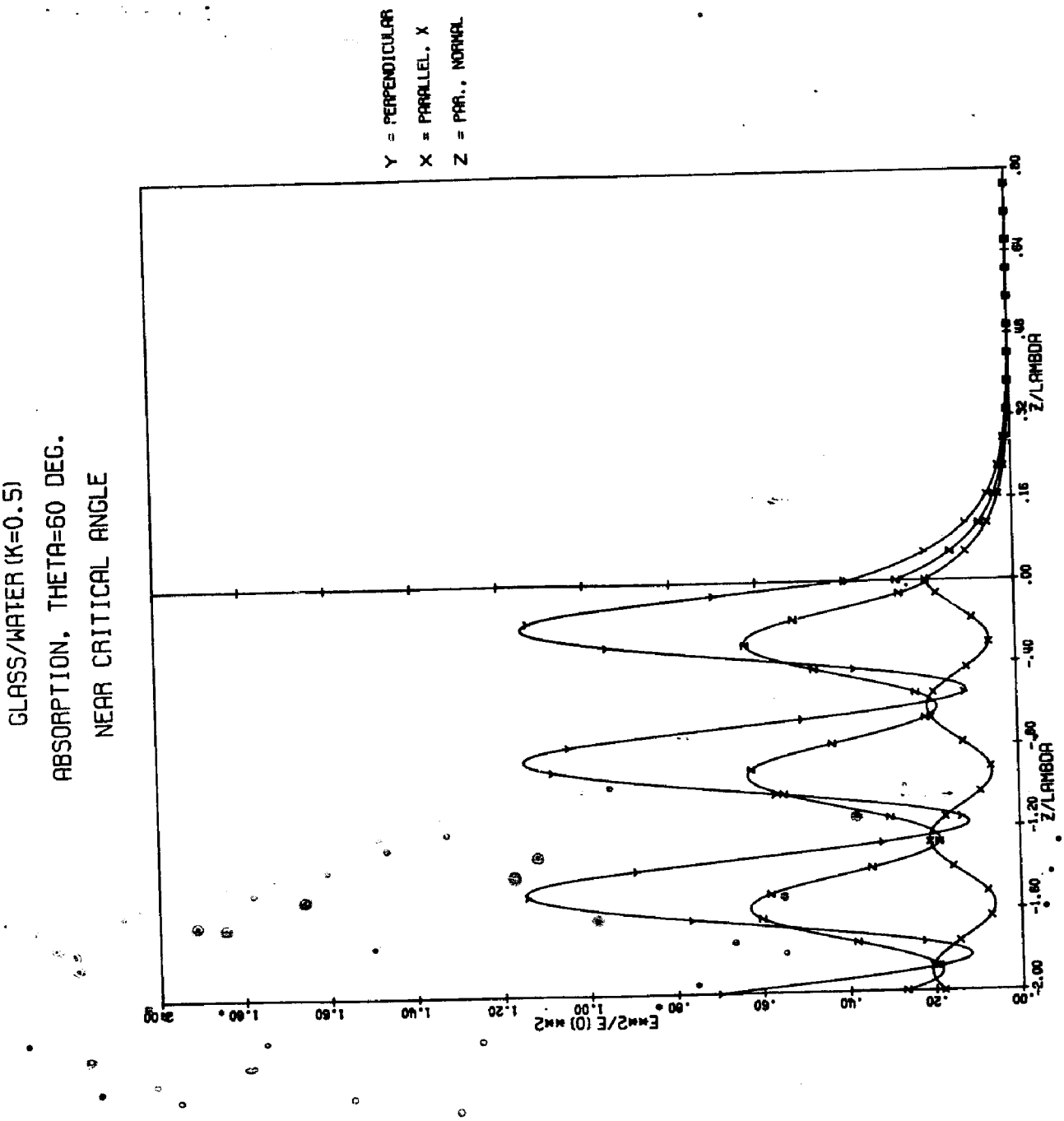
GLASS/WATER (K=0.5)
ABSORPTION, THETA=60 DEG.
NEAR CRITICAL ANGLE
Y = PERPENDICULAR
X = PARALLEL, X
Z = PAR., NORMAL
Emm2/E (0) mm2
Z/LAMBDA
Z/LAMBDA

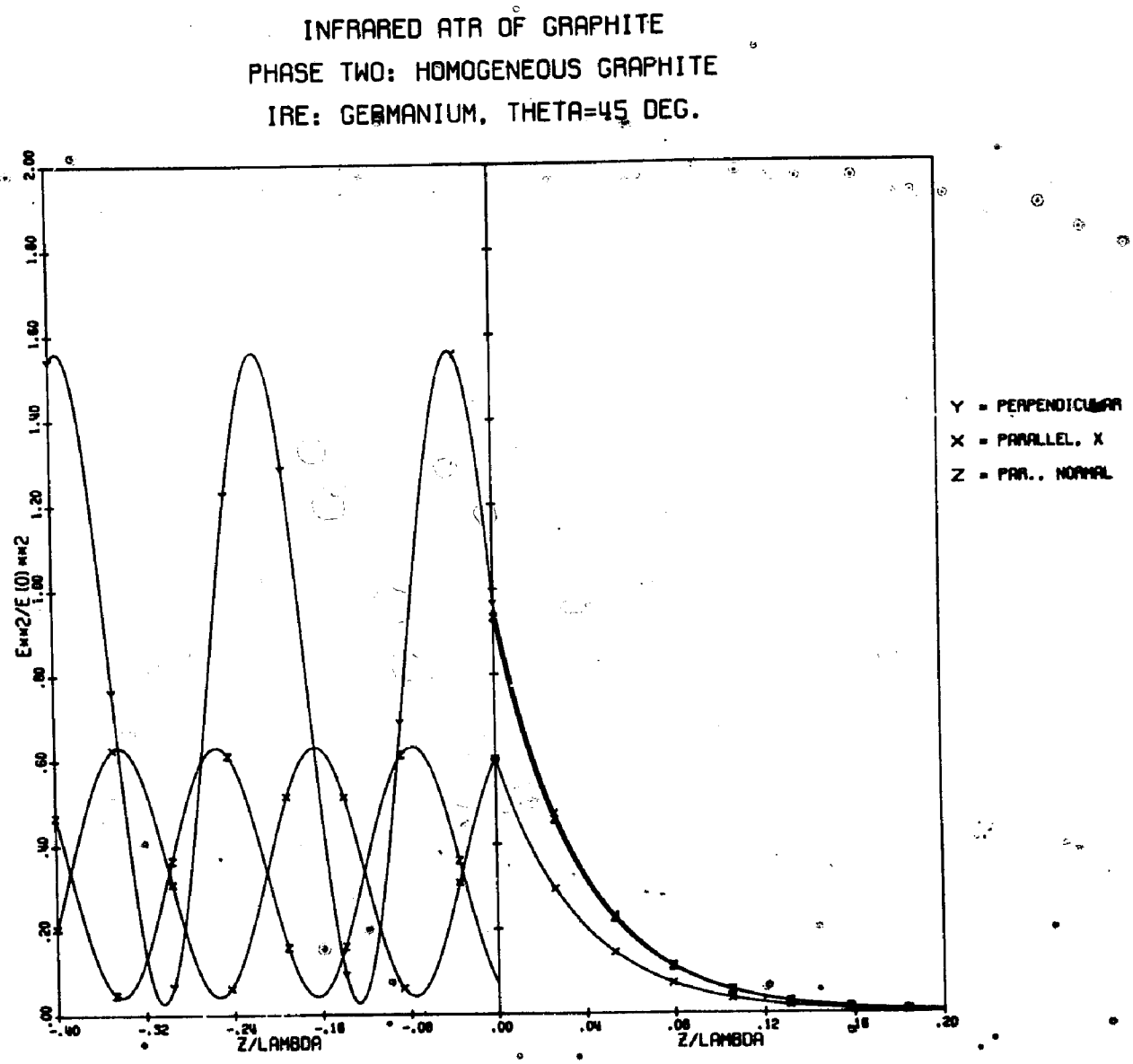

Fig. 36.--Homogeneous, highly absorbing ($\tilde{K} = 0.7$) graphite will interact strongly with the intense evanescent field observed on the right. The loss of energy is proportional to the area beneath the exponentially decaying curve.

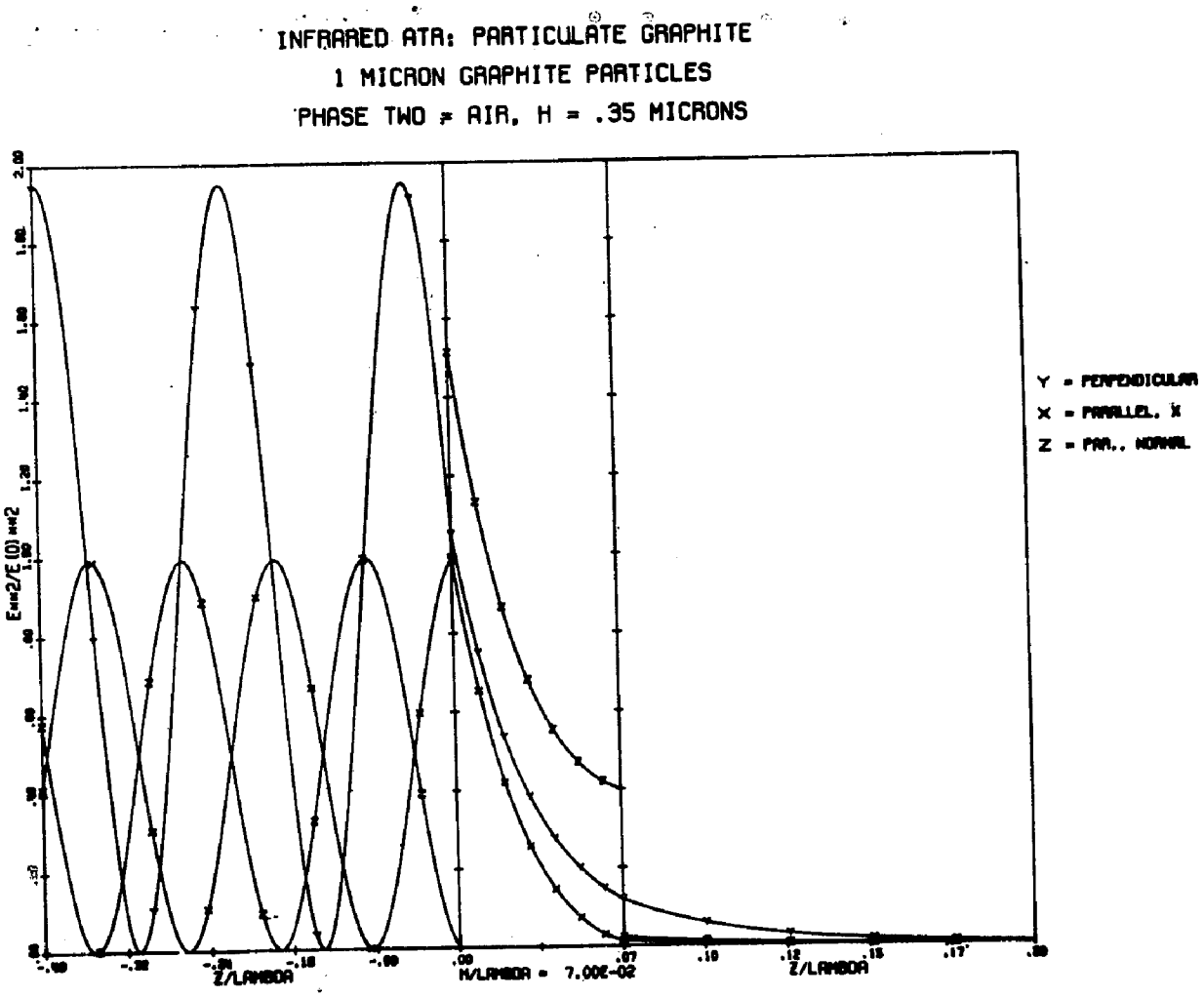

Fig. 37.--Particulate graphite, with a thin film of air separating the sample from the IRS crystal. The observed interaction, proportional to the area beneath the exponentially decaying curve in the sample medium (far right), is very weak.

attenuated electric field components, actually representing the time-averaged intensity of the electric field, is referred to as the evanescent wave. The absorption of energy from the evanescent wave is proportional to the product of the electric field intensity and the product of the optical constants, nk, of the sample (51). The complex refractive index of a substance is defined by $\hat{n} = n + ik$, (68) (Chapter 3). The evanescent wave, in addition to its exponential attenuation in the z direction, is propagated in the x direction, parallel to the reflecting interface. The evanescent wave has electric field components in all three directions in phase 2, including a non-zero E_x in the direction of propagation. This means that the evanescent wave is non-transverse, sometimes referred to as an inhomogeneous wave.

The distance into phase 2 required for the intensity of the evanescent wave to decay to 1/e of its value at the interface is called the depth of penetration (for an exponential curve, the integral from zero to infinity under the curve is the same as the product of the value of the function at zero times the depth of penetration). The depth of penetration is directly proportional to the wavelength in vacuo, λ.

The negative log of the reflectance, the "reflectance absorbance", is directly proportional to nk for an internal reflection spectrum, whereas in transmission spectroscopy the

absorbance is proportional to nk/λ. The practical consequence of the dependence of the reflectance absorbance on nk rather than nk/λ is that the relative intensities of IRS absorption peaks will be distorted in comparison to those observed for the same subtances in transmission spectra, with the peaks at longer wavelengths appearing to be enhanced in IRS (51), except in the case of a thin film of sample (51), in which case distortion is not observed.

The depth of penetration is an important effect when the rarer phase includes a powdered sample, as the rarer medium is a complex mixture of homogeneous supporting medium and irregularly shaped absorbing particles.

The evanescent field is perturbed by discontinuous variations in nk due to the particulate nature of the sample. The interaction of the evanescent field with an inhomogeneous sample is not a simple problem (51). Fried and co-workers (69, 70) have treated the interaction of a propagated wave with an inhomogeneous medium, for the case where the inhomogeneities are of dimensions $>>\lambda$. For an inhomogeneous mixture with dimensions $<<\lambda$, a refractive index for the mixture can be approximated by mixing the polarizabilities of the individual components. Thus, for a uniform mixture, the overall refractive index n_{mix} can be determined from the relationship (71).

$$3\left[\frac{n_{mix}^2 + 1}{n_{mix}^2 + 2}\right] = N_1\alpha_1 + N_2\alpha_2 + N_3\alpha_3 + \cdots$$

where N_i is the mole fraction of component i, and α_i is the polarizability of the ith component,

$$3\left[\frac{n_i^2 - 1}{n_i^2 + 2}\right] = \alpha_i$$

The sample materials of interest, however, contain particles with dimensions on the order of the wavelength employed for analysis. These are in the range of particle diameters from $\lambda/10$ to 10λ. For these systems, approximations given in the above relations are not valid. In Figure 34, the evanescent field retains sufficient intensity in the rarer phase for interaction as far as 0.8λ from the boundary. Particles which are within a distance of about 2λ from the reflecting interface can be expected to interact to some extent with the evanescent field and produce an attenuation of the reflected beam. However, the situation depicted in Figure 34 is an extreme case. The refractive indices of the two media are very close ($n_1 = 1.55$, $n_2 = 1.33$), and the angle employed is within one degree of the critical angle, thus producing a large depth of penetration. For a system such as germanium-air,

where the refractive indices are very far apart ($n_1 = 4.2$, $n_2 = 1$), and at an angle sufficiently removed from the critical angle, the attenuation of the evanescent field is much steeper, as shown in Figure 35. In this case the particles must be considerably closer to the interface in order to absorb energy from the evanescent field. Figures 36 and 37 illustrate the effect of a small amount of separation between the germanium surface and a particle of homogeneous graphite ($n = 2.2$, $k = 0.7$, $\lambda = 5\mu$) (47). In Figure 36, the graphite is in contact with the reflecting interface, and the reflectance (computed from equations 1-57 of Hansen (53) $R = 1/2(R_{TE} + R_{TM}) = 46.74\%$. This large attenuation of the reflected beam is a result of the high intensity of the evanescent field directly adjacent to the interface, in the region where the particle is located. Figure 37 illustrates the effect of a thin film ($0.35\ \mu$) of air between the germanium and the graphite. Because of the weak evanescent field at $0.35\ \mu$, the observed reflectance is $R = 1/2(R_{TE} + R_{TM}) = 96.73\%$. The wavelength for this example is $5\ \mu$, and a separation of less than $\lambda/10$ decreases the attenuation from 53.26% to only 3.27%, more than an order of magnitude. This illustrates the steepness of the decay of the evanescent field intensity near the reflecting interface under certain conditions.

Those situations where the depth of penetration into the supporting medium is small compared to the dimensions of the particle present a different problem than the three cases mentioned earlier, and it is to the solution of this problem that the present discussion is directed. This problem may be approached by first assuming that the propagative nature of the evanescent wave is not a significant contributor to the interaction, as there are few particles in the region where the evanescent field is intense. Those particles which are in this region will tend primarily to absorb energy rather than to scatter it, as this problem is a subdivision of that in which the diameters of the particles are on the same order as the wavelength. This may explain why scattering effects have not been observed in IRS spectra of powders. The interaction which is observed is therefore primarily the absorption of energy from the evanescent field by the portions of the particles immediately adjacent to the reflecting interface. This would include the points of contact and some of the area of the particles in the neighborhood of the contact points. By using the equations of Hansen, a model system which includes a three-phase system (as in Figure 37) with a middle phase of varying thickness can be set up. Calculation of the surface area of spherical particles as a function of the distance perpendicular

to the boundary, taking into account the particle size distribution, should give a fairly accurate representation of the observed attenuation.

The main physical sample requirement thus is that the phase which is to be analyzed must be able to conform closely to the planar reflecting surface. The evanescent field can only interact effectively if the sample is within a distance of approximately $\lambda/5$ of the reflecting interface. The minimum average distance from the reflecting interface to the boundary of a sphere will be about R/5, where R is the particle radius. As the evanescent field is exponentially decreasing in the direction perpendicular to the boundary, those surfaces of the particle within this range from the reflecting interface will have an exponentially larger contribution to the net observed interaction than those surfaces further removed from the interface. It can readily be seen that the principal physical requirements for a sample are good packing characteristics and small particle size. The smaller the particles, the closer they are, on the average, to the reflecting interface, and the stronger the attenuation observed in the reflected beam.

REFERENCES

1. I. Langmuir, J. Amer. Chem. Soc., 37, 1139 (1915).

2. A. Smith, Proc. Roy. Soc., A12, 424 (1863).

3. H. P. Boehm, Advan. Catal. 16, 179 (1964).

4. H. P. Boehm, E. Diehl, W. Heck, R. Sappok, Angew. Chem. Internat. Ed., 3, 669 (1964).

5. R. W. Coughlin and F. S. Ezra, Environ. Sci. Technol., 2, 291 (1968).

6. B. R. Puri, "Proc. 5th Conf. Carbon, Vol. I," Pergamon Press, New York, 1962, p. 165.

7. B. R. Puri, D. D. Singh, L. R. Sharma, J. Phys. Chem., 62, 756 (1958).

8. B. R. Puri, D. D. Singh, J. Nath, L. R. Sharma, Ind. Eng. Chem., 50, 1071 (1958).

9. B. R. Puri, K. Murari, D. D. Singh, J. Phys. Chem., 65, 37 (1961).

10. B. R. Puri and R. C. Bansal, Carbon, I, 451 (1964).

11. B. R. Puri and R. C. Bansal, ibid., 457 (1964).

12. B. R. Puri, Carbon, 4, 391 (1966).

13. Y. A. Zarif'yanz, V. F. Kiselev, N. N. Lezhnev, D. V. Nikitina, Carbon, 5, 127 (1967).

14. F. J. Vastola and P. L. Walker, Jr., J. Chim. Phys., 58, 20 (1961).

15. G. R. Hennig, J. Chim. Phys., 58, 12 (1961).

16. G. R. Hennig, "Proc. 5th Conf. Carbon, Vol. I," Pergamon Press, New York, 1962, p. 143.

17. V. A. Garten, D. E. Weiss, J. B. Willis, Australian J. Chem., 10, 295 (1957).

18. J. S. Mattson, H. B. Mark, Jr., W. J. Weber, Jr., Anal. Chem., 41, 355 (1969).

19. J. S. Mattson and H. B. Mark, Jr., J. Colloid Interface Sci., 31, 131 (1969).

20. J. S. Mattson, H. B. Mark, Jr., L. Lee, W. J. Weber, Jr., J. Colloid Interface Sci., (in press).

21. H. Harker, C. Jackson, W. F. K. Wynne-Jones, Proc. Roy. Soc., A262, 328 (1961).

22. H. Harker, J. T. Gallagher, A. Parkin, Carbon, 4, 401 (1966).

23. K. Antonowicz, "Proc. 5th Conf. Carbon, Vol. I," Pergamon Press, New York, 1962, p. 46.

24. G. G. Fedorov, Y. A. Zarif'yanz, V. F. Kiselev, Zh. Fiz. Khim., 37, 2344 (1963).

25. N. R. Laine, F. J. Vastola, P. L. Walker, Jr., "Proc. 5th Conf. Carbon, Vol. 2," Pergamon Press, New York, 1963, p. 211.

26. A. Frumkin, Kolloid Z., 51, 123 (1930).

27. H. R. Kruyt and G. S. de Kadt, Kolloid Z., 47, 44 (1929).

28. B. Steenberg, "Adsorption and Exchange of Ions on Activated Charcoal," Almquist & Wiksells, Uppsala, Sweden, 1944.

29. V. A. Garten and D. E. Weiss, Rev. Pure Appl. Chem., 7, 69 (1957).

30. J. D. Roberts and M. C. Caserio, "Basic Principals of Organic Chemistry," W. A. Benjamin, Inc., New York, 1964.

31. E. R. Lippincott, R. R. Stromberg, W. H. Grant, G. L. Cessac, Science, 164, 1482 (1969).

32. B. V. Deryagin, M. V. Talaev, N. N. Fedyakin, Proc. Acad. Sci. USSR Phys. Chem., 165, 807 (1965).

33. R. A. Horne, "Marine Chemistry; The Structure of Water and the Chemistry of the Hydrosphere," Wiley-Interscience Publishers, New York, 1969.

34. M. L. Moss, J. H. Elliot and R. T. Hall, Anal. Chem., 20, 784 (1948).

35. H. H. Willard, L. L. Merritt, Jr., and J. A. Dean, "Instrumental Methods of Analysis, 4th Ed.," D. Van Nostrand Co., Inc., Princeton, N. J., 1965, p. 569.

36. "Handbook of Chemistry and Physics, 44th Ed.," Chemical Rubber Publishing Co., Cleveland, Ohio, 1963, p. 1753.

37. D. S. Villars, J. Amer. Chem. Soc., 69, 214 (1947).

38. M. L. Studebaker, E. W. D. Huffman, A. C. Wolfe, L. G. Nabors, Ind. Eng. Chem., 48, 162 (1956).

39. M. L. Studebaker, "Proc. 5th Conf. Carbon, Vol. II," Pergamon Press, New York, 1963, p. 189.

40. J. V. Hallum and H. V. Drushel, J. Phys. Chem., 62, 110 (1958).

41. J. F. Jones and R. C. Kaye, J. Electroanal. & Interface Electrochem., 20, 213, (1969).

42. J. K. Brown, J. Chem. Soc. (London), 1955, 744.

43. R. A. Friedel and J. A. Queiser, Anal. Chem., 28, 22 (1956).

44. R. C. Smith and H. C. Howard, J. Amer. Chem. Soc., 59, 234 (1937).

45. J. R. Dyer, "Applications of Absorption Spectroscopy of Organic Compounds," Prentice-Hall, Inc., Englewood Cliffs, N. J., 1965.

46. S. Ergun, in "Chemistry and Physics of Carbon," Vol. 3, Philip L. Walker, Ed., Marcel Dekker, Inc., New York, 1968, pp 45-119.

47. P. J. Foster and C. R. Howarth, Carbon, 6, 719 (1968).

48. W. W. Wendlandt and H. G. Hecht, "Reflectance Spectroscopy," Interscience Publishers, New York, 1966.

49. F. A. Digiano and W. J. Weber, Jr., Technical Report T-69-1, Department of Civil Engineering, University of Michigan, 1969.

50. V. L. Snoeyink, W. J. Weber, Jr., and H. B. Mark, Jr., Environ. Sci. Technol., 3, 918 (1969).

51. N. J. Harrick, "Internal Reflection Spectroscopy," Interscience Publishers, New York, 1967.

52. J. S. Mattson, H. B. Mark, Jr., M. D. Malbin, W. J. Weber, Jr., and J. C. Crittenden, J. Colloid & Interface Sci., 31, 116 (1969).

53. W. N. Hansen, J. Opt. Soc. Amer., 58, 380 (1968).

54. J. S. Mattson, J. C. Crittenden, and H. B. Mark, Jr., Nuclear Applications and Tech., 7, 383 (1969).

55. Carl Leistner, Ultra Carbon Corp., Bay City, Michigan, personal communication.

56. J. S. Mattson, H. B. Mark, Jr., W. J. Weber, Jr., in "Proc. 20th Mid-America Symposium on Applied Spectroscopy," Plenum Press (in press).

57. R. G. Zhbankov, "Infrared Spectra of Cellulose and its Derivatives," trans. by A. B. Densham, Consultants Bureau, New York, 1966.

58. K. Freudenberg, in "Lignin Structure and Reactions," Advances in Chemistry Series 59, American Chemical Society, Washington, D.C., 1966, pp. 1-21.

59. V. L. Snoeyink and W. J. Weber, Jr., Environ. Sci. Technol., 1, 228 (1967)

60. C. H. Giles, T. H. MacEwen, S. N. Nakhwa and D. Smith, J. Chem. Soc., 1960, 3973.

61. Charles R. Nichols, West Virginia Pulp and Paper Co., Covington, Va., personal communication.

62. A. W. Adamson, "Physical Chemistry of Surfaces," Interscience Publishers, New York, 1967 (Second Edition).

63. J. J. Kipling, "Adsorption From Solutions of Non-electrolytes," Academic Press, London, 1965.

64. C. R. Jones, M. S. Thesis, University of Maryland, 1968.

65. E. S. Gould, "Mechanism and Structure in Organic Chemistry," Holt, Rinehart and Winston, New York, 1959, p. 30.

66. R. S. Drago, R. J. Niedzielski, R. L. Middaugh, J. Amer. Chem. Soc., 86, 1694 (1964).

67. M. R. Tamres, J. Chem. Ed., 45, 221 (1968)

68. M. Born and E. Wolf, "Principles of Optics," 3rd Ed., Pergamon Press, Oxford, England, 1965, p. 613.

69. D. L. Fried and J. D. Cloud, J. Opt. Soc. Amer., 56, 1667 (1966).

70. D. L. Fried and J. B. Seidman, J. Opt. Soc. Amer., 57, 181 (1967); and D. L. Fried, G. E. Mevers, M. P. Keister, J. Opt. Soc. Amer., 57, 787 (1967).

71. R. P. Feynman, R. B. Leighton, M. Sands, "The Feynman Lectures on Physics, Vol. II," Section 32, Addison-Wesley Publishing Co., Reading, Mass., 1964.